Characterization of a “hypothetical protein”, EF1025, from *Enterococcus faecalis*: role in cell length and shape

A Thesis Presented to

the College of Graduate and Postdoctoral Studies

in Partial Fulfilment of the Requirements

for the Degree of Doctor of Philosophy

in the Department of Microbiology and Immunology

University of Saskatchewan

Saskatoon

By

Kusum Sharma

PERMISSION TO USE

In presenting this thesis/dissertation in partial fulfilment of the requirements for a Postgraduate degree from the University of Saskatchewan, I agree that the Libraries of this University may make it freely available for inspection. I further agree that permission for copying of this thesis/dissertation in any manner, in whole or in part, for scholarly purposes may be granted by the professor or professors who supervised my thesis/dissertation work or, in their absence, by the Head of the Department or the Dean of the College in which my thesis work was done. It is understood that any copying or publication or use of this thesis/dissertation or parts thereof for financial gain shall not be allowed without my written permission. It is also understood that due recognition shall be given to me and to the University of Saskatchewan in any scholarly use which may be made of any material in my thesis/dissertation.

Requests for permission to copy or to make other uses of materials in this thesis/dissertation in whole or part should be addressed to:

Department Head
Biochemistry, Microbiology and Immunology
College of Medicine
University of Saskatchewan
107 Wiggins Road
Saskatoon, Saskatchewan S7N 5E5
Canada

or

Dean
College of Graduate and Postdoctoral Studies
University of Saskatchewan
116 Thorvaldson Building, 110 Science Place
Saskatoon, Saskatchewan S7N 5C9
Canada

Abstract

DivIVA plays multifaceted roles in Gram-positive organisms by associating with various cell division and non-cell division proteins. While the interaction of DivIVA with other proteins has been studied in many Gram-positive bacteria, no information is available about DivIVA- associating proteins in *E. faecalis.* This research reports a novel $DivIVA_{Ef}$ interacting protein named EF1025 (encoded by *EF1025*) (confirmed using Bacterial Two-Hybrid, Glutathione S-Transferase pull-down, and co-immunoprecipitation assays) that affects cell length and morphology in *E. faecalis*.

EF1025 is predominantly conserved in Gram-positive bacteria and contains a conserved N-terminal DNA binding Helix-turn-Helix (HTH) domain and two Cystathionine β-Synthase (CBS) domains located centrally and at the C-terminus. The protein, EF1025, oligomerizes to form a higher-order oligomer and the two CBS domains are responsible for its self-interaction. Viable cells were recovered after insertional inactivation or deletion of *EF1025* only through complementation of *EF1025 in trans*. These cells were longer than the average length of *E. faecalis* cells and had distorted shapes. Overexpression of *EF1025* also resulted in cell elongation but had no effect on cell shape. Immuno-staining revealed comparable localization patterns of EF1025 and $DivIVA_{Ef}$ in the later stages of division in *E. faecalis* cells.

The EF1025 homologue in *Bacillus subtilis*, CcpN, is a transcriptional repressor in *Bacillus subtilis*. In the presence of glucose, CcpN binds to the promoter region of *gapB* and *pckA* and downregulates their expression. CcpN interacted with DivIVA of *B. subtilis* in B2H and GST-pull down assays. A heterologous interaction between EF1025 and $DivIVA_{Bs}$ was also identified in a GST-pull down assay. Insertional inactivation of *ccpN* leads to cell elongation and growth of cells in straight chains. These findings suggest an additional function of CcpN in *B. subtilis*, therefore, CcpN is a dual function performing protein involved in both gluconeogenesis and cell elongation.

E. faecalis contains homologues of divisome proteins FtsZ, FtsA, FtsK, FtsQ, FtsL, FtsI and FtsB, however, the cell division interactome of *E. faecalis*, by contrast, is not presently known. This thesis also presents the unique interactome of *E. faecalis* divisome proteins (i.e. $FtsZ_{Ef}$, $FtsA_{Ef}$, $FtsQ_{Ef}$, $FtsL_{Ef}$, $FtsI_{Ef}$, $FtsW_{Ef}$, $DivIVA_{Ef}$, and $FtsB_{Ef}$), established using Bacterial-two hybrid system. The interaction of FtsA with FtsI, FtsL, and FtsZ, is common among *E. faecalis, S. pneumoniae and S. aureus* cell division interactomes. One unique

interaction i.e. $FtsZ_{Ef}$-$FtsI_{Ef}$ was identified in *E. faecalis* cell division interactome. While studying the divisome interactome of *E. faecalis*, it was observed that EF1025 is not a part of the divisome machinery in *E. faecalis* as it did not interact with any divisome protein except $DivIVA_{Ef}$.

Acknowledgements

This thesis would not have been possible without the support of numerous people from my professional and personal life and everyone deserve a note of thankfulness from me.

I take great pleasure in expressing my profound gratitude and indebtedness to my Ph.D. supervisor and mentor Prof. Jo-Anne R Dillon for her constant support, inspiring guidance, encouraging comments and constructive criticism throughout my PhD. This work would not have been possible without her timely advice from the very early stages of my work.

Besides my advisor, I would like to thank the rest of my thesis committee: Prof. Peter Howard, Prof. Scott Napper, and Dr. Aaron White, for their encouragement, and insightful comments throughout my research work at the University of Saskatchewan.

I would also like to give my thanks to staff at Vaccine and Infectious Disease Organization-International Vaccine Center (VIDO-InterVac), especially Dr. Robert Brownie, for being a great late-night lab mate and his invaluable comments on my experiments.

My hearty thanks to previous lab members (Dr. Mingmin Liao, Cherise Hedlin, Dr. Dorota Sikora, Monica Wang and Kristen Pedrizet) who laid the foundation of this project. Special thanks to my lab mates (in no specific order) Dr. Yinan Zou, Dr. Nidhi Gohil, Dr. Reema Singh, and Sumudu Perera among numerous others who have given me their support during times of need.

This work wouldn't be possible if it weren't for some very important people in my life. Beginning with my mother, father, my sisters, Mowgli and my other family i.e. Dr. Bharath Raja and Jyotsnamani Mohanta, who I'm so happy to have in my life. I was under a misapprehension that my accomplishments were mine alone. Nothing could be further from the truth. I have been encouraged, sustained, inspired and tolerated not only by my family but by the greatest group of friends anyone ever had. I apologize if I haven't been the person you deserve. But I want you all to know in my way, I love you all and thank you.

“There is enough magic in this world if you do not understand science”

- Unknown

Table of Contents

List of Tables

List of Figures

Chapter 1

Chapter 2

List of Figures (Contd…)

List of abbreviations

AA	amino acids
Chl	chloramphenicol
Kan	kanamycin
Bs	*Bacillus subtilis*
Sp	*Streptococcus pneumoniae*
Ss	*Streptococcus suis*
Lm	*Listeria monocytogenes*
Mt	*Mycobacterium tuberculosis*
Ms	*Mycobacterium smegmatis*
bp	base pair
DAPI	4',6-diamidino-2-phenylindole
dcw	division cell wall cluster
DNA	deoxyribonucleic acid
dNTP	deoxynucleoside triphosphate
Ec	*Escherichia coli*
Fts	filamentous temperature sensitive
GST	glutathione S-transferase
GTP	Guanosine 5′-triphosphate
HMW	high-molecular-weight
HTH	helix-turn-helix
CBS	cystathionine β-synthase
IPTG	isopropyl β-D-1-thiogalactopyranoside
Kb	kilobase
kDa	Kilodalton
LB	Luria broth
BHI	Brain Heart Infusion
LMW	low-molecular-weight
MIC	minimum inhibitory concentration
Ng	*Neisseria gonorrhoeae*
OD	Optical density
ONPG	o-nitro-phenyl-D-galactopyranoside
ORF	Open reading frame

PBP	penicillin binding protein
PBS	phosphate buffered saline
PCR	polymerase chain reaction
PPIs	protein-protein interactions
PG	peptidoglycan
Rpm	rotations per minute
SDS-PAGE	sodium dodecyl sulphate polyacrylamide gel electrophoresis
SPR	surface plasmon resonance
SEM	scanning electron microscopy
TEM	transmission electron microscopy
AFM	atomic force microscopy
Tm	Melting temperature
Y2H	Yeast Two-Hybrid assay

Chapter 1. General introduction

1.1. Genus- Enterococcus

Enterococci are facultative anaerobic, non-sporulating cocci, firmicute bacteria that belong to the low GC branch of Gram-positive bacteria and are commonly found growing in hostile conditions (Paulsen et al., 2003; Van Tyne and Gilmore, 2014). In the 19th century, Thiercelin described an intestinal saprophytic disease-causing coccus which was termed as "enterococcus" (Lebreton et al., 2014). The genus Enterococcus belongs to the Enterococcaceae family (Whitman et al., 2003), and includes species found in the gastrointestinal (GI) tracts of humans, animals, and insects (Mundt, 1961, 1963). The other habitats for enterococci include fermented food and dairy products (Lebreton et al., 2014), as well as soil, water and plants as well (Mundt, 1961; Mundt et al., 1962). In the fermentation industry, the members of this genus have been reported to play an important role in the ripening of food and the production of unique aromas of various cheeses and dry sausages (Franz et al., 2003; Foulquié Moreno et al., 2006; Hammerum, 2012). Several strains of "enterococcus" produce bacteriocin/enterocin, an antimicrobial compound that is widely used in the food ripening industry as a food preservative (Vuyst and Vandamme, 1994; Cleveland et al., 2001; Yang et al., 2014; Kurushima et al., 2015). Initially, enterococci were classified as group D streptococci but later, *Streptococcus faecalis* and *Streptococcus faecium* were reclassified as *Enterococcus faecalis* and *Enterococcus faecium*, respectively (Schleifer and Kilpper-Bälz, 1984). Although the genus Enterococcus consists of more than 40 ecologically different species (Jett et al., 1994; Huycke et al., 1998); approximately 90 per cent of enterococcal human infections are caused by two species: *E. faecalis* and *E. faecium* (Maki and Agger, 1988; Murray, 1990; Hidron et al., 2008).

1.2. *E. faecalis*- an important human pathogen

From a lethal case of endocarditis, MacCallum and Hastings were the first to describe a species and its pathogenic capabilities which we now call as *E. faecalis* (MacCallum and Hastings, 1899). *E. faecalis* is an opportunistic pathogen that among all Gram-positive cocci, lives most abundantly in the gastrointestinal tract of healthy humans or animals and is commonly associated with hospital-acquired infections (HAIs)/ nosocomial infections (Murray, 1990; Sievert et al., 2013). It has been known to cause various infectious diseases, including urinary infectious disease, bacteremia, meningitis, infective endocarditis, and

neonatal infections (Murray, 1990; Jett et al., 1994). Rare dental diseases such as periodontitis, periimplantitis and caries have also been found to involve *E. faecalis* (Kouidhi et al., 2011; Dahlén et al., 2012; Rams et al., 2013). Recently Al-Ahmad et al., (2009, 2010) showed incorporation of *E. faecalis* from food into the oral biofilms in the human mouth leading to dental diseases. They also showed that consumption of cheese can lead to food-borne enterococci which can integrate into the oral biofilm (Al-Ahmad et al., 2009, 2010). Larsen et al. (2010) and Gelsomino et al. (2002) have reported transmission of *E. faecalis* of porcine origin through food to the human gastrointestinal tract (Gelsomino et al., 2002; Larsen et al., 2011).

1.3. Identification of *E. faecalis* in biological specimens

The basic morphological and physiological characteristics for identifying *E. faecalis* include being Gram-positive, non-spore forming, spherical or ovoid cells that are arranged individually, in pairs, or in short chains (MacCallum and Hastings, 1899). *E. faecalis* is facultatively anaerobic, catalase-negative, fermentative chemoorganotroph that grows optimally at 35°C in a broth containing 6.5% NaCl, and bile esculin in the presence of 40% bile salts along with a number of amino acids (including Val, Leu, Ile, Ser, Met, Glu, Arg, His and Trp) and vitamins like biotin, nicotinic acid, pantothenate, pyridoxine, riboflavin, and folic acid (Lebreton et al., 2014).

1.4. Virulence of *E. faecalis*

E. faecalis colonizes both human tissue and medical devices (e.g., central venous catheters, endotracheal tubes and Foley catheters) by establishing surface communities (biofilms) (Sandoe et al., 2003; Arias-Moliz et al., 2012), which make them difficult to treat. Due to their additional ability to form a biofilm, catheter-related urinary tract infections are difficult to treat effectively with conventional antibiotics (Mohamed and Huang, 2007). Biofilms act as a barrier and prevent absorption and delivery of antibiotics from reaching their intended targets (Otto, 2006). The enterococcal surface protein (*esp*) is a large surface protein encoded by an Esp-containing pathogenicity island which aids in adsorption and colonization of cells on abiotic surfaces by biofilm formation (Toledo-Arana et al., 2001; Paganelli et al., 2012). Likewise, aggregation substance (AS), an adhesin of proteinaceous nature, also aids in adherence and invasion of host cells and biofilm establishment (Kreft et al., 1992), Another important virulence factor is cytolysin (*cyl*, beta-hemolysin), a plasmid-encoded bacteriocin

(Gilmore et al., 1994; Van Tyne et al., 2013). Cytolysin is known to lyse a number of Gram-positive bacteria using two extracellular proteins i.e. the activator and lytic components (Brock et al., 1963; Segarra et al., 1991). Similar to cytolysin, gelatinase (*gelE*), is an extracellular metalloprotease that hydrolyzes gelatin, collagen, and haemoglobin, which in turn furthers bacterial adherence and biofilm formation (Kayaoglu and Ørstavik, 2004). Hyaluronidase, a degradative enzyme, encoded by the chromosomal *hyl* gene, depolymerizes the mucopolysaccharide moiety of host tissue, thereby facilitating *E. faecalis* spread (Fisher and Phillips, 2009). Other virulence factors include extracellular superoxide (Huycke et al., 1996; Huycke and Gilmore, 1997), surface carbohydrates, (Guzmàn et al., 1989) and *E. faecalis* endocarditis antigen A (*efaA*) (Singh et al., 1998). The presence of these virulence factors makes *E. faecalis* a hypervirulent pathogen and provides a competitive edge to grow in hostile environments and resist host defences.

1.5. Antibiotic resistance in *E. faecalis*

The first case of antibiotic resistance in the treatment of enterococcal endocarditis using penicillin was reported in the early 1950s (Geraci Joseph E. and Martin William J., 1954). In 1981, the first β-lactamase-producing *E. faecalis* isolates were identified in Texas (Murray, 1990) and today, almost all enterococcal strains show low-levels of susceptibility to penicillin and ampicillin and resistance to cephalosporins and all semi-synthetic penicillins (Kristich et al., 2014). The first clinical isolate of vancomycin-resistant *E. faecalis*, strain V583, was isolated from the bloodstream of a patient in the United States (Sahm et al., 1989). Ever since, enterococcal resistance to vancomycin i.e. Vancomycin-resistant enterococci (VRE), has been growing (Gilmore et al., 2013). Outbreaks of VRE have since occurred in England, France and the United States (Leclercq et al., 1988; Uttley et al., 1988; Sahm et al., 1989). At that time, there was a lack of awareness about the emergence of antibiotic resistance among health-care workers, but a recent increase in the prevalence of antibiotic resistance to all antibiotics in *E. faecalis* is worrisome and poses a major setback in treating *E. faecalis* infections. The majority of clinical isolates of *E. faecalis* today are ampicillin-resistant and continue to carry high-level resistance (HLR) to aminoglycosides (e.g. gentamicin and streptomycin), vancomycin, and other glycopeptides, providing *E. faecalis* the status of "multidrug-resistant" (Murray, 2000; Kristich et al., 2014).

The standard treatment protocol for *E. faecalis* infections involves administration of β-lactam antibiotics such as the amino-penicillins (e.g. ampicillin) and ureidopenicillins (e.g.

piperacillin), along with penicillin G and carbapenems (Kristich et al., 2014). In the cases of β-lactam allergy, vancomycin is reserved for treatment purposes (Kristich et al., 2014). In certain infections such as endocarditis, an association of a β-lactam with an aminoglycoside produces efficient bactericidal effects (Moellering and Weinberg, 1971). The usual regimen to treat VRE infections involves the administration of high-dose ampicillin, chloramphenicol alone or with rifampin (Mekonen et al., 1995; Norris et al., 1995; Murray, 2000). Other VRE treatment antibiotics include tetracycline and doxycline (Gransden et al., 1998).

In addition to possessing specific virulence and resistance genes, *E. faecalis* is noted for incorporating mobile elements into its genome (Manson et al., 2010; Paganelli et al., 2012). This capability leads to the distribution and transmission of many genes responsible for conferring antibiotic resistance by horizontal gene transfer (Paganelli et al., 2012). Multidrug-resistant enterococcal genomes consist of more than 25% of mobile elements representing a widespread accumulation of drug-resistant elements and virulence factors (Paulsen et al., 2003). The transfer of vancomycin resistance genes from *E. faecalis* to methicillin-resistant *Staphylococcus aureus* has been recorded in the late 90s and early 2000 (Willems et al., 2001; Palmer et al., 2010).

Enterococcal infections have become a major health care problem due to increasing numbers of multidrug-resistant isolates and difficulties in eradicating biofilms (Flemming and Wingender, 2010; Arias and Murray, 2012). The recent emergence of hypervirulent and multidrug-resistant *E. faecalis* strains, therefore, requires an in-depth understanding of the enterococcal biology, genetics and underlying factors contributing to the virulence of this pathogen (Stinemetz et al., 2017). New therapeutic targets (such as the process of cell division or metabolism pathway) and strategies need to be identified to combat enterococcal infections. Despite the status of "hypervirulent and multidrug-resistant" that *E. faecalis* has acquired over the past few decades, there have been only a few research studies that have dealt with the process of cell division in this pathogen (Ramirez-Arcos, 2005; Rigden et al., 2008; Stinemetz et al., 2017).

1.6. Division Cell Wall (*dcw*) Gene Cluster

Due to evolutionary dynamics, there exist highly conserved gene clusters throughout bacterial genomes (Weber et al., 2016), such a cluster for cell division is called the *dcw* (division and cell wall) gene cluster (Ayala et al., 1994; Tamames et al., 2001). The

conservation of *dcw* genes, their regulation and, in general, their cluster structure, are remarkably conserved in bacterial groups of similar taxon and cell size (Tamames et al., 2001). Since the proteins encoded by the *dcw* genes are involved in cell division and peptidoglycan synthesis, bacterial *dcw* gene clusters are mostly essential (Boyle and Donachie, 1998; Kobayashi et al., 2003). In addition to regulatory mechanisms, their conserved gene order can ensure successful synchronization of growth and division (Mingorance et al., 2004). The filamentous temperature-sensitive (Fts) phenotype was first described in *E. coli* when the filamentous temperature-sensitive (*fts*) genes were mutated (Bi and Lutkenhaus, 1991). These mutations were found to be restricted to a region, which was later named the *dcw* cluster (Ayala et al., 1994; Vicente and Errington, 1996; Rothfield and Justice, 1997). The *dcw* genes have been studied intensively in model organisms such as *B. subtilis* and *E. coli*, but due to numerous regulatory features such as protein ratios, internal promoters and transcript stability, their regulation is not fully understood (Weber et al., 2016).

Although the *dcw* cluster is highly conserved in bacterial species (Pucci et al., 1997), the organization of various genes within the dcw cluster varies in different bacterial species as found in *E. coli*, *B. subtilis*, *S. aureus*, *E. faecalis*, *S. pyogenes*, and *S. pneumoniae* (Fig. 1.1.) (Massidda et al., 1998; Francis et al., 2000; Snyder et al., 2001; Fadda et al., 2003; Ramirez-Arcos, 2005; Real and Henriques, 2006). Genes like *ftsZ* and *ftsA*, are highly conserved between Gram-negative and Gram-positive bacteria, as are their position within the *dcw* cluster.

1.6.1. *dcw* cluster of *B. subtilis*

The first bacterial *dcw* cluster was deduced in the *E. coli* which comprises 16 genes (i.e. $mraZ_{Ec}$, $mraW_{Ec}$, $ftsL_{Ec}$, $ftsI_{Ec}$, $murE_{Ec}$, $murF_{Ec}$, $mraY_{Ec}$, $murD_{Ec}$, $ftsW_{Ec}$, $murG_{Ec}$, $murC_{Ec}$, $ddlB_{Ec}$, $ftsQ_{Ec}$, $ftsA_{Ec}$, $ftsZ_{Ec}$ and $envA_{Ec}$) (Ayala et al., 1994; Mingorance et al., 2004). The organization of the *dcw* cluster in *B. subtilis*, the Gram-positive model organism for studying cell division (Harwood, 2007), is similar to that in *E. coli*, the Gram-negative model organism, with respect to 17 different identified genes ($mraZ_{Bs}$, $mraW_{Bs}$, $ftsL_{Bs}$, $ftsI_{Bs}$, $spoVD_{Bs}$, $murE_{Bs}$, $murF_{Bs}$, $mraY_{Bs}$, $murD_{Bs}$, $ftsW_{Bs}$, $murG_{Bs}$, $murB_{Bs}$, $ftsQ_{Bs}$, $ylxW_{Bs}$, $ylxX_{Bs}$, $ftsA_{Bs}$ *and* $ftsZ_{Bs}$) (Fig. 1.1) (Mingorance et al., 2004; Real and Henriques, 2006). *E. coli mraW* is the antagonist of $mraZ_{Ec}$, a highly conserved transcriptional regulator in most of the bacteria (Eraso et al., 2014). The *mur* genes, including $mraY_{Ec}$ and $ddlB_{Ec}$, are essential genes for the synthesis of peptidoglycan precursors (Pilhofer et al., 2008). However, the *B. subtilis dcw* cluster also

contains, *spoVD*$_{Bs}$ and *spoVE*$_{Bs}$, that encode sporulation-specific proteins for endospore cortex peptidoglycan synthesis (Daniel et al., 1994). *spoVD*$_{Bs}$ shares 33% identity with the upstream *ftsI*$_{Bs}$ (Daniel et al., 1994; Vicente et al., 2004). The other difference is that there is an internal transcription terminator between *ftsI*$_{Bs}$ and *spoVD*$_{Bs}$. An important cell division protein is DivIVA$_{Bs}$, encoded by *divIVA*$_{Bs}$ which does not belong to the *dcw* cluster of *B. subtilis*.

1.6.2. *dcw* cluster in other microorganisms

The Gram-positive bacteria, *S. pyogenes* and *S. pneumoniae* have distinctive *dcw* cluster organization (Fig. 1.1) (Massidda et al., 1998). The *S. pneumoniae dcw* cluster is distributed into three separate regions on the chromosome where the first region, *dcw1*, contains eight genes i.e. *pbp2b*$_{Sp}$, *recM*$_{Sp}$, *ddl*$_{Sp}$, *murF*$_{Sp}$, *mutT*$_{Sp}$, *orf1*, *ftsA*$_{Sp}$ *and ftsZ*$_{Sp}$. The second region contains five genes, *murG*$_{Sp}$, *divIB*$_{Sp}$, *pyrF*$_{Sp}$, *and pyrE*$_{Sp}$, and the third region, *dcw3*, is composed of the *yllC*$_{Sp}$, *yllD*$_{Sp}$, *pbp2x*$_{Sp}$, and *mraY*$_{Sp}$ genes (Massidda et al., 1998). Four putative genes are located downstream of *ftsZ*$_{Sp}$ (Massidda et al., 1998) and the protein encoded by the last gene shares 65% similarity with *B. subtilis* DivIVA which is involved in Gram-positive bacteria cell division (Cha and Stewart, 1997; Edwards and Errington, 1997). The *dcw* cluster of *S. pyogenes* is distributed in two clusters where *dcw1* and *dcw2*, each contains five genes i.e. *murG*$_{Spy}$, *murD*$_{Spy}$, *divIB*$_{Spy}$, *ftsA*$_{Spy}$ *and ftsZ*$_{Spy}$, and *yllC*$_{Spy}$, *yllD*$_{Spy}$, *pbpN-ter*$_{Spy}$, *pcpC-ter*$_{Spy}$, and *mraY*$_{Spy}$, respectively. Understanding the role of important proteins in the division of cells, however, is essential for understanding bacterial cell division initiation and regulation.

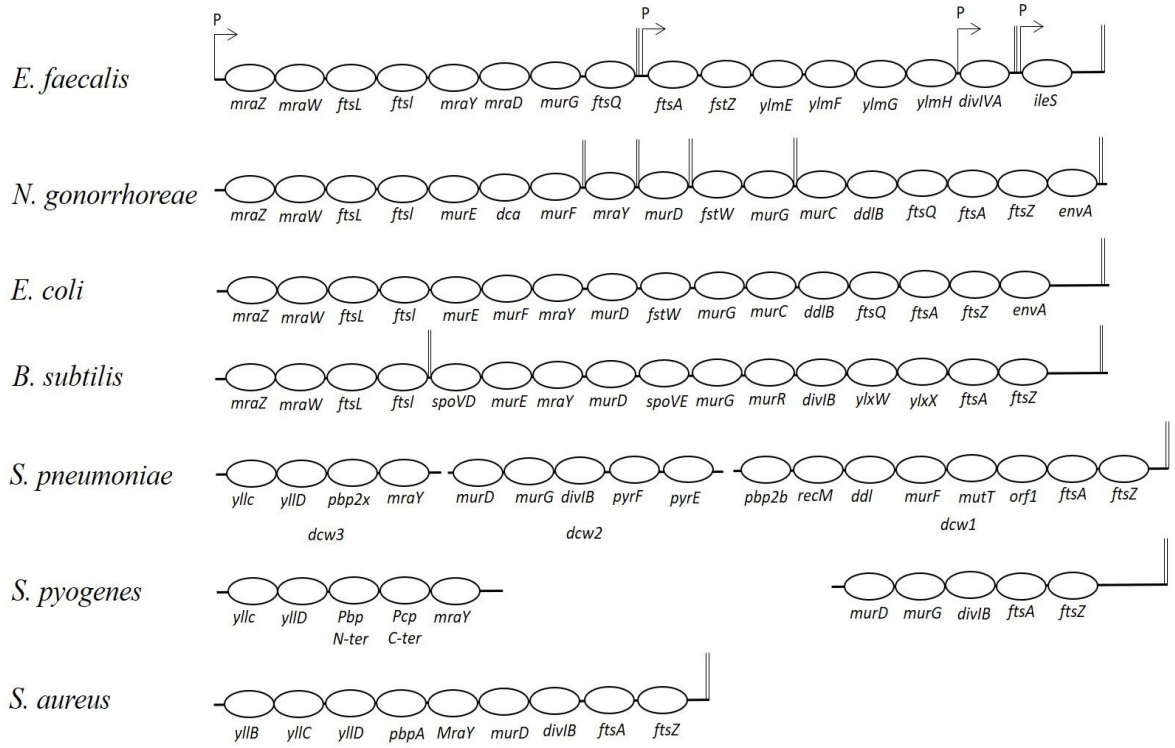

Figure 1.1. *dcw* clusters of *E. faecalis* (Ramirez et al., 2005), *N. gonorrhoeae* (Francis et al., 2000), *E. coli* (Ayala et al., 1994; Mingorance et al., 2004), *B. subtilis* (Mingorance et al., 2004; Real and Henriques, 2006), *S. pneumoniae* (Vicente et al., 2004), *S. pyogenes* (Massidda et al., 1998) and *S. aureus* (Massidda et al., 1998). Arrows indicate the direction of transcription of *dcw* cluster genes. Transcriptional terminators are indicated as two vertical lines. P- predicted promoter region.

1.7. Bacterial cell division

Bacterial cells are critically dependent on their ability to divide for growth, development, and reproduction. Cell division is a complex mechanism orchestrated by the coordinated interaction of a large number of proteins forming a macromolecular complex called the divisome. Divisome assembly happens in at least two steps (Gamba et al., 2009). First, in a spatially and temporally controlled manner, the Z ring is assembled on the cytoplasmic membrane between segregated chromosomes using membrane tethering proteins (Jensen et al., 2005). In the second step, to form the complete divisome, other essential and non-essential cell division proteins are added to the Z ring depending on the bacterial species (Levin et al., 1999; Gueiros-Filho and Losick, 2002; Hamoen et al., 2006; Haeusser et al., 2007; Singh et al., 2007; Tavares et al., 2008; Lenarcic et al., 2009; Król et al., 2012; Cleverley et al., 2014; Taguchi et al., 2019). The process of divisome assembly is followed by the third step that involves peptidoglycan (PG) remodelling so that the daughter cells can separate after septal cell wall synthesis has initiated (Domínguez-Escobar et al., 2011; Garner et al., 2011). This step is very tightly regulated so that cell wall degrading enzymes are only activated at the correct place and time (Uehara and Bernhardt, 2011).

B. subtilis has served as a model organism for studying and understanding the process of cell division in Gram-positive bacteria for decades (Pavlendová et al., 2007; Errington and Wu, 2017; Barák et al., 2019). *E. coli* has served the same role for Gram-negative bacteria (Lutkenhaus and Du, 2017). The basic elements of the cytokinetic machinery that comprises a core of essential components used by many bacteria, were compared in these two species. The intensive investigation of these model organisms resulted in the development of many genetic tools, techniques and resources specifically for the investigation.

1.7.1. Divisome assembly in *B. subtilis*

In *B. subtilis*, the divisome assembles in two distinct steps where the first step involves $FtsZ_{Bs}$-ring assembly along with the recruitment of "early" divisome proteins $FtsA_{Bs}$, $SepF_{Bs}$, $ZapA_{Bs}$ and $EzrA_{Bs}$ in a sequential manner (Wang and Lutkenhaus, 1993; Gueiros-Filho and Losick, 2002; Anderson et al., 2004; Jensen et al., 2005; Hamoen et al., 2006; Singh et al., 2007; Gamba et al., 2009). Cell division starts with the midcell assembly of a contractile ring by the central component of the divisome, $FtsZ_{Bs}$, a structural and biochemical homologue of the eukaryotic tubulin (Anderson et al., 2004; Jensen et al., 2005; Gamba et al., 2009). $FtsZ_{Bs}$

assembles into proto-filaments that self-interact and form a dynamic circumferential ring (i.e. Z-ring) which defines the site of cell division and recruits, directly or indirectly, multiple protein components of the divisome (Gamba et al., 2009). FtsZ assembles *in vitro* in a head to tail fashion to form single-stranded protofilaments, which can further assemble into bundles, sheets or rings at the Z-ring (Peters et al., 2007; Gamba et al., 2009). This ring undergoes cycles of turnover/polymerization, regulated by the binding and hydrolysis of GTP (Bi and Lutkenhaus, 1991; Peters et al., 2007).

The Z-ring is tethered to the membrane by the recruitment of the "early" divisome proteins $FtsA_{Bs}$ or $SepF_{Bs}$ which use their amphipathic helices to bind to the cell membrane (Fig. 1.2.) (Jensen et al., 2005; Hamoen et al., 2006). $FtsA_{Bs}$ and $SepF_{Bs}$ specifically interact with the C-terminal domain of $FtsZ_{Bs}$ and forms high molecular weight (MW) dynamic complexes (Jensen et al., 2005; Ishikawa et al., 2006; Król et al., 2012). Sequentially, the two positive regulators i.e. $ZapA_{Bs}$ and $EzrA_{Bs}$ then interact with the Z-ring maintaining FtZ_{Bs} polymerization (Levin et al., 1999; Gueiros-Filho and Losick, 2002; Singh et al., 2007; Cleverley et al., 2014). $ZapA_{Bs}$ acts as a promoter of $FtsZ_{Bs}$ bundling by interacting directly with $FtsZ_{Bs}$ and encouraging both $FtsZ_{Bs}$ polymerization and lateral connection *in vitro*, producing both single and bundled filaments (Gueiros-Filho and Losick, 2002; Low et al., 2004). $EzrA_{Bs}$ anchors the membrane protofilaments and stops protofilament bundle formation locally (Haeusser et al., 2007; Land et al., 2014).

The complex comprised of $FtsZ_{Bs}$-$FtsA_{Bs}$-$SepF_{Bs}$-$ZapA_{Bs}$-$EzrA_{Bs}$ then recruits the 'late' cell division proteins i.e. $FtsW_{Bs}$, $PBP1_{Bs}$, $PBP2B_{Bs}$, $DivIB_{Bs}$, $DivIC_{Bs}$ and $FtsL_{Bs}$, $DivIVA_{Bs}$ and $GpsB_{Bs}$ (Fig. 1.2.) (Perry and Edwards, 2004; Tavares et al., 2008; Gamba et al., 2009; Lenarcic et al., 2009; den Blaauwen, 2018; Taguchi et al., 2019). These proteins do not directly interact with $FtsZ_{Bs}$ and are primarily proteins with major extracellular domains or integral membrane proteins (Ishikawa et al., 2006) which includes proteins for septal cell wall biosynthesis ($FtsW_{Bs}$, $PBP1_{Bs}$, $PBP2B_{Bs}$) and scaffolding proteins ($DivIB_{Bs}$, $DivIC_{Bs}$ and $FtsL_{Bs}$) (Ishikawa et al., 2006; Taguchi et al., 2019). $DivIVA_{Bs}$ and $GpsB_{Bs}$ are recruited in the later stages of division in the presence of early and late divisive components (Halbedel and Lewis, 2019). Various other regulatory proteins, including $MinJ_{Bs}$, $MinD_{Bs}$ and $MinC_{Bs}$ arrive at about the same time or slightly later, depending on the initiation of the membrane or PG ingrowth (Gamba et al., 2009).

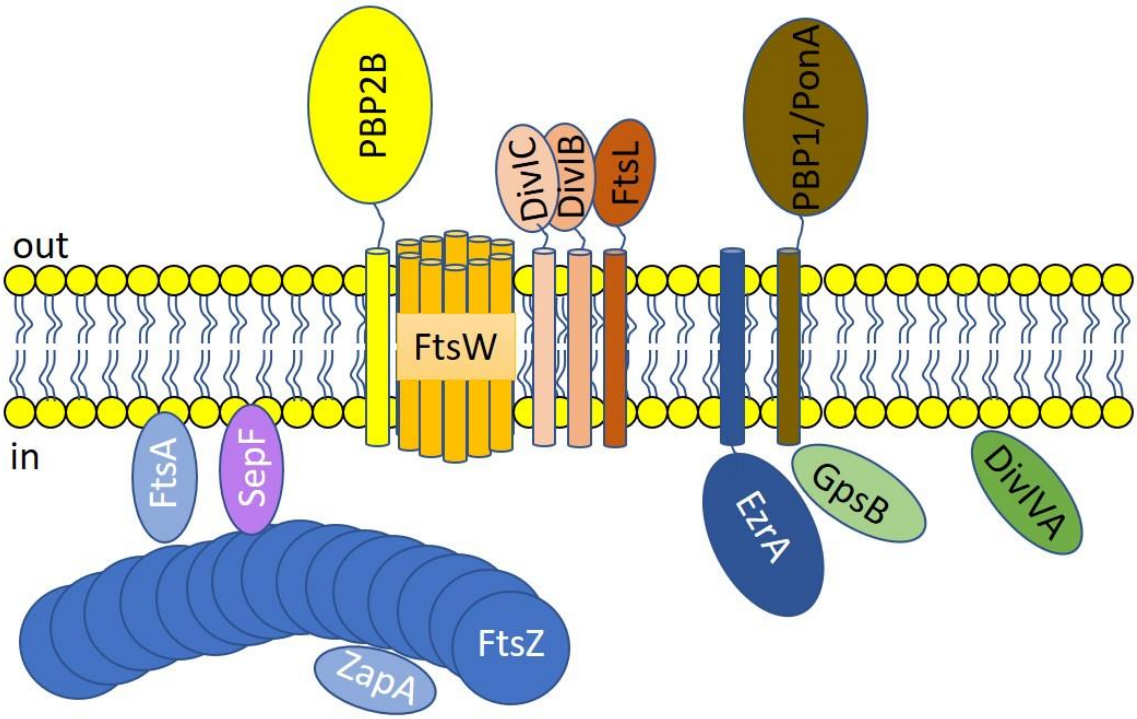

Figure. 1.2. The two-step assembly of the divisome in *B. subtilis*. Adapted from (Halbedel and Lewis, 2019). Early cell division proteins are indicated in white font whereas late proteins are in black font.

1.7.2. *S. pneumoniae* divisome assembly

Streptococcus pneumoniae is an important ovococcal opportunistic Gram-positive pathogen that causes a variety of infections including middle ear infections, sinusitis, pneumonia, bacteraemia and meningitis (Weiser et al., 2018). *S. pneumoniae* contains the majority of the cell division proteins present in *B. subtilis* and other Gram-positive bacteria (Errington and Wu, 2017). *S. pneumoniae* contains genes encoding homologues of $YlmF_{Sp}$/$SepF_{Sp}$ and $DivIVA_{Sp}$ that are involved in chromosome segregation, cell morphology and cell division in various species (Massidda et al., 1998; Fadda et al., 2003, 2007; Flärdh, 2003; Ramos et al., 2003; Miyagishima et al., 2005; Ramirez-Arcos, 2005; Hamoen et al., 2006; Ishikawa et al., 2006; Kabeya et al., 2010). Two interdependently operating cell wall synthesis machineries are utilized by *S. pneumoniae* for peripheral growth and cell division (Lleo et al., 1990; Massidda et al., 1998; Morlot et al., 2003, 2004; Noirclerc-Savoye et al., 2005; Le Gouëllec et al., 2008; Zapun et al., 2008). Although an exact order of recruitment of cell division proteins to mid cell has not yet been established, fluorescence studies show that like *B. subtilis*, divisome formation in pneumococci occurs in at least two steps (Fadda et al., 2003; Morlot et al., 2004).

The cell division initiator proteins $FtsZ_{Sp}$ and $FtsA_{Sp}$ localize to mid-cell first (Morlot et al., 2003; Lara et al., 2005) followed by the septal markers $DivIB_{Sp}$ ($FtsQ_{Sp}$), $DivIC_{Sp}$ ($FtsB_{Sp}$), $FtsL_{Sp}$, $FtsW_{Sp}$, $PBP2X_{Sp}$ ($FtsI_{Sp}$), $PBP1a_{Sp}$ (Morlot et al., 2003, 2004b; Noirclerc-Savoye et al., 2005), and the cell division protein $DivIVA_{Sp}$ (Fadda et al., 2007; Beilharz et al., 2012). The exact function of these essential Fts proteins during the initial steps of cell division is not known (Mura et al., 2017). Z-ring formation requires about half of the cell cycle before septation can occur (Fadda et al., 2007) where $FtsZ_{Sp}$ and $FtsA_{Sp}$ self-interact and with each other (Lara et al., 2005; Maggi et al., 2008) and with other cell division proteins, including $ZapA_{Sp}$ and $EzrA_{Sp}$ (Song et al.; Thanassi et al., 2002). $SepF_{Sp}$, a crucial protein required for Z-ring stability in *B. subtilis* (Hamoen et al., 2006; Ishikawa et al., 2006), results in severe division defects when inactivated in *S. pneumoniae* (Massidda et al., 1998; Fadda et al., 2003). Maggi et al. (2008) used a bacterial two-hybrid system to study the interaction between various divisome proteins. They found that pneumcoccal $FtsK_{Sp}$ interacts with itself, $FtsZ_{Sp}$, $ZapA_{Sp}$, $FtsQ_{Sp}$ and $FtsL_{Sp}$ (Maggi et al., 2008). Other cell division proteins, $FtsQ_{Sp}$ ($DivIB_{Sp}$), $FtsB_{Sp}$ ($DivIC_{Sp}$) and $FtsL_{Sp}$ (Buddelmeijer and Beckwith, 2004), form a trimeric complex by interacting with each other before this complex is incorporated into the *S. pneumoniae*

divisome (Fig. 1.3.) (Noirclerc-Savoye et al., 2005; Masson et al., 2009). *S. pneumoniae* FtsW, late cell division protein, interacts with $FtsQ_{Sp}$ ($DivIB_{Sp}$) and $FtsL_{Sp}$ (Morlot et al., 2004; Maggi et al., 2008).

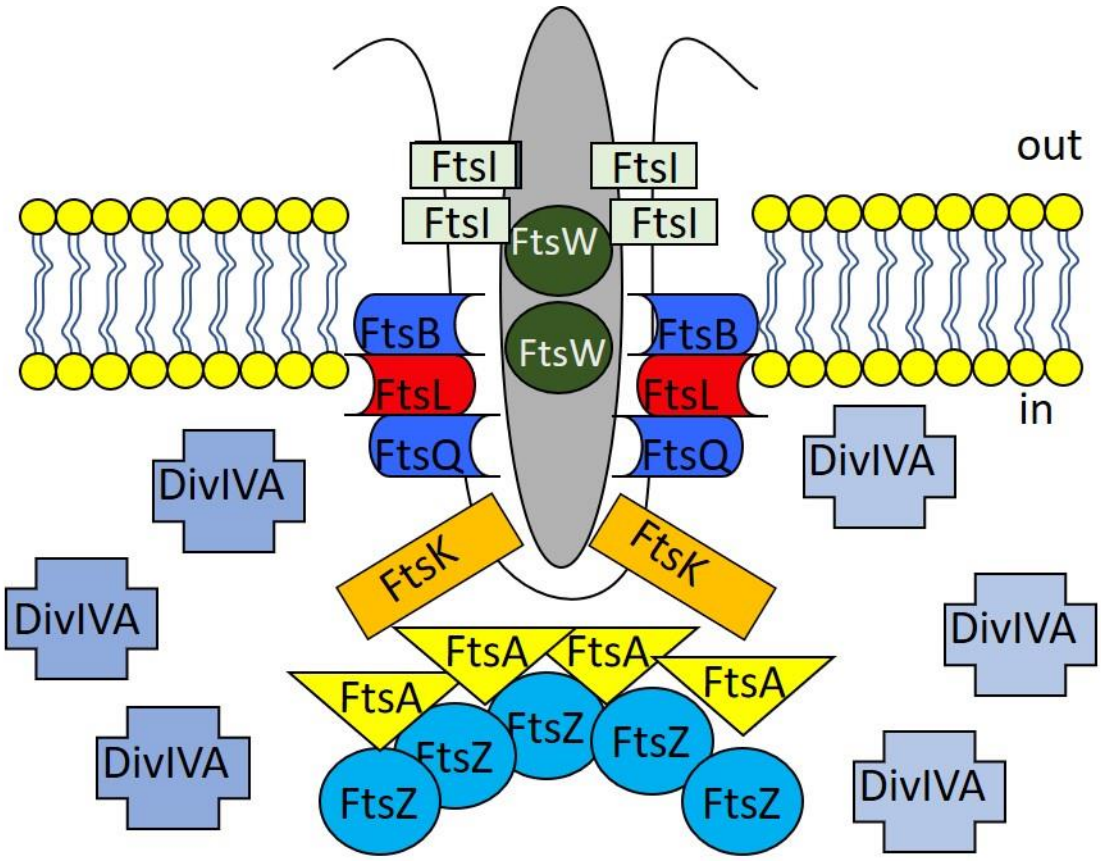

Figure 1.3. Proposed assembly of cell division proteins in *S. pneumoniae* divisome. Derived from the data developed by Fadda et al. (2007) using the bacterial two-hybrid assay.

1.8. DivIVA- An important Gram-positive cell division protein

DivIVA is a highly conserved, "late" cell division protein that is crucial for septum determination. Homologues of *B. subtilis* DivIVA are present in most Gram-positive bacteria, especially in bacterial subgroups such as actinobacteria and the firmicutes interacting with different partners and performing a variety of functions (Fadda et al., 2003; Kang et al., 2008; Rigden et al., 2008; Donovan et al., 2012; Massidda et al., 2013; Kaval et al., 2014; Bottomley et al., 2017; Ni et al., 2018; Halbedel and Lewis, 2019). DivIVA homologues have also been reported to be present in extremophiles such as *Deinococcus, Synergistaceae, Nitrospira,* and *Deltaproteobacteria* species, and few of the Chlorobi/Fibrobacter/Bacteroidetes group (Halbedel and Lewis, 2019). Lluch-Senar et al., 2010 reported uncharacterized DivIVA homologues from *Mycoplasma* species (Lluch-Senar et al., 2010). Although most of the *divIVA* genes from firmicutes are non-essential (Cha and Stewart, 1997; Fadda et al., 2003; Pinho and Errington, 2004; Claessen et al., 2008; Halbedel et al., 2012; Fleurie et al., 2014; Rismondo et al., 2016; Bottomley et al., 2017), exceptions exist (Ramirez-Arcos, 2005). The *divIVA* homologue in Actinobacteria, also called *wag31* in mycobacteria, is essential for cell viability and growth (Kang et al., 2008). There are no DivIVA homologues in humans, making DivIVA an excellent target for novel antimicrobials (Halbedel and Lewis, 2019).

1.8.1. DivIVA from *B. subtilis*

$DivIVA_{Bs}$ is a crucial protein in *B. subtilis* which is involved in the differentiation of the cell poles (Edwards and Errington, 1997). $DivIVA_{Bs}$ localizes at the division site and cell poles upon divisome assembly by associating with the Min proteins (Edwards and Errington, 1997). Although $divIVA_{Bs}$ is an important gene of *B. subtilis,* it is not located in the *dcw* cluster (Mingorance et al., 2004; Real and Henriques, 2006). $DivIVA_{Bs}$ is a small cytoplasmic protein that is homologous to eukaryotic cytoskeletal protein, myosin, a protein involved in cytokinesis (Edwards et al., 2000; Oliva et al., 2010). The N-terminus of $DivIVA_{Bs}$ is a highly conserved domain connected to the α-helical coiled-coil central and C-terminus region with a linker (Edwards et al., 2000; Oliva et al., 2010). $DivIVA_{Bs}$ self-interacts and oligomerizes using its coiled-coil region and utilizes its N-terminal region for interaction with lipid membranes (Muchová et al., 2002; Stahlberg et al., 2004; Rigden et al., 2008; Lenarcic et al., 2009; Rismondo et al., 2016). The interaction of $DivIVA_{Bs}$ with membrane uses a hairpin structure with conserved exposed basic and hydrophobic residues in the N-terminal protein domain (Oliva et al., 2010). $DivIVA_{Bs}$ oligomers have a high affinity for the negative curvature of the

membrane, which occurs in the invaginating division septa in dividing cells (Lenarcic et al., 2009; Ramamurthi and Losick, 2009; Eswaramoorthy et al., 2014). Once the curvature has been generated, $DivIVA_{Bs}$ localizes to each side of the growing septum preventing the contraction of the divisome and division at polar sites in the dividing cell (Eswaramoorthy et al., 2011). In non-dividing *B. subtilis* cells, $DivIVA_{Bs}$-GFP concentrated at the hemispheric cell poles (Eswaramoorthy et al., 2011). However, in dividing cells, $DivIVA_{Bs}$ remodelling took place and a portion of the $DivIVA_{Bs}$ molecules remained at the pole, while some protein migrated to the new division site (Bach et al., 2014).

1.8.2. DivIVA interacting partners in *B. subtilis*

B. subtilis DivIVA interacts with at least seven different interacting partners (Fig. 1.4.) (Perry and Edwards, 2006; Bramkamp et al., 2008; Patrick and Kearns, 2008; Lenarcic et al., 2009; Briley et al., 2011; dos Santos et al., 2012; Halbedel et al., 2014; Schumacher, 2017; Halbedel and Lewis, 2019) utilizing different interacting sites (Halbedel and Lewis, 2019). Such a variety of interacting partners confer a variety of functions to $DivIVA_{Bs}$ in cellular processes that includes chromosome segregation (Perry and Edwards, 2006), cell division (Bramkamp et al., 2008; Patrick and Kearns, 2008), competence development (Briley et al., 2011; dos Santos et al., 2012), sporulation (Lenarcic et al., 2009) and protein secretion (SecA) (Halbedel et al., 2014).

$DivIVA_{Bs}$ acts as a "topological specificity" determinant for MinJ, RacA, and ComN for their recruitment to the septum and the cell poles (Ben-Yehuda et al., 2003; Bramkamp et al., 2008; dos Santos et al., 2012). With $MinJ_{Bs}$, a transmembrane protein, which acts as a molecular bridge between $DivIVA_{Bs}$ and the FtsZ-inhibiting $MinCD_{Bs}$ complex, $DivIVA_{Bs}$ interacts to recruit itself and $MinCD_{Bs}$ complex at the division site and the cell poles for correct cell division (Bramkamp et al., 2008; Patrick and Kearns, 2008). $DivIVA_{Bs}$ is necessary for sporulation where it associates with the DNA binding protein $RacA_{Bs}$, acting as a bridge between the *oriC* region and the cell poles, anchoring chromosomes at the poles (Ben-Yehuda et al., 2003). Subsequently, $DivIVA_{Bs}$ and $RacA_{Bs}$ attract Spo0J and Soj to the chromosome, participating in chromosome segregation (Ben-Yehuda et al., 2003; Wu and Errington, 2003). The *spo0J-soj* system determines the orientation and positioning of the chromosome early in sporulation (Wu and Errington, 2003). The correct localization of $DivIVA_{Bs}$ ensures the $RacA_{Bs}$ mediated securing of the chromosome to the distal side of the prespore during sporulation (Errington and Wu, 2017). $ComN_{Bs}$, a small protein from *B. subtilis* has been

described as a polarly localized, posttranscriptional regulator of competence gene expression (Ogura and Tanaka, 2009). Such a unique localization by $ComN_{Bs}$ is achieved by a direct interaction with $DivIVA_{Bs}$ which leads to the accumulation of $comE_{Bs}$ (ComN's target mRNA) to septal and polar sites (dos Santos et al., 2012). Although $ComN_{Bs}$ is non-essential for the polar assembly of the core competency DNA uptake machinery, its delocalization resulted in a significant reduction in the efficiency of competencies (dos Santos et al., 2012). $DivIVA_{Bs}$ also binds to Maf_{Bs}, a protein involved in cell division arrest in competent cells of *B. subtilis* (Briley et al., 2011). This highly conserved protein is synthesized in competent cells under the direct control of $ComK_{Bs}$, a transcriptional factor (Briley et al., 2011). A point mutation in maf_{Bs} inhibits its interaction with $DivIVA_{Bs}$ and also cell division (Briley et al., 2011). The interaction between $DivIVA_{Bs}$ and $SecA_{Bs}$, the secretion ATPase, is important for correct localization of $DivIVA_{Bs}$ during cell division (Halbedel et al., 2014). Mutation in $SecA_{Bs}$ leads to inhibition of sporulation and $DivIVA_{Bs}$ delocalization (Halbedel et al., 2014).

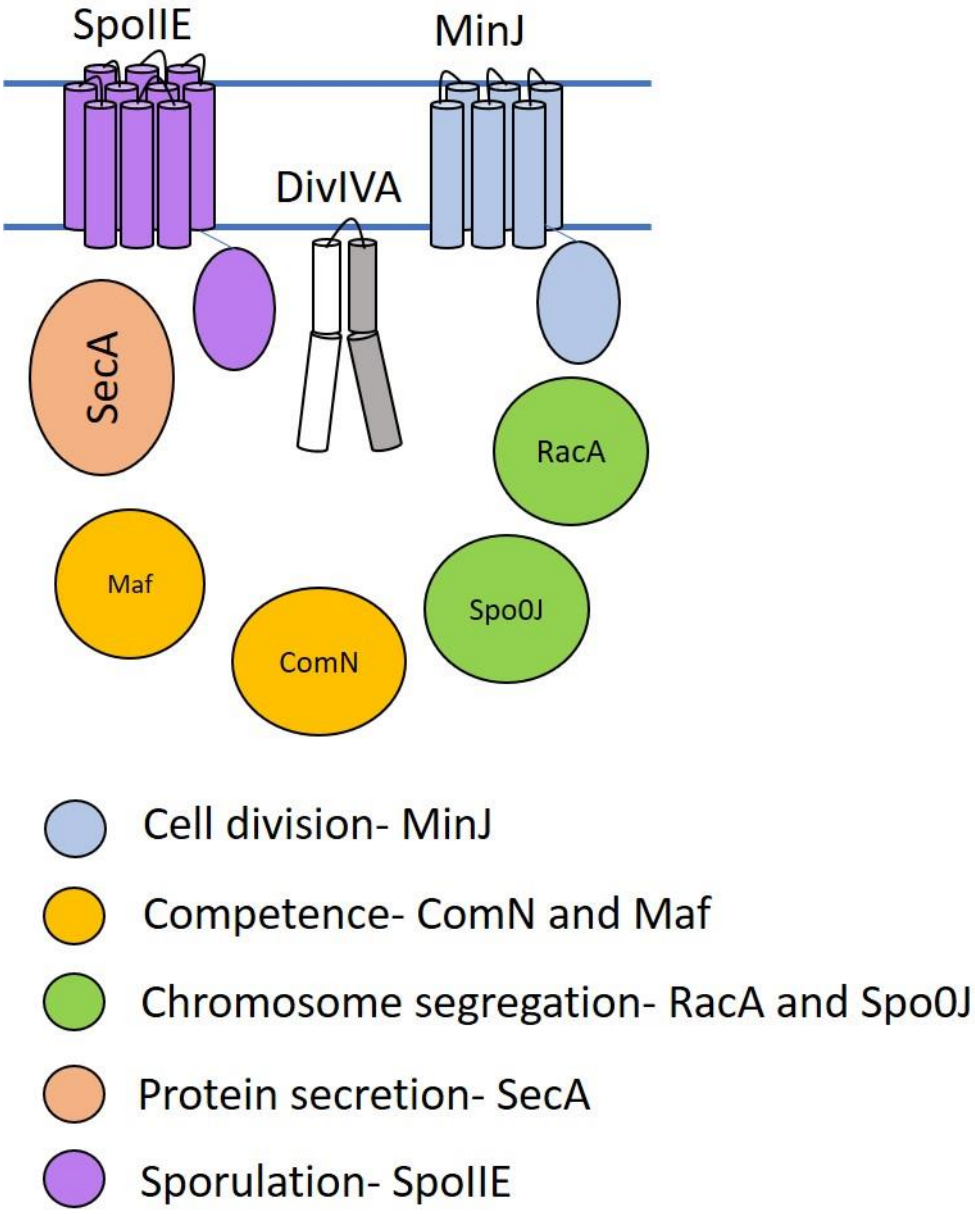

Figure 1.4. DivIVA interacting partners in *Bacillus subtilis* (Halbedel et al., 2019).

1.8.3. DivIVA interacting partners in other bacteria

The range of DivIVA interacting partners changes from one Gram-positive bacterial species to another (Table 1.1). For example, in *Listeria monocytogenes*, another Gram-positive human pathogen, $DivIVA_{Lm}$ performs three functions that include precise positioning of the septum at midcell, assistance in the secretion of autolysins, and enabling swarming motility of *L. monocytogenes* (Kaval et al., 2014); each of these functions are governed by different domains of DivIVA (Kaval et al., 2017). In *L. monocytogenes*, MinC and MinD localizes at the cell poles in a $DivIVA_{Lm}$-dependent fashion unlike MinJ (Kaval et al., 2014). Other than these interacting partners, $DivIVA_{Lm}$ also interacts with SecA2, the accessory secretion ATPase, to assist the secretion of two autolysins p60 (CwhA) and MurA (NamA) (Lenz and Portnoy, 2002) through the SecA2-dependent secretion pathway (Kaval et al., 2014). *divIVA* mutants had impaired autolysin secretion levels (Kaval et al., 2014) which lead to cell chaining and defective division site selection (Lenz and Portnoy, 2002; Machata et al., 2005).

The *S. pneumoniae* homologue of DivIVA is crucial for normal growth by ensuring proper septum placement, and chromosome segregation (Fadda et al., 2003; Nováková et al., 2010). $DivIVA_{Sp}$ interacts with several divisome proteins from the *dcw* cluster including $FtsZ_{Sp}$, $FtsA_{Sp}$, $ZapA_{Sp}$, $FtsK_{Sp}$, $FtsI_{Sp}$, $FtsB_{Sp}$, $FtsQ_{Sp}$ and $FtsW_{Sp}$ (Fadda et al., 2007). A point mutation at the N-terminal coiled-coil of $DivIVA_{Sp}$ (A78T) significantly reduced DivIVA interaction with the "late" divisome proteins $FtsL_{Sp}$, $FtsQ_{Sp}$, $FtsB_{Sp}$ and $FtsW_{Sp}$ (Fadda et al., 2007; Vicente and García-Ovalle, 2007). Other than these cell division proteins, $DivIVA_{Sp}$ also interacted with ParB (Fadda et al., 2007) through ParA that helps in chromosome segregation. In *Streptococcus suis* serotype 2, an important swine pathogen, Ser/Thr kinases (STK) encoded by *stk*, directly phosphorylates $DivIVA_{Sp}$ (Thr-199) and affects cell growth and division (Nováková et al., 2010a; Ni et al., 2018). $DivIVA_{Ss}$ is one of the target substrates for STK, which when mutated exhibits abnormal growth and asymmetrical division, including lower viability, enlarged cell mass (Nováková et al., 2010a; Ni et al., 2018). STK regulates the cell growth and virulence of *S. suis* by phosphorylating targeted substrates that are involved in different biological processes (Ni et al., 2018). Similarly in *S. pneumoniae,* StkP also phosphorylates $DivIVA_{Sp}$ affecting cell division and morphogenesis (Giefing et al., 2008; Nováková et al., 2010). DivIVA of *Corynebacterium glutamicum* and *Streptomyces coelicolor* interacts with ParB/Spo0J (Donovan et al., 2012, 2013; Sieger et al., 2013), which binds to chromosomal origins of replication via ParA for chromosomal segregation (Mierzejewska and Jagura-Burdzy, 2012). Additionally in *Streptomyces coelicolor*, another rod-shaped Gram-positive

bacterium, DivIVA is involved in apical growth and control of cell polarity by establishing sites for hyphal branching and for cell wall growth (Flärdh, 2010).

S. aureus also encodes a homologue of $DivIVA_{Sa}$, that associates with various divisome proteins to ensure cell division and chromosome segregation (Bottomley et al., 2017). A highly conserved molecular chaperone, $DnaK_{Sa}$, interacts with and stabilizes $DivIVA_{Sa}$ in *S. aureus* (Bukau and Walker, 1989; Bottomley et al., 2017). Bottomley et al., 2017 also reported an indirect function of $DivIVA_{Sa}$ in chromosomal segregation by its interaction with the chromosome segregation protein, SMC, where these two act collectively to maintain accurate chromosome segregation (Bottomley et al., 2017).

In the rod-shaped bacteria, *Mycobacterium smegmatis* and *M. tuberculosis*, DivIVA, also called as Wag31, controls cell growth, morphology and cell wall synthesis (Nguyen et al., 2007; Kang et al., 2008; Meniche et al., 2014). *M. tuberculosis* Wag31 interacts with the penicillin-binding protein, PBP3 (Mukherjee et al., 2009) and ParB (Donovan et al., 2012), and *wag31* in *M. tuberculosis* is essential for cell viability (Donovan et al., 2012). $Wag31_{Ms}$ interacts with ParA, a member of the mycobacterial chromosome segregation machinery for cell separation (Donovan et al., 2012; Ginda et al., 2013).

In conclusion, DivIVA plays a pivotal function in Gram-positive bacteria by interacting with a variety of interacting partners in different genera. A variety of interacting partners confer a variety of functions to DivIVA in cellular processes ranging from the synthesis of the cell wall (Nguyen et al., 2007; Kang et al., 2008), cell growth (Flärdh, 2010), chromosome segregation (Perry and Edwards, 2006; Fadda et al., 2007; Donovan et al., 2012; Bottomley et al., 2017), cell division (Bramkamp et al., 2008; Giefing et al., 2008; Patrick and Kearns, 2008; Mukherjee et al., 2009; Nováková et al., 2010; Ni et al., 2018), competence development (Briley et al., 2011; dos Santos et al., 2012), sporulation (Perry and Edwards, 2006; Lenarcic et al., 2009) and protein secretion (Nováková et al., 2010; Halbedel et al., 2012, 2014; Kaval et al., 2014; Ni et al., 2018).

Table 1.1. DivIVA interacting partners from different Gram-positive bacteria.

DivIVA homologue from:	Interacting partners
Bacillus subtilis	$MinJ_{Bs}$ (Bramkamp et al., 2008; Patrick and Kearns, 2008) $RacA_{Bs}$ (Ben-Yehuda et al., 2003) $ComN_{Bs}$ (dos Santos et al., 2012) Maf_{Bs} (Briley et al., 2011) $SecA_{Bs}$ (Halbedel et al., 2014) $Spo0J_{Bs}$ (Perry and Edwards, 2006) $SpoIIE_{Bs}$ (Eswaramoorthy et al., 2014)
Streptococcus pneumoniae	$FtsZ_{Sp}$, $FtsA_{Sp}$, $ZapA_{Sp}$, $FtsK_{Sp}$ and $FtsI_{Sp}$, $FtsB_{Sp}$, $FtsQ_{Sp}$ and $FtsW_{Sp}$ (Fadda et al., 2007) STK_{Sp} (Ser/Thr kinases) (Giefing et al., 2008)
Streptococcus suis	STK_{Ss} (Ser/Thr kinases) (Nováková et al., 2010)
Corynebacterium glutamicum	$ParB_{Cg}$ (Donovan et al., 2013) $RodA_{Cg}$ (Sieger et al., 2013)
Listeria monocytogenes	MinCD (Kaval et al., 2014) SecA2 (Kaval et al., 2014)
Streptomyces coelicolor	$ParB_{Sc}$ (Donczew et al., 2016)
S. aureus	$DnaK_{Sa}$, $FtsZS_{Sa}$, $FtsA_{Sa}$, $EzrA_{Sa}$, $DivIC_{Sa}$, $DivIB_{Sa}$, $PBP1_{Sa}$ and $PBP2_{Sa}$ (Bottomley et al., 2017) Chromosome segregation protein (SMC) (Bottomley et al., 2017)
Mycobacterium smegmatis (Wag31)	ParA (Donovan et al., 2012; Ginda et al., 2013)
Mycobacterium tuberculosis (Wag31)	PBP3 (Mukherjee et al., 2009) ParB (Donovan et al., 2012)

1.9. Cell division interactome

While the gene arrangement in the *dcw* cluster varies in different bacteria species, key cell division proteins are relatively conserved (Pucci et al., 1997). For examples, proteins like FtsZ, FtsA, ZipA, FtsQ/DivIB, FtsL, FtsW, FtsB/DivIC, FtsI and FtsK are highly conserved in almost all cell-walled Eubacteria (Margolin, 2000; Harry et al., 2006). But additional proteins like Min proteins, ZipA, ZapA, EzrA, FtsN or SepF, may or may not be present depending on the bacterial species (Margolin, 2000). All these proteins interact with one another to form one large multicomponent complex spanning the cytoplasmic membrane. Using *in vivo* and *in vitro* biochemical techniques such as bacterial two-hybrid (B2H) assay, GST-pull down assay, Co-immunoprecipitation (Co-IP) and Surface Plasmon Resonance (SPR) cell division protein-protein interaction networks have been established for only four bacterial species i.e. *E. coli* (Di Lallo et al., 2003; Karimova et al., 2005), *N. gonorrhoeae* (Zou et al., 2017), *S. aureus* (Steele et al., 2011) and *S. pneumoniae* (Fadda et al., 2007; Maggi et al., 2008).

1.9.1. Cell division interactome in Gram-positive bacteria

Maggi et al. (2008) tested 11 streptococcal cell division proteins for interactions using a B2H assay and co-immunoprecipitation from *S. pneumoniae*. A total of 37 homo- and/or hetero-dimeric interactions were observed where each protein interacted with at least two or more interacting partners except for PBP1A which had only one interacting partner (Maggi et al., 2008). There were 7 unique interactions i.e. $FtsA_{Sp}$–$FtsK_{Sp}$, $FtsA_{Sp}$–$FtsL_{Sp}$, $FtsZ_{Sp}$–$FtsW_{Sp}$, $FtsZ_{Sp}$–$FtsQ_{Sp}$/$DivIB_{Sp}$, $FtsZ_{Sp}$–$FtsL_{Sp}$, $FtsK_{Sp}$–$FtsW_{Sp}$, $FtsL_{Sp}$–$FtsI_{Sp}$/$PBP2X_{Sp}$, when compared with the *E. coli* interactome (Maggi et al., 2008). Using co-immunoprecipitation, seventeen confirmed interactions (i.e. $FtsZ_{Sp}$ with $FtsA_{Sp}$, $FtsK_{Sp}$, $FtsQ_{Sp}$, $FtsB_{Sp}$, $FtsL_{Sp}$, and $FtsW_{Sp}$; $FtsA_{Sp}$ with $FtsK_{Sp}$, $FtsL_{Sp}$, and $FtsL_{Sp}$; $FtsK_{Sp}$ with $FtsQ_{Sp}$, $FtsI_{Sp}$, and $FtsW_{Sp}$; $FtsQ_{Sp}$ with $FtsL_{Sp}$, and $FtsW_{Sp}$; $FtsB_{Sp}$-$FtsW_{Sp}$; and $FtsL_{Sp}$ with $FtsI_{Sp}$, and $FtsW_{Sp}$) were observed among nine cell division proteins that included $FtsZ_{Sp}$, $FtsA_{Sp}$, $FtsK_{Sp}$, $DivlB_{Sp}$, $DivlC_{Sp}$, $FtsL_{Sp}$, $FtsW_{Sp}$, and $PBP2x_{Sp}$ (Maggi et al., 2008).

In *S. aureus*, the potential interactions between thirteen divisome proteins (i.e. $FtsZ_{Sa}$, $FtsA_{Sa}$, $EzrA_{Sa}$, $GpsB_{Sa}$, $SepF_{Sa}$, $Pbp1_{Sa}$, $Pbp2_{Sa}$, $Pbp3_{Sa}$, $DivIB_{Sa}$, $DivIC_{Sa}$, $FtsL_{Sa}$, $FtsW_{Sa}$ and $RodA_{Sa}$) were mapped using a B2H assay by Steele et al. (2011). Around 49 homo-and/or hetero-dimeric protein interactions were identified and almost all proteins were found to interact with multiple interacting partners except for $SepF_{Sa}$ and $GpsB_{Sa}$ which interacted with

only $EzrA_{Sa}$ (Steele et al., 2011). $SepF_{Sa}$ interaction with $FtsZ_{Sa}$ has been well-studied in *B. subtilis* (Hamoen et al., 2006) but was not observed in *S. aureus* (Steele et al., 2011). When compared with the interactome of *S. pneumoniae*, following interactions were observed to be conserved: $FtsA_{Sa}$ with $FtsZ_{Sa}$, all division-specific PBPs, $FtsW_{Sa}$, $DivIC_{Sa}$ and $FtsL_{Sa}$; $FtsW_{Sa}$ with $FtsL_{Sa}$ and all division-specific PBPs; $DivIC_{Sa}$, $DivIB_{Sa}$ and $FtsL_{Sa}$ with all division-specific PBPs; and $FtsL_{Sa}$ with $DivIC_{Sa}$. $EzrA_{Sa}$ interacted with all thirteen cell division proteins (Fig. 1.5.) (Steele et al., 2011).

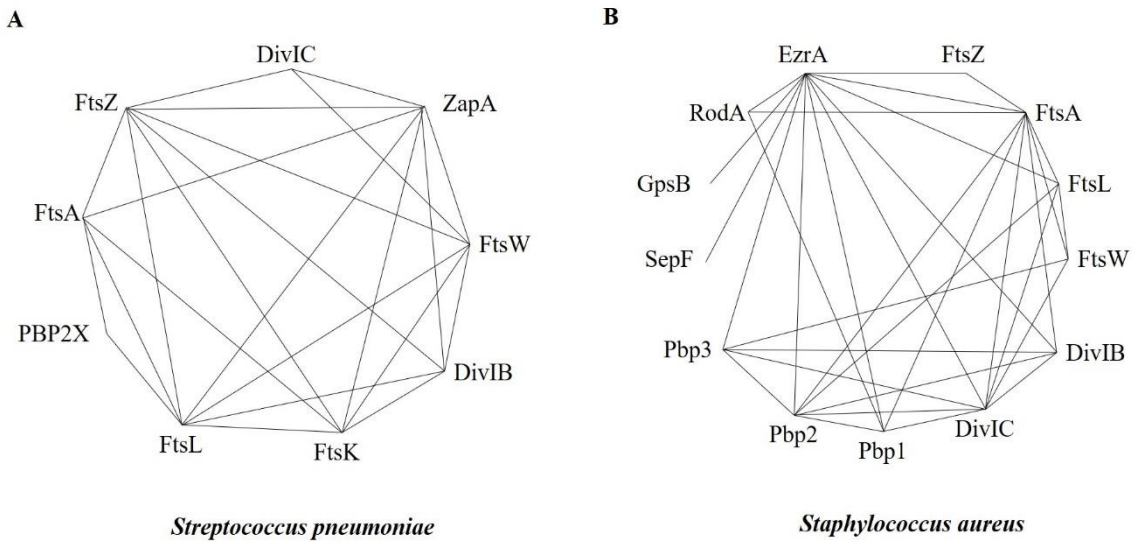

Figure 1.5. Characterized cell division interactomes from A) *S. pneumoniae* (Maggi et al., 2008), and B) *S. aureus* (Steele et al., 2011).

1.9.2. Cell division interactome in Gram-negative bacteria

Di Lallo et al. (2003) were first to use B2H assay to deduce the cell division interactome network in *E. coli* using 9 divisome proteins (i.e. $FtsZ_{Ec}$, $FtsA_{Ec}$, $ZipA_{Ec}$, $FtsK_{Ec}$, $FtsQ_{Ec}$, $FtsL_{Ec}$, $FtsI_{Ec}$, $FtsW_{Ec}$, and $FtsN_{Ec}$). Karimova et al. (2005) later expanded on this knowledge using their own version of a B2H assay i.e. the bacterial adenylate cyclase two-hybrid (BACTH) system, which relies on the reconstruction of a cyclic AMP (cAMP) signalling cascade upon interaction (Karimova et al., 1998). They reconfirmed all the interactions showed by Di Lallo et al. (2003) and included FtsB for testing possible interactions with other cell division proteins. Collectively in *E. coli*, 16 interactions (i.e. $FtsZ_{Ec}$ with $FtsA_{Ec}$, $ZipA_{Ec}$, $FtsK_{Ec}$; $FtsA_{Ec}$ with $FtsI_{Ec}$, $FtsN_{Ec}$, $FtsQ_{Ec}$; $FtsK_{Ec}$ with $FtsI_{Ec}$, $FtsQ_{Ec}$; $FtsQ_{Ec}$ with $FtsB_{Ec}$, $FtsL_{Ec}$, $FtsI_{Ec}$, $FtsN_{Ec}$, $FtsW_{Ec}$; $FtsB_{Ec}$ with $FtsL_{Ec}$, $FtsI_{Ec}$; $FtsL_{Ec}$ with $FtsI_{Ec}$, $FtsW_{Ec}$; $FtsI_{Ec}$ with $FtsW_{Ec}$, $FtsN_{Ec}$; and $FtsW_{Ec}$ with $FtsN_{Ec}$) between ten cell division proteins (i.e. including $FtsZ_{Ec}$, $FtsA_{Ec}$, $ZipA_{Ec}$, $FtsK_{Ec}$, $FtsQ_{Ec}$, $FtsB_{Ec}$, $FtsL_{Ec}$, $FtsI_{Ec}$, $FtsW_{Ec}$, and $FtsN_{Ec}$) were identified (Di Lallo et al., 2003; Karimova et al., 2005). Maggi et al. (2008) compared S. *pneumoniae* interactome with *E. coli* and observed 8 unique interactions that were absent in *E. coli* interactome which was a reflection of distinct cell division mechanisms in these two organisms (Di Lallo et al., 2003; Karimova et al., 2005; Maggi et al., 2008).

Zou et al. (2017) characterized cell division interactome from *Neisseria gonorrhoeae*, another Gram-negative coccal bacterium, using B2H and GST-pull down assays. Nine positive interactions (i.e. $FtsZ_{Ng}$-$FtsA_{Ng}$, $FtsZ_{Ng}$-$FtsK_{Ng}$, $FtsZ_{Ng}$-$FtsW_{Ng}$, $FtsA_{Ng}$-$FtsK_{Ng}$, $FtsA_{Ng}$-$FtsQ_{Ng}$, $FtsA_{Ng}$-$FtsW_{Ng}$, $FtsA_{Ng}$-$FtsN_{Ng}$, $FtsI_{Ng}$-$FtsW_{Ng}$, and $FtsK_{Ng}$-$FtsN_{Ng}$) were observed among 8 cell division proteins i.e. $FtsZ_{Ng}$, $FtsA_{Ng}$, $ZipA_{Ng}$, $FtsK_{Ng}$, $FtsQ_{Ng}$, $FtsI_{Ng}$, $FtsW_{Ng}$, and $FtsN_{Ng}$, that defined the cell division interactome. $FtsA_{Ng}$ did not homodimerize or interact with $FtsZ_{Ec}$ but interacted with $FtsN_{Ng}$ which is unlike *E. coli* interactome (Fig. 1.6) (Di Lallo et al., 2003; Karimova et al., 2005; Zou et al., 2017).

1.9.3. Conserved cell divisome interactions

When cell division interactomes from *E. coli* (Di Lallo et al., 2003; Karimova et al., 2005), *N. gonorrhoeae* (Zou et al., 2017), *S. aureus* (Steele et al., 2011) and *S. pneumoniae* (Fadda et al., 2007; Maggi et al., 2008) were compared, the interaction between FtsZ and FtsA was found to be conserved in all four interactomes. The interaction between FtsZ and FtsK was positive in *E. coli*, *N. gonorrhoeae*, and *S. pneumoniae* but *S. aureus* was not tested.

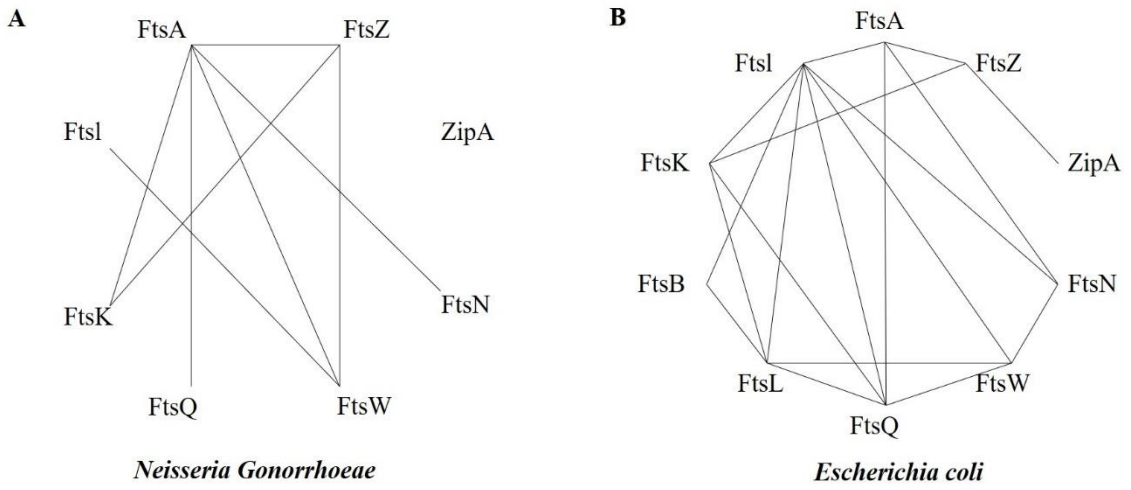

Figure 1.6. Characterized cell division interactomes from Gram-positive organisms: A) *Neisseria gonorrhoeae* (Zou et al., 2017); B) *E. coli* (Karimova et al., 2005; Di Lallo et al., 2003).

1.10. Cell division in *E. faecalis*

1.10.1. *E. faecalis* Division Cell Wall (*dcw)* cluster

Enterococcus faecalis dcw gene cluster was identified first by Pucci et al. (1997) and Massidda et al. (1998) reported its resemblance with *E. hirae.* Ramirez et al. (2005) extended the information on the *E. faecalis* dcw cluster and reported the presence of 16 genes organized in four operons (Fig. 1.1). The first operon contains promoter region located upstream of *mraZ$_{Ef}$* followed by *mraW$_{Ef}$, ftsL$_{Ef}$, ftsI$_{Ef}$, mraY$_{Ef}$, murG$_{Ef}$ and ftsQ$_{Ef}$*, followed by a terminator sequence located immediately downstream of *ftsQ$_{Ef}$* (Ramirez-Arcos, 2005). The second operon in the *dcw* cluster contains *ftsA$_{Ef}$, ftsZ$_{Ef}$, ylmE$_{Ef}$, ylmF$_{Ef}$, ylmG$_{Ef}$,* and *ylmH$_{Ef}$* with the promoter sequence located upstream of *ftsA$_{Ef}$* (Ramirez-Arcos, 2005). The third and fourth operons contain *divIVA$_{Ef}$* and *ileS$_{Ef}$* respectively (Ramirez-Arcos, 2005). All the genes within the enterococcal *dcw* cluster are transcribed in the same direction using four σ70 promoter sequence and three predicted ρ-independent transcriptional terminators (Ramirez-Arcos, 2005). Among all enterococcal *dcw* cluster genes, only *divIVA$_{Ef}$* has been studied so far (Ramirez-Arcos, 2005; Rigden et al., 2008). Ramirez et al. 2005 also postulated that *divIVA$_{Ef}$* might be co-transcribed with other upstream cell division protein encoding genes.

1.10.2. DivIVA from *E. faecalis*

Unlike the *dcw* clusters from other Gram-positive bacteria, such as *B. subtilis, S. pyogenes, S. pneumoniae* and *S. aureus, divIV$_{Ef}$,* is located within the *dcw* cluster of *E. faecalis* (Ramirez-Arcos, 2005). *E. faecalis divIV$_{Ef}$* encodes DivIVA$_{Ef}$ which comprises predominantly of coiled-coil domains, one at the N-terminus, one at the C-terminus, and two in the central region of the protein that is responsible for the self-interacting properties of DivIVA$_{Ef}$ (Rigden et al., 2008). Both, the N-terminal and central coiled-coil regions were indispensable for DivIVA$_{Ef}$ function (Rigden et al., 2008). An N-terminal point mutation in DivIVA$_{Ef}$ resulted in aberrant phenotypes, such as irregular shape, aggregation, and enlargement, indicating disruption of normal cell division (Rigden et al., 2008). DivIVA$_{Ef}$ is essential for cell viability and is involved in cell division and chromosome segregation (Ramirez-Arcos, 2005), similar to its counterpart in *S. pneumoniae* (Fadda et al., 2003, 2007). *divIVA* inhibits proper cell division when absent (Ramirez-Arcos, 2005). Its absence leads to abnormal cell clusters possessing rounded enlarged cells instead of the characteristic ovodiplococcal cells (Ramirez-Arcos, 2005). Overexpression of DivIVA$_{Ef}$ in *E. coli* KJB24

resulted in enlarged cells with disrupted cell division (Ramirez-Arcos, 2005). *E. faecalis* DivIVA failed to complement the cell division defects of either *S. pneumoniae* or *B. subtilis divIVA* mutants, reflecting the variety of DivIVA functions in different microorganisms and indicating that DivIVA could be playing a species-specific function (Ramirez-Arcos, 2005).

1.10.3. Discovery of a novel $DivIVA_{Ef}$ interacting partner

To identify novel $DivIVA_{Ef}$ interacting proteins in *E. faecalis*, a Y2H system was used to screen an *E. faecalis* genomic DNA library using $DivIVA_{Ef}$ as the bait protein. Fifteen positive clones were identified from ~$3x10^4$ transformed yeast colonies. Thirteen of the positive clones had inserts corresponding to full-length $divIVA_{Ef}$ and the remaining two positive clones contained a 400bp DNA fragment from an unknown ORF (unpublished data). Upon bioinformatic analysis, this 400bp DNA fragment was found to encode a peptide corresponding to the C-terminus of the hypothetical protein EF1025 (GenBank accession # NP_814759) in *E. faecalis.* This thesis builds in part upon the characterization of this novel protein.

1.11. Hypothesis and objectives

1.11.1. Background

The diverse functionality of DivIVA in Gram-positive organisms across species, suggests that DivIVA associates with different proteins in different bacterial species performing a variety of functions. These DivIVA-associating proteins are not a part of divisome and indirectly assist DivIVA in cell growth and division. Although DivIVA interacting partners have been reported from many bacterial species, there is a lack of information regarding DivIVA-associating proteins in *E. faecalis.* We have identified a novel $DivIVA_{Ef}$ interacting protein i.e. EF1025, but its characteristics and the biological function is unknown.

The cell division interactome presents a network of assembly of divisome proteins. The cell division interactomes of only *E. coli, N. gonorrhoeae*, *S. aureus and S. pneumoniae* have been characterized (Di Lallo et al., 2003; Maggi et al., 2008; Steele et al., 2011; Zou et al., 2017). These interactomes show the existence of multiple unique interactions within the divisome proteins that might help in stabilizing the macromolecular complex, divisome (Maggi et al., 2008, 2008). The *dcw* cluster of *E. faecalis* contains homologues of divisome proteins FtsZ, FtsA, FtsK, FtsQ (DivIB), FtsL, FtsI and probably FtsB (DivIC), EzrB and ZapA. The cell division interactome of *E. faecalis*, by contrast, is not presently known.

1.11.2. Hypothesis

The hypothesize of this thesis is that EF1025 is a cell division protein in *E. faecalis*, which interacts with $DivIVA_{Ef}$ and affects cell division. I also hypothesize that homologues of EF1025 may interact with DivIVA from other species. Like other functionally characterized DivIVA interacting partners, EF1025 might not also be a part of divisome and will be assisting during the process of cell division.

1.11.3. Objectives

1. To biochemically, biologically, and functionally characterize EF1025 from *E. faecalis* by:

    a. Bioinformatically characterizing EF1025, its homologues and domains.

b. Researching the interaction of EF1025 and domains present in EF1025 with $DivIVA_{Ef}$ using GST pull-down assay and re-analyze previous B2H and Co-immunoprecipitation assay results for this interaction.

c. Studying the oligomerization properties of EF1025 using size exclusion chromatography (SEC), Dynamic light scattering (DLS) and SEC- multi-angle light scattering (SEC-MALS) techniques.

c. Creating an *E. faecalis EF1025* deletion mutant and *EF1025* overexpressing strain.

d. Ascertaining the morphological changes in *E. faecalis* when *EF1025* is deleted or overexpressed by electron microscopy and atomic force microscopy.

2. To investigate CcpN, an EF1025 homologue from *B. subtilis* by:

a. Ascertaining whether there is an interaction between CcpN and $DivIVA_{Bs}$ by B2H and GST pull-down assays.

b. Ascertaining the heterologous interaction between EF1025 and $DivIVA_{Bs}$ by GST pull-down assay.

c. Ascertaining the morphological changes by electron microscopy and atomic force microscopy in *B. subtilis* when *ccpN* is insertionally inactivated.

3. To establish a preliminary cell division interactome of *E. faecalis* by:

a. Testing *E. faecalis* cell division protein-protein interactions between $FtsZ_{Ef}$, $FtsA_{Ef}$, $FtsQ_{Ef}$, $FtsL_{Ef}$, $FtsI_{Ef}$, $FtsW_{Ef}$, $DivIVA_{Ef}$, and $FtsB_{Ef}$, using B2H assays and re-analyze previous B2H data using statistical methods.

b. Identifying whether EF1025 interacts with *E. faecalis* cell division proteins i.e. $FtsZ_{Ef}$, $FtsA_{Ef}$, $FtsQ_{Ef}$, $FtsL_{Ef}$, $FtsI_{Ef}$, $FtsW_{Ef}$, $DivIVA_{Ef}$, and $FtsB_{Ef}$, using B2H assays and re-analyze previous B2H data using statistical methods.

Chapter 2. EF1025, a hypothetical protein from *Enterococcus faecalis*, interacts with DivIVA and affects cell length and cell shape

Kusum Sharma[1, 2], Taranum Sultana[3], Mingmin Liao[1,2], Tanya E S Dahms[3]

and Jo-Anne R Dillon[1,2*]

Department of Microbiology and Immunology,[1] Vaccine and Infectious Disease Organization,[2] University of Saskatchewan, Saskatoon, SK, Canada.

Department of Chemistry and Biochemistry[3], University of Regina, Regina, SK, Canada.

Accepted in **Frontiers in Microbiology** on 15th Jan 2020.

Running title: A novel DivIVA interacting protein in *E. faecalis*.

Keywords: Gram-positive bacteria, *Enterococcus faecalis*, cell division, DivIVA, protein-protein interaction, *Bacillus subtilis*.

*Corresponding author:

Prof Jo-Anne R Dillon

j.dillon@usask.ca

Author contributions:

Kusum Sharma designed and completed the majority of the experiments, analyzed results and drafted the article. We are grateful to Monica Wang for performing Immunoflorescense microscopy experiment; Cherise Hedlin and Dr Mingmin Liao for performing Y2H and Co-IP experiments. Dr Taranum Sultana and Prof Tanya Dahms designed and analyzed AFM experiments and edited the manuscript. Dr Jo-Anne R Dillon directed the project and its implementation, analyzed data, edited manuscript drafts and approved the final submission in collaboration with all authors.

2.1. Abstract

DivIVA plays multifaceted roles in Gram-positive organisms through its association with various cell division and non-cell division proteins. We report a novel DivIVA interacting protein in *Enterococcus faecalis*, named EF1025 (encoded by *EF1025*), which is conserved in Gram-positive bacteria. The interaction of EF1025 with $DivIVA_{Ef}$ was confirmed by Bacterial Two-Hybrid, Glutathione S-Transferase pull-down, and co-immunoprecipitation assays. EF1025, which contains a DNA binding domain and two Cystathionine β-Synthase (CBS) domains, forms a decamer mediated by the two CBS domains. Viable cells were recovered after insertional inactivation or deletion of *EF1025* only through complementation of *EF1025 in trans*. These cells were longer than the average length of *E. faecalis* cells and had distorted shapes. Overexpression of *EF1025* also resulted in cell elongation. Immuno-staining revealed comparable localization patterns of EF1025 and $DivIVA_{Ef}$ in the later stages of division in *E. faecalis* cells. In summary, EF1025 is a novel DivIVA interacting protein influencing cell length and morphology in *E. faecalis*.

2.2. Introduction

A key protein in Gram-positive bacteria is DivIVA which is implicated in cell division and other functions (Cha and Stewart, 1997; Ben-Yehuda et al., 2003; Fadda et al., 2003; Pinho and Errington, 2004; Ramirez-Arcos, 2005; Briley et al., 2011; Halbedel and Lewis, 2019). DivIVA self-interacts, oligomerizes and associates with a functionally different array of proteins in different Gram-positive bacteria (Halbedel and Lewis, 2019). In *Bacillus subtilis* (Bs), $DivIVA_{Bs}$ functions as a mid-cell determinant by attracting the MinC/MinD protein complex to the cell poles, thereby preventing cell division at the polar region (Cha and Stewart, 1997; Edwards and Errington, 1997; Marston and Errington, 1999; Edwards et al., 2000; Karoui and Errington, 2001; Harry and Lewis, 2003). $DivIVA_{Bs}$ also associates with the DNA binding protein RacA, which acts as a bridge between the *oriC* region and the cell poles, anchoring the chromosome at the poles during sporulation (Ben-Yehuda et al., 2003). In addition, $DivIVA_{Bs}$ interacts with Spo0J, participating in chromosome segregation during sporulation (Ben-Yehuda et al., 2003; Wu and Errington, 2003; Perry and Edwards, 2006); ComN which is involved in competence development (dos Santos et al., 2012); and, with Maf, a regulator of cell shape and division (Butler et al., 1993). The interaction between Maf and $DivIVA_{Bs}$ arrests cell division in competent cells (Briley et al., 2011). DivIVA of *Corynebacterium glutamicum* interacts with RodA and ParB, (Donovan et al., 2012; Sieger et al., 2013), which binds the origin of replication with ParA, resulting in chromosomal segregation (Mierzejewska and Jagura-Burdzy, 2012). DivIVA is involved in apical growth and control of cell polarity in *Streptomyces coelicolor* (Flärdh, 2010), by interacting with ParB to co-ordinate chromosomal segregation. (Donczew et al., 2016). DivIVA in *S. pneumoniae* interacts with several proteins implicated in divisome formation, including FtsZ, FtsA, ZapA, FtsK and FtsI, FtsB, FtsQ and FtsW (Fadda et al., 2007). These studies highlight the diverse functionality of DivIVA in Gram-positive organisms. There is no information regarding DivIVA-associating proteins in *Enterococcus faecalis* (Ef).

E. faecalis, an opportunistic, commensal, Gram-positive, ovococcal pathogen is recognized for its resistance to multiple antibiotics and for causing hospital-acquired infections (Murray, 1990; Cross and Jacobs, 1996; Hidron et al., 2008a, 2008b; Sievert et al., 2013). Enterococcal infections are potentially fatal, causing neonatal and wound infections, endocarditis, meningitis, and urinary tract infections (Hidron et al., 2008a, 2008b; Torelli et al., 2017). Due to its ability to form biofilms, catheter-related urinary tract infections with *E. faecalis* are difficult to treat (Mohamed and Huang, 2007). To formulate new therapeutic agents

and targets for resisting antibiotic resistant *E. faecalis* infections, a greater understanding of enterococcal biology, physiology and genetics is required.

*E. faecali*s contains DivIVA (Ramirez-Arcos, 2005). This research describes a novel DivIVA-interacting protein, EF1025, which was annotated as a hypothetical protein in *E. faecalis* strain V583 (Paulsen et al., 2003). EF1025, which is conserved in most Gram-positive bacteria, contains a DNA binding domain at its N-terminus and two highly conserved Cystathionine β-Synthase (CBS) domains at the central and C-terminal regions. Bacterial Two-Hybrid (B2H), Glutathione S-Transferase (GST) pull-down, and Co-Immunoprecipitation (Co-IP) assays were used to demonstrate an interaction between EF1025 and $DivIVA_{Ef}$. EF1025 self-interacts and forms a decamer. It was not possible to obtain viable cells after the deletion or insertional inactivation of *EF1025* without *in trans* expression of the gene. These rescued cells grew more slowly than wild type *E. faecalis*. Scanning electron microscopy (SEM) and atomic force microscopy (AFM) revealed cell elongation and aberrant cell shape in rescued cells. Cell elongation was also observed in SEM images when *EF1025* was overexpressed in *E. faecalis* cells. Using an *E. coli* model, overexpression of *EF1025* in *E.coli* PB103 resulted in filamentation. Immunofluorescence microscopy showed that EF1025 localized comparably to $DivIVA_{Ef}$ localization during the later stages of cell division.

2.3. Materials and methods

2.3.1. Strains, plasmids and growth conditions

Strains and plasmids used in this study are listed in Tables S1 and S2. *E. coli* XL1-Blue or DH5α were used as hosts for cloning. *E. coli* C41 (DE3) was used to overexpress cloned proteins, *E. coli* PB103 (de Boer et al., 1988) for heterologous overexpression of *E. faecalis* proteins, and *E. coli* R721 (Di Lallo et al., 2001, 2003) was used for the bacterial-two hybrid evaluations. *E. coli* strains were grown at 37°C in Luria-Bertani (LB) medium (Difco, Detroit, MI) and antibiotics were included in the following concentrations as required: ampicillin (Amp) 100 µg/mL, kanamycin (Kan) 50 µg/mL and erythromycin (Ery) 125 µg/mL. *E. faecalis* JH2-2 (Jacob and Hobbs, 1974), the parental strain, was used for the preparation of genomic DNA. *E. faecalis* was cultured at 37°C without aeration in Brain Heart Infusion (BHI) broth (Difco, Detroit, MI) and supplemented with appropriate antibiotics if required (Ramirez-Arcos, 2005; Rigden et al., 2008). *Saccharomyces cerevisiae* SFY526, used in yeast two-hybrid (Y2H) assays (Clontech Laboratories, Inc., CA), was grown at 30°C for 2-4 days on yeast extract-peptone-dextrose-adenine medium (YPDA) or appropriate synthetic dropout media (Yeast Protocols Handbook, Clontech).

2.3.2. Bioinformatic analysis

DNA sequences interacting with $DivIVA_{Ef}$, identified after screening Y2H libraries of *E. faecalis* JH2-2 (Supplementary methods) were blasted against the *E. faecalis* V583 genome (Paulsen et al., 2003) using NCBI BLAST (http://blast.ncbi.nlm.nih.gov/Blast.cgi). A putative open reading frame, named *EF1025* (GenBank accession number NC_004668), was identified from the *E. faecalis* V583 genome. The upstream sequence of *EF1025* (~ 480bp) was analyzed for promoter prediction (http://www.fruitfly.org/cgi-bin/seq_tools/promoter.p1) and the deduced amino acid sequence of EF1025 was ascertained using ProtParam (http://us.expasy.org/tools/protparam.html). Homologues of EF1025 were identified using BLASTp (https://blast.ncbi.nlm.nih.gov/Blast.cgi?PAGE=Proteins) against the non-redundant protein sequences database. EF1025 was also analyzed by PROSITE (Sigrist et al., 2010) (http://ca.expasy.org/cgi-bin/prosite/mydomains) to identify functional domains. Transmembrane motifs in EF1025 were predicted using TMbase (http://www.ch.embnet.org/cgi-

bin/TMPRED_form_parser) and potential coiled-coil structures were predicted using COILS (http://www.ch.embnet.org/software/COILS_form.html).

2.3.3. EF1025-DivIVA interactions in the Bacterial Two-Hybrid (B2H) assays

The B2H system of Di Lallo et al. (2001 and 2003) was used to investigate interactions between $DivIVA_{Ef}$ and EF1025 and its various domains. This particular assay involves a hybrid repressor which recognizes a chimeric operator. Potential interacting proteins are cloned at the two chimeric regions at the C-terminus of this hybrid repressor. The dimerization of the heterologous proteins permits reconstitution of the hybrid repressor which recognizes the chimeric operator and downregulates the activity of the downstream reporter gene, *lacZ* (Di Lallo et al., 2001). Modified B2H vectors pcI434-L and pcIp22-L, containing a linker with multiple endonuclease restriction sites were used in B2H assays (Table S2A). *EF1025*, *EF1025CBS12* (encoding AA80-209 of EF1025) and $divIVA_{Ef}$ were PCR-amplified from the *E. faecalis* JH2-2 using primers EF1025-F/R, EF1025C-F/R and CBdivIVA-F/R, respectively (Supplementary Materials, Table S3A) and cloned into the modified B2H vectors, resulting in plasmids pdivIVA22, pdivIVA434, pEF1025434, p22CBS1CBS2 and p434CBS1CBS2, respectively (Table S2A). These plasmids were transformed into *E. coli* R721 alone or in combination (Di Lallo et al., 2001, 2003; Greco-Stewart et al., 2007). Freshly transformed single colonies were grown overnight in 4 mL LB medium supplemented with Amp 50µg/mL and Kan 30 µg/mL. Cells were diluted 1:100 using fresh LB medium containing the same antibiotics and were incubated for ~1 hr (OD600 ~0.1) at 37°C, followed by the addition of 0.1 mM isopropyl β-D-1-thiogalactopyranoside (IPTG). Cells were further incubated to mid-log phase (i.e. OD600 ~0.5) at 37°C, harvested, and tested for β-galactosidase activity, as previously described (Di Lallo et al., 2001). Each experiment was performed in triplicate and the average percentage β-galactosidase activity was calculated.

2.3.4. GST pull-down assays

To create a GST-$DivIVA_{Ef}$ fusion, $divIVA_{Ef}$ was PCR-amplified from genomic DNA from *E. faecalis* JH2-2 (see supplementary methods) using primers IVA-5/IVA-11 (Table S3B) (Ramirez-Arcos, 2005). The amplicon was cloned into pGEX-2T, generating plasmid pGST-Div (Supplementary Materials, Table S2B). *EF1025* was PCR-amplified from *E. faecalis* JH2-2 DNA using primers EF1025F-F/R (Table S3B) and cloned into pET30a(+), resulting in plasmid

pETEF1025 (Table S2B). The two CBS domains i.e. CBS1 and CBS2, of EF1025 were PCR-amplified from *E. faecalis* JH2-2 DNA using primers EF1025-CF/R and cloned into pET30a(+), resulting in plasmid pETEF1025CBS12 (Table S2B and 3B).

GST-DivIVA$_{Ef}$, 6×His-EF1025, or 6×His-EF1025CBS12 fusions were overexpressed in *E. coli* C41 (DE3)(Ramirez-Arcos, 2005). The GST-DivIVA$_{Ef}$ fusion protein was purified using GST affinity beads (GST-Bind Kit, Novagen, USA). 6×His-EF1025 or 6×His-EF1025CBS12 were purified from 200 mL log-phase growth of *E. coli* C41 by sonication in 5 mL Interaction Buffer (IB, 20 mM Tris/HCl pH 7.5, 10% glycerol, 50 mM KCl, 0.5 mM EDTA, 1% Triton X100, 1 mM DTT). The cell lysate was centrifuged and the supernatant (50 µL) was incubated with 20 µL GST-DivIVA$_{Ef}$ bound beads, pre-equilibrated with IB buffer, at 4°C for 2 hrs. Beads were washed with cold IB buffer 3× and the retained protein was eluted using a 40 µL 1×SDS loading buffer and heating at 95 C for 10 min. Eluted protein was separated by SDS-PAGE, followed by Western blot analysis using anti-6×His monoclonal antibody (Biorad, USA). The same protocol was used to study DivIVA$_{Ef}$ and EF1025CBS12 interaction. Purified GST protein was used as a control and was produced in *E. coli* C41 (DE3) from plasmid pGEX2T.

2.3.5. Production of anti-EF1025 polyclonal antibody

6×His-EF1025 was overexpressed in *E. coli* C41DE3 from plasmid pETEF1025 (Table S2B) and was purified as described previously (Ramirez-Arcos, 2005). Female New Zealand White rabbits were injected with ~30 µg/mL purified 6×His-EF1025 in Freund's adjuvant (Sigma; v/v=1:1) at the Animal Core Facility of the Vaccine and Infectious Diseases Organization (University of Saskatchewan) with a booster dose on day 21 after the initial injection. Polyclonal IgG antibody was purified by affinity purification of antiserum using Protein-A sepharose beads (Pharmacia Bioscience; (Ramirez-Arcos, 2005). Antibody specificity was tested by western blotting assay using an *E. faecalis* JH2-2 whole cell protein extract which was prepared by sonicating 50 mL of cell culture and resuspending the cells in 2.5 mL of Tris buffer (Fig. S1). Previously prepared anti-DivIVA$_{Ef}$ (Ramirez-Arcos, 2005) was used as a positive control.

2.3.6. Co-immunoprecipitation (Co-IP)

An overnight culture of *E. faecalis* JH2-2 was diluted 1:100 in BHI broth and incubated for 16-20 hrs at 37°C without aeration. 200 mL were centrifuged at 10,000 rpm for 10 minutes and

the pellet was re-suspended in 5 mL Co-IP buffer (25 mM HEPES pH7.9, 100 mM NaCl, 5% glycerol, 0.5 mM EDTA, 0.1% Triton X100, 1 mM DTT and 0.5 mM PMSF). The suspension was sonicated, on ice, 3×, for 30 seconds each, with an interval of 20 seconds. The cell lysate was centrifuged under the same conditions (above) and the supernatant was collected for Co-IP assays.

Protein-A Sepharose beads (Pharmacia Inc., Canada) were cross-linked with 20 µg of either anti-DivIVA$_{Ef}$ or anti-EF1025 polyclonal antibody in 200 µL PBS as follows: antibody was incubated with 50 µL Protein-A Sepharose beads at room temperature (RT) for 1 h. Beads were washed with PBS once and then washed twice with 0.2 M sodium borate (pH 9.0). Dimethylpimelimdate (Sigma) was added to the beads to a final concentration of 20 mM and incubated for 30 min at RT to allow cross-linking. The reaction was stopped by adding 0.2 M ethanolamine (final concentration 20 mM) pH8.0 (Sigma) and incubating at RT for 2 hrs. Beads were then washed with PBS and stored at 4°C for later use. Prior to Co-IP, 20 µL antibody-bound beads were incubated with 10 mg/mL BSA overnight at 4°C to block non-specific binding sites. Beads were then equilibrated with Co-IP buffer and subsequently incubated with 200 µL of *E. faecalis* JH2-2 cell extract for 2 hrs at 4°C. After removing the supernatant, beads were washed with Co-IP buffer 3× for 10 min each. Proteins retained on the beads were eluted in 80 µL 1×SDS loading buffer, separated on 12% SDS-PAGE, and transferred onto a nitrocellulose membrane for Western blot assay. Blots were probed with either anti-DivIVA$_{Ef}$ or anti-EF1025 polyclonal antibody. Beads alone or beads cross-linked with anti-MinC$_{Ng}$ polyclonal antibody (Ramirez-Arcos et al., 2001) were used as negative controls.

2.3.7. EF1025 self-interaction

To determine whether EF1025 self-interacts, and to map the sites responsible for self-interaction, the predicted functional domains of EF1025 were constructed, in different combinations, in Y2H vectors as follows: EF1025CBS12 (AA80-204) carrying CBS1 and CBS2 domains, NCBS1-EF1025 (AA6-204) containing the N-terminus HTH domain and CBS1 domain, CBS2-EF1025 (AA144-204) containing the CBS2 domain, and N-EF1025 (AA6-50) containing the N-terminus HTH domain. *E. faecalis* JH2-2 DNA was used as a template for PCR amplification of these fragments. Primers for the amplification of various fragments are described in Supplementary Table S3C. These amplicons were cloned into the vectors pGAD424 and pGBT9 resulting in plasmids pGADEF1025CBS12, pGBDEF1025CBS12, pGADEF1025NCBS1,

pGBDEF1025NCBS1, pGADEF1025CBS2, pGBDEF1025CBS2, pGADEF1025-N and pGBDEF1025-N, respectively (Table S2C). Each plasmid construct was co-transformed with a plasmid expressing full-length EF1025 (e.g. pGADEF1025 or pGBDEF1025) into *S. cerevisiae* SFY526. Transformation efficiencies were calculated by plating 50 µL of diluted transformants on separate plates followed by counting the number of colonies produced. Transformants were selected on complete synthetic medium lacking leucine and tryptophan (SD-leu-trp) (Clontech). Transformation efficiencies were calculated by plating 50 µL of diluted transformants on separate plates followed by counting the number of colonies produced. After 3-4 days of incubation at 30°C, using a colony lift assay (Clontech, CA), cells were screened for blue color development in the presence of 5-Bromo-4-chloro-3-indolyl-β-D-galactopyranoside (X-Gal, Sigma-Aldrich; St. Louis, MS) to study the self-interaction ability of EF1025. Positive clones were further subcultured in SD-leu-trp broth and a spectrophotometric assay for β-galactosidase activity, using the substrate o-nitrophenyl-β-$_D$-galactopyranoside (Ramirez-Arcos, 2005).

SEC-MALS, the combination of Size Exclusion Chromatography with Multi-Angle Light Scattering analysis (Wyatt Technology, USA), was used to determine the oligomerization state of EF1025. Using His-bind resin (Novagen, Canada), 1mg of purified 6×His-EF1025 was loaded onto a Superdex 200 column (Biorad) equilibrated with a buffer comprising 50 mM Tris base, 400 mM NaCl, pH 7.4. A single peak, corresponding to EF1025 eluted by SEC, was detected by the MALS detector to estimate molar mass.

2.3.8. Overexpression of *EF1025* in *E. faecalis* JH2-2

To overexpress *EF1025* in *E. faecalis* JH2-2, *EF1025* was cloned into pMSP3545 (Supplementary Materials, Table S2). pMSP3545 was first modified by introducing an Amp-encoding gene that was PCR amplified from pcDNA3.1(+) using primer pairs AmpF/R (Table S3D), into pMSP3545 creating pMSP3545A (Table S2D). Linkers LinkA/B (Table S3D), which contained restriction sites BamHI and NcoI, were ligated to the Amp gene amplicon prior to ligation in pMSP3545. pMSP3545A was electroporated into electrocompetent *E. faecalis* JH2-2 cells using previously described methods (Ramirez-Arcos, 2005) and colonies were selected on BHI supplemented with Ery (125 µg/mL), creating *E. faecalis* MK0. *E. faecalis* JH2-2 and *E. faecalis* MK0 served as controls for all electroporation experiments. *EF1025* and 80 bp upstream which included the predicted promoter sequence was PCR amplified using primers

EF1025npF/R, and the amplicon was digested with NcoI and XbaI, purified and subcloned into pMSP3545A, digested with the same enzymes, creating pMSPEF1025A (Table S2D). pMSPEF1025A was transformed into *E. coli* DH5α and transformants were selected for Amp resistance. Clones were confirmed for the presence of EF1025 using restriction digestion and PCR amplification with primers EF1025npF/R. pMSPEF1025A was electroporated into electrocompetent *E. faecalis* JH2-2 cells creating *E. faecalis* MK23 (Table S1) using previous methods (Ramirez-Arcos, 2005). To ascertain whether *EF1025* was expressed from its native promoter in pMSPEF1025A, pMSPEF1025-flag was created by fusing a flag-tag encoding sequence which was PCR amplified from pcDNA3.1(+) using primers flagF/R (Table S3D). The amplicon was ligated in pMSPEF1025A downstream of *EF1025* and electroporated into electrocompetent *E. faecalis* JH2-2 cells to create *E. faecalis* MK24 (Table S1). *EF1025* expression from pMSPEF1025-flag in *E. faecalis* MK24 was evaluated using an anti-flag monoclonal antibody (GenScript, USA) by Western blot analysis. Whole cell extracts of both *E. faecalis* JH2-2, *E. faecalis* MK23 and *E. faecalis* MK24 were prepared for these blots. In a separate Western blot, an anti-EF1025 antibody was used to compare EF1025 expression levels in the same strains.

2.3.9. Complementation *of EF1025* deletions and insertional mutants in *E. faecalis JH2-2*

Clones of insertionally inactivated or deleted *EF1025* in *E. faecalis* JH2-2 could not be recovered unless *EF1025* was expressed *in trans*. Therefore, *E. faecalis* JH2-2 was co-transformed both with plasmids expressing *EF1025* (i.e. either pMSPEF1025-pro or pMSPEF1025A) and plasmid constructs designed to insertionally inactive (i.e. p3ERMEF1025::Kan) or delete (i.e. p3ERMΔEF1025::Cat) *EF1025*.

To create p3ERMEF1025::Kan, first the N-terminal sequence of *EF1025* (AA1-55) was PCR-amplified from *E. faecalis* JH2-2 using primers CBSDPF/CBS55R-Hind (Table S3D). The amplicon was digested and ligated to predigested pUC18 resulting in pUCEF1025-N (Table S2D). Then, a kanamycin cassette (*Kan*^{R}) was PCR-amplified from pTCV-lac (Table S2D; Poyart and Trieu-Cuot, 1997) with primers KanF/R (Table S3D), and the amplicon was inserted into pUCEF1025-N at its *Hind*III/*Sma*I sites, producing plasmid pUCEF1025-N-Kan (Supplementary Materials, Table S2D). The C-terminal sequence of *EF1025* (AA56-209) was PCR-amplified from *E. faecalis* JH2-2 with primers CBS55F-SmaI/EF1025-R-BamHI (Table S3D) and the amplicon

was inserted into pUCEF1025-N-Kan creating the plasmid pUCEF1025::Kan (Supplementary Materials, Table S2D). Finally, pUCEF1025::Kan was digested with EcoRI and BamHI, yielding a fragment containing *EF1025-N, Kan*^{R} and *EF1025-C.* This fragment was ligated into p3ERM-H, creating the suicide vector p3ERMEF1025::Kan (Table S2D; Ramirez-Arcos, 2005). This plasmid was electroporated into *E. faecalis* JH2-2 (Ramirez-Arcos, 2005) with selection attempted using BHI agar containing Kan 500 µg/mL and incubation at 37°C for 2-3 days. Transformants were never obtained after multiple attempts, so p3ERMEF1025::Kan was co-electroporated with the shuttle plasmid pMSPEF1025-Pro that expresses wild type *EF1025 in trans* from its native promoter (Table S2D) into *E. faecalis* JH2-2 to create *E. faecalis* MJ26 (Table S3C; Ramirez-Arcos, 2005). Transformants were selected on BHI supplemented with Ery (125 µg/mL) and Kan (500 µg/mL). For each electroporation experiment, we used *E. faecalis* JH2-2 and MK0 as controls for growth on BHI supplemented with erythromycin. *E. faecalis* JH2-2 failed to grow in the presence of erythromycin while *E. faecalis* MK0 grew well. To confirm that transformants contained both an insertionally inactivated chromosomal *EF1025* as well as *EF1025* expressed *in trans* from pMSPEF1025-pro in *E. faecalis* MJ26, primers mutF/Kan-R, KanF/KanR, EF1025-Pro/KanR and KanF/CBSDPR were used to amplify chromosomal and plasmid fragments, followed by DNA sequencing of all amplified fragments for confirmation of the insertion (Table S3D).

To ensure that phenotypes observed in *E. faecalis* MJ26 were not caused by polar effects of the insertional mutagenesis of *EF1025* on the downstream gene, *EF1026*, qPCR was performed to study the expression of both genes (Supplementary Methods).

A second strategy to inactivate *EF1025* in *E. faecalis* JH2-2 involved the nonpolar deletion of chromosomal *EF1025* (LeDeaux et al., 1997) by the introduction of the suicide plasmid pERMΔEF1025::Cat. Partial overlapping flanking primers ppdkF/R-BamHI (Table S3D) were used to amplify 500 bp upstream (includes the native promoter of *EF1025*) of the start codon of *EF1025* and 500 bp downstream of the stop codon of *EF1025* using primers 1026F/R-EcoRI (Table S3D) of *E. faecalis* JH2-2 DNA. A chloramphenicol cassette was amplified from pLemo (NEB) using primers CatF/R (Table S3D). The three fragments were combined by overlap PCR amplification (Hussain and Chong, 2016), creating a fragment that contained the chloramphenicol cassette flanked by the 500 bp upstream fragment and 500 bp downstream fragment. The resultant fragment was purified, digested and ligated into p3ERM-H, creating the suicide vector

p3ERMΔEF1025::Cat (Table S2D). As no transformants were recovered after electroporation of p3ERMΔEF1025::Cat into *E. faecalis* JH2-2, this plasmid along with pMSPEF1025A (Table S2D) were co-electroporated into *E. faecalis* JH2-2 (Shepard and Gilmore, 1995) creating *E. faecalis* MK12. Transformants were selected on BHI agar plates containing Chl 5 µg/mL and Ery 125 µg/mL, incubated at 37°C for 2-3 days. The deletion of *EF1025* in *E. faecalis* MK12 was confirmed by PCR-amplification using primers ppdkF/EF26b-R, mutF/EF26b-R, ppdkF/EF1025npR, EF1025npF/1026R, CatF/1026R and CatF/R (Table S3C and D) followed by DNA sequencing of these amplified fragments (data not shown). *E. faecalis* JH2-2 did not grow at this concentration of chloramphenicol. As a positive control, p3ERMΔEF1025::Cat was electroporated into *E.coli* DH5α and transformants were selected on LB agar plates containing Chl 33 µg/mL at after incubation for 24 hrs at 37°C.

2.3.10. Microscopy

SU8010 Cold Field Emission Ultra-High-Resolution scanning electron microscope (WCVM, University of Saskatchewan, Saskatoon, Saskatchewan) was used to image *E. faecalis* strains JH2-2, MK0, MK12, MJ26, MK23, MK24 (Table S1). Strains were cultured in BHI medium with or without appropriate antibiotics, without agitation, at 37°C, either overnight (~20 hrs) or to stationary phase. Cells were fixed on poly-l-lysine coverslips, dehydrated in ethanol, critical point dried, sputter coated with gold and imaged (Ramirez-Arcos et al., 2001). Length measurements were performed across the poles of the diplococcal bacteria and the percentage of elongated cells was calculated by measuring the lengths of 110-250 cells.

A Hitachi HT7700 High Contrast High-Resolution Digital Transmission Electron Microscope (WCVM, University of Saskatchewan, Saskatoon, Saskatchewan) was used to image *E. faecalis* strains JH2-2 and MJ26 prepared as previously described (Ramirez-Arcos, 2005).

2.3.11. Immuno-fluorescence microscopy of *E. faecalis* JH2-2

To visualize $DivIVA_{Ef}$ and EF1025 localization, *E. faecalis* JH2-2 cells in exponential phase were collected and fixed using a procedure modified from Harry and Lewis (2003). One mL of cell culture was harvested and the resuspended pellet was fixed with 1 ml fixation buffer (2.5% paraformaldehyde, 0.03% glutaradehyde in 30 mM sodium phosphate buffer pH 7.5) for 30 min, at RT, then for 2 hrs at 4°C. Cells were washed 3× with 1×PBS and resuspended in 200 µL GTE

(50 mM glucose, 20 mM Tris-HCl pH 7.5, 10 mM EDTA) to which a freshly prepared lysozyme solution (2 mg/mL) was added. This volume was transferred to and fixed on poly-L-lysine coated coverslips. Cells attached to the coverslips were blocked with BSA-PBST (3% bovine serum albumin [wt/vol] and 0.2% Triton X-100 [vol/vol] in PBS) for 2 hrs at RT. Cells were then incubated with either anti-$DivIVA_{Ef}$ (1:200) or anti-EF1025 (1:100) in BSA-PBST for 3 hrs at RT. After washing with PBST, cells were incubated with a fluorescence-labeled secondary antibody (1:500 dilutions in BSA-PBST, goat anti-rabbit Alexa Fluor 488, Invitrogen) for 45 min. Images were acquired using U-M655 and U-M665 filters and processed using *InVitro* 3 and ImagePro 6.0 software (Media Cybernetics). Each experiment was performed 4× using 2 independent cell cultures, and about 300 cells were counted for each immuno-staining. Cells were also stained with DAPI (Thermofischer, CA) and were mounted and observed under a 100X oil immersion objective using an Olympus BX61 microscope with standard filters. DAPI-stained cells were divided into five cell division stages. Stage 1 was defined as a single cell with a central condensed chromosome. Stage 2 cells contained segregating chromosome as the cell started to divide. Stage 3 and 4 were defined by the presence of two newly replicated cells with segregated chromosome. As the cell completed one round of cell division, Stage 5 comprised of two daughter cells with condensed DNA in the center. *E. faecalis* MWMR16 cells were used as a negative control which contains point mutations in the coiled-coil region of $DivIVA_{Ef}$ (Rigden et al., 2008).

2.4. Results

2.4.1. Identification and *in silico* analysis of a novel DivIVA$_{Ef}$ interacting protein in *E. faecalis*

To identify DivIVA$_{Ef}$ interacting proteins from *E. faecalis*, a Y2H system was used to screen an *E. faecalis* genomic DNA library using DivIVA$_{Ef}$ as the bait protein (data not shown). Positive clones were sequenced and bioinformatic analysis indicated a sequence corresponding to the C-terminus of the hypothetical protein EF1025 (GenBank accession # NP_814759) of the *E. faecalis* V583 genome; *EF1025* spans nucleotide positions 983760-984389 (Fig. 2.1A). *In silico* analysis of *EF1025* indicated that a ribosome binding site (GGAGG) is located at nucleotide position (nt) –6 to –10, and a putative promoter at position nt -36 to -87. *EF1025* has a transcriptional orientation (Fig. 2.1B) similar to the downstream gene *EF1026*, a hypothetical protein with a kinase phosphoprotein phosphatase (PPPase) domain. A predicated terminator sequence is located downstream of *EF1026*. The upstream gene, *EF1024*, is transcribed in the opposite orientation of *EF1025* and *EF1026* and encodes a putative pyruvate phosphate dikinase (PPDK) domain (Fig. 2.1B).

EF1025 comprises 209 amino acids (AA), with a molecular weight of ~23kDa and a theoretical isoelectric point of 6.75. Domain prediction studies (Fig. 2.1B) showed that EF1025 contains an N-terminal Helix-turn-Helix (HTH) DNA binding domain (AA 6-50), and two CBS domains (i.e. CBS1, AA 80-137 and CBS2, AA 144-204). The CBS1 domain is in the central region of EF1025 and CBS2 is located at the C-terminus. EF1025 does not contain any transmembrane motifs (suggesting that it is a cytosolic protein), nor does it contain coiled-coil regions.

The EF1025 protein sequence was used as a query in BLASTp against 10000 targeted sequences in the non-redundant (nr) protein sequences database (last accessed May 2019). EF1025 was identified as belonging to the CBS pair superfamily and is conserved predominantly in Gram-positive bacteria, primarily in Firmicutes, As with EF1025, Gram-positive homologues contain an N-terminal HTH domain and two CBS domains located identically. In *B. subtilis,* the EF1025 homologue is named CcpN and is involved in the gluconeogenic pathway (Servant et al., 2005).

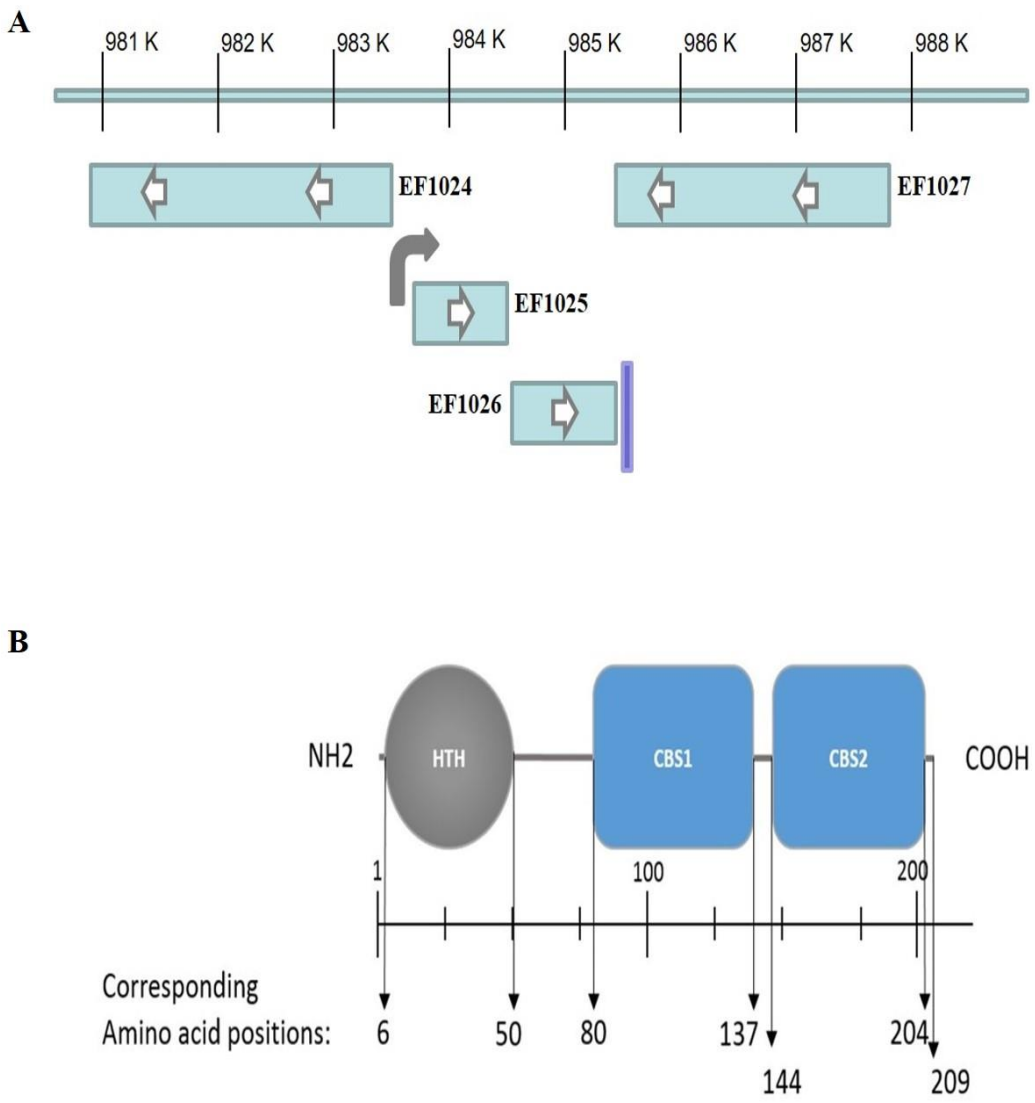

Figure. 2.1. (A) *EF1025* position in *E. faecalis* V583 genome. Transcriptional orientation of genes upstream (i.e. EF1024) and downstream (i.e. EF1026 and EF1027) to *EF1025* (i.e. EF1025). The direction of an arrow within the rectangle indicates the transcriptional orientation of the gene. The bent arrow indicates promoter region upstream of EF1025 and vertical line indicates terminator region. (B) EF1025 domain prediction. N: N-terminus; C: C-terminus; HTH: Helix-turn-helix domain; CBS: Cystathionine-β-Synthase domain. Space in between domains constitutes hinge regions.

2.4.2. EF1025 oligomerizes and self-interacts

To determine whether EF1025 self-interacts, fragments comprising different combinations of domains of *EF1025* were cloned into Y2H vectors and initially tested for interactions using colony lift assay (data not shown), followed by a quantitative assay for increased β-galactosidase activity. The quantitative assay indicated that EF1025 strongly self-interacts (Fig. 2.2). Furthermore, the EF1025CBS12, containing the CBS1 and CBS2 domains, strongly interacted with EF1025. Fragments containing the N-terminus HTH domain and the central CBS1 domain (i.e. EF1025NCBS1) and fragments EF1025CBS2 (contains CBS2 domain) and EF1025-N (i.e. N-terminus HTH domain) showed no interaction with EF1025.

6×His-EF1025 was found to be a decamer, with an estimated molecular mass of 222 kDa, using a combination of Size Exclusion Chromatography (SEC) with Multi-Angle Light Scattering (MALS) analysis (Fig. S2). Reduced disulfide linkages did not change the overall molecular weight of 6×His-EF1025.

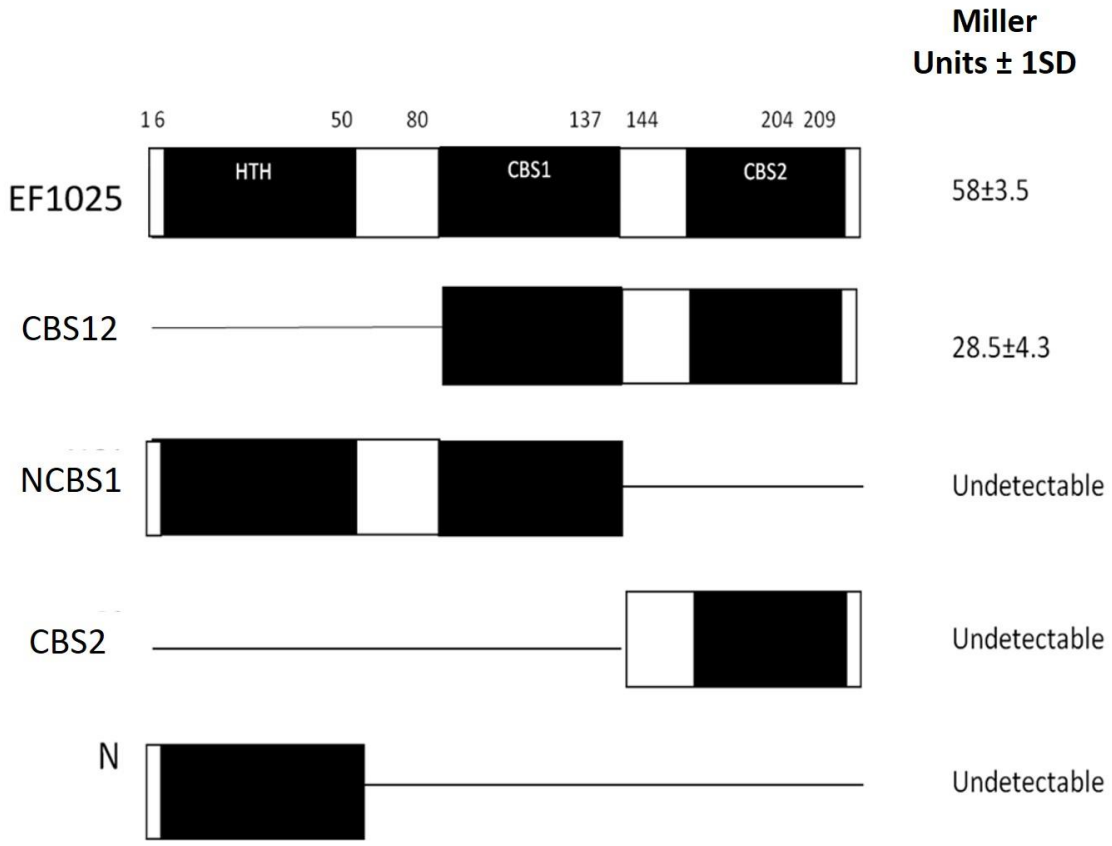

Figure 2.2. **EF1025 self-interacts using CBS1 and CBS2 domains.** EF1025 self-interacts in the Y2H assay. Bars represent full-length and truncations of EF1025. Amino acid positions are indicated on the top. Open bars—predicted domains; closed bars—hinge regions; HTH - helix-turn-helix domain; CBS –cystathionine-β-synthase; Full-length EF1025 contains 209 amino acids (AA1-209); CBS12— EF1025 CBS1 and CBS2 domains together (AA80-204); NCBS1—N-terminus and CBS1 domain of EF1025 (AA1-131); CBS2—CBS2 domain of EF1025 (AA131-209); N—N-terminus of EF1025 (AA1-50). ND—Not detectable. The experiment was performed three times in triplicate. SD— standard deviation. Miller Units represent β-galactosidase activity.

2.4.3. EF1025 interacts with DivIVA$_{Ef}$ *in vitro* and *in vivo*

A B2H system was used to confirm preliminary Y2H results showing the interaction of EF1025 with DivIVA$_{Ef}$. In this assay, less than 50% residual β-galactosidase activity is indicative of positive interaction (Di Lallo et al., 2001; Zou et al., 2017). *E. coli* R721 cells showed a baseline residual β-galactosidase activity of 100%. *E. coli* R721 transformed, with one of pdivIVA22, pdivIVA434, pEF1025434, p434CBS1CBS2, or p22CBS1CBS2, showed residual β-galactosidase activities of 78%, 82%, 55%, 66% and 77%, respectively, and served as negative controls. The positive control (*E. coli* R721 cells containing plasmids pdivIVA22 and pdivIVA434), which demonstrated the self-interaction of DivIVA$_{Ef}$ (Ramirez-Arcos, 2005), displayed 36% residual β-galactosidase activity. Our results indicated an interaction between DivIVA$_{Ef}$ and EF1025 (Fig. 2.3; pdivIVA434 and p22EF1025 together) with the residual β-galactosidase activity of 21%. The two CBS domains together (i.e. p22CBS1CBS2 or p434CBS1CBS2) also interacted with DivIVA$_{Ef}$ (pdivIVA434 or pdivIVA22) with 14% residual β-galactosidase activity.

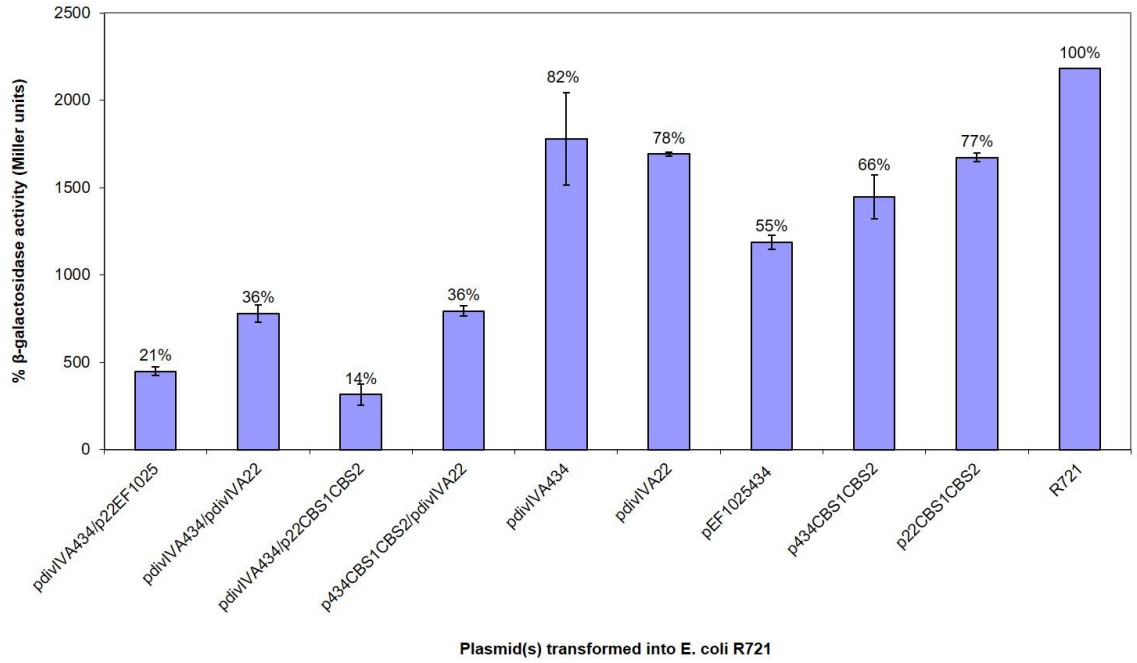

Figure 2.3. EF1025 interacts with $DivIVA_{Ef.}$ in B2H assay. The β-galactosidase activity was expressed in percentage Miller Units (y-axis). The x-axis shows the combination of B2H plasmids used in the experiment. Average values were obtained from three independent assays that were performed in triplicate. Values of less than 50% indicate a positive interaction. The error bars represent 1 standard deviation.

The interaction between EF1025 and $DivIVA_{Ef}$ was also ascertained using a GST-pull down assay. A Western blot using anti-EF1025 antibody revealed that GST-$DivIVA_{Ef}$ was pulled down by 6×His-EF1025 (Fig. 2.4A, Lane 3) or 6×His-EF1025CBS12 (Fig. S3, Lane 3). GST did not interact with 6×His-EF1025 (Fig. 2.4A, Lane 2) or 6×His- EF1025-C (Fig. S3, Lane 2).

The *in vitro* interaction between EF1025 and $DivIVA_{Ef}$ was also determined using a Co-IP assay. EF1025 co-precipitated with $DivIVA_{Ef}$ using an anti-$DivIVA_{Ef}$ antibody (Fig. 2.4B, Lane 2), and $DivIVA_{Ef}$ co-precipitated with EF1025 with anti-EF1025 antibody (Fig. 2.4C, Lane 2). As a negative control, anti-$MinC_{Ng}$ (MinC from *N. gonorrhoeae*) antiserum failed to precipitate EF1025 or $DivIVA_{Ef}$ (Fig. 4B and C Lane 4).

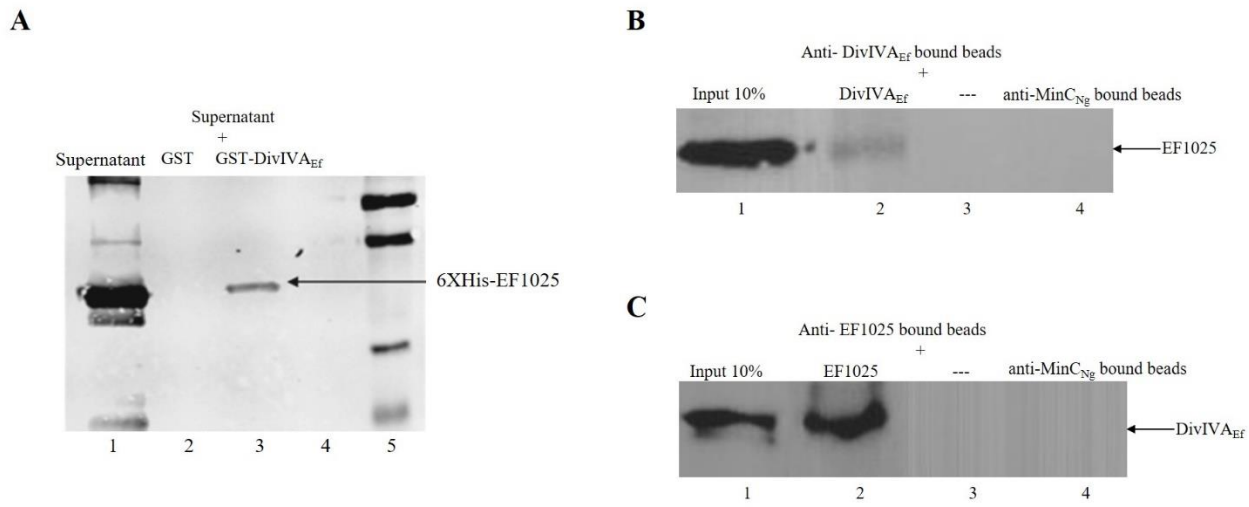

Figure 2.4. Interaction of EF1025 with DivIVA$_{Ef}$. (A) GST pull-down assay. Shown is the Western blot probed with anti-6×His (BioRad, CA) monoclonal antibody to check the presence of EF1025. Lane 1: supernatant containing overexpressed EF1025 representing 10% input of EF1025; Lane 2: GST bound beads; Lane 3: GST-DivIVA$_{Ef}$ bound beads; Lane 5: Protein ladder. (B) Co-immunoprecipitation assay of EF1025. EF1025 was co-precipitated with DivIVA$_{Ef}$ using the anti-DivIVA$_{Ef}$ antibody as bait. The blot was probed with the anti-EF1025 polyclonal antibody. Lane 1: *E. faecalis* extracts representing 10% input in Co-IP assays; Lane 2: anti-DivIVA$_{Ef}$ antibody bound beads; Lane 3: beads alone; Lane 4: anti-MinC$_{Ng}$ antibody bound beads. (C) Co-immunoprecipitation assay of DivIVA$_{Ef}$. DivIVA$_{Ef}$ with EF1025 using anti-EF1025 antibody as bait. The blot was probed with an anti-DivIVA$_{Ef}$ polyclonal antibody. Lane 1: *E. faecalis* extracts representing 10% input in Co-IP assays; Lane 2: anti-EF1025 antibody bound beads; Lane 3: beads alone; Lane 4: anti-MinC$_{Ng}$ antibody bound beads. --- indicates the empty lane.

2.4.4. *In trans* complementation of inactivated or deleted *EF1025*

Two strategies were used to inactivate or delete *EF1025* in *E. faecalis* JH2-2. First, we attempted to insert a *Kan*^{R} cassette at position nt151 (AA50 and Fig. S4A) of *EF1025* using p3ERMEF1025::Kan. No transformants were recovered after several attempts. The second strategy, in which an *EF1025* deletion mutant would be created by in frame replacement of *EF1025* (p3ERM EF1025::Cat) with a *Cat*^{R} cassette (Fig. S4B) in *E. faecalis* JH2-2 also failed to produce transformant colonies. Expression of *EF1025* was rescued by co-transformation with plasmid combinations p3ERMEF1025::Kan and pMSPEF1025-pro, and p3ERMΔEF1025::Cat and pMSPEF1025A. These rescue strategies were successful, creating transformant strains *E. faecalis* MJ26 and MK12, respectively (Fig. S4C and D). Taken together, the data suggest that *EF1025* may be an essential gene. *E. faecalis* MJ26 and MK12 grew more slowly than *E. faecalis* JH2-2 (Fig. S5).

The expression *EF1026* in *E. faecalis MJ26* was determined by RT-PCR to ascertain that the lethal effects of the Kan^R insertion in *EF1025* was not due to polar effects on *EF1026*. Amplified DNA fragments corresponding to the various regions of *EF1026* indicated that the gene was transcribed (Fig. S6). Expression levels (i.e. ΔC_T values) for *EF1026* in *E. faecalis* JH2-2 (i.e. 16.88 ± 0.13) and *E. faecalis* MJ26 (i.e. 16.79 ± 0.04) were equal.

The phenotypes of *E. faecalis* MJ26 and MK12 differed from wild type *E. faecalis* JH2-2. SEM of *E. faecalis* JH2-2 showed cells with symmetrical division at the mid-cell with characteristic ovococcal cell morphology (Fig. 2.5A). *E. faecalis* MJ26 and *E. faecalis* MK12 cells formed elongated cells with distorted cell shapes (Fig. 2.5B and C) which were aggregated, failed to segregate (Fig. 2.5B) and had multiple division sites within a single elongated cell (Fig. 2.5C). Compared to the length of the wild type *E. faecalis* JH2-2 cells (1.16 ± 0.14 µm, n=141), 47% of *E. faecalis* MJ26 (1.63 ± 0.29 µm, n=174) and 49% of *E. faecalis* MK12 (1.74 ± 0.27 µm, n=127) cells were significantly (p<0.05) longer (Fig. 2.5D) when measured across the poles. The control *E. faecalis* MK0 (i.e. contains empty plasmid pMSP3545A) had a cell length (1.15 ± 0.18 µm, n=165) identical (p<0.05) to *E. faecalis* JH2-2 (Fig. 2.5D). Transmission electron microscopy showed that 10% of *E. faecalis* MJ26 cells were aggregated (n=273) with abnormal septation, resulting in daughter cells of different sizes and shapes (Fig. 2.6B, C and D). AFM images showed larger aggregated cell clusters for *E. faecalis* MK12 as compared to *E. faecalis* JH2-2 (Fig. S7).

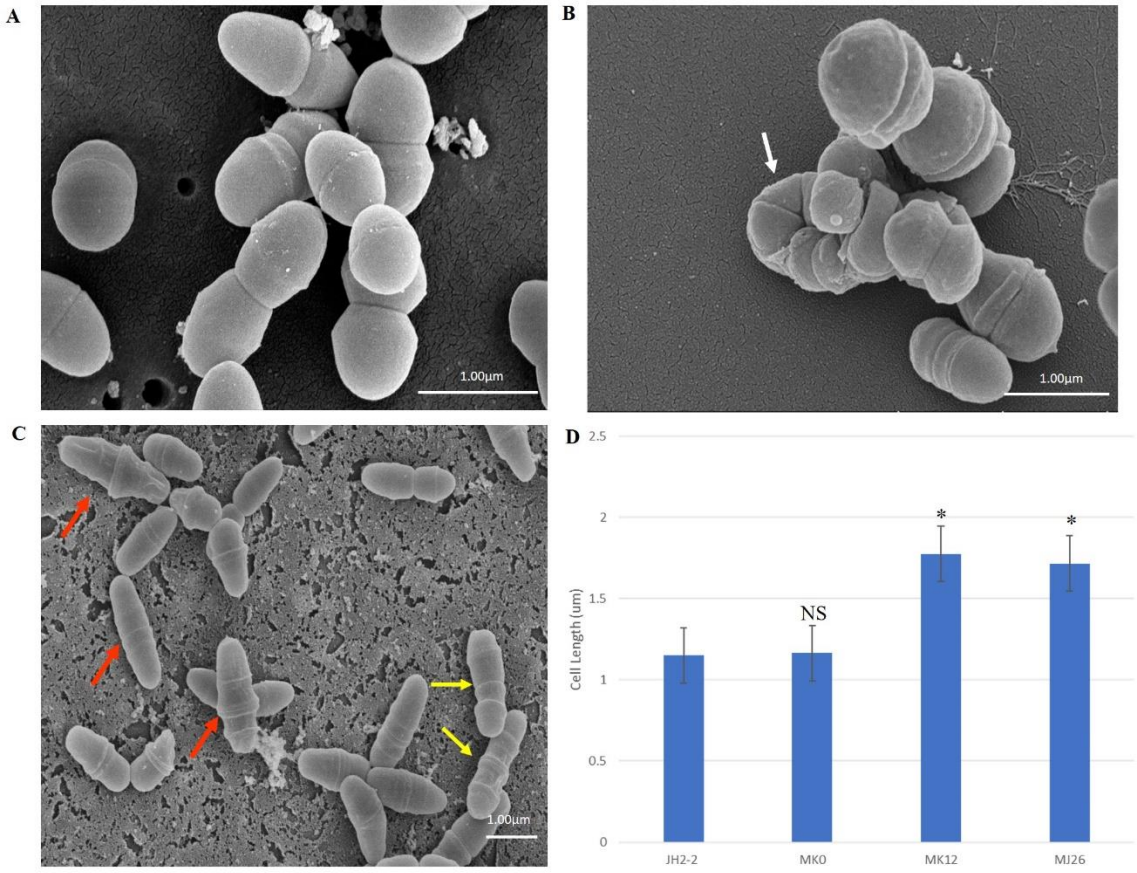

Figure. 2.5. Rescued *E. faecalis* cells (i.e. *E. faecalis* MJ26 and MK12) showed compromised cell division phenotypes. Scanning electron micrographs showing (A) Normal *E. faecalis* JH2-2 lancet-shaped cells; (B) aggregated *E. faecalis* MJ26 cells with impaired segregation; (C) *E. faecalis* MK12 cells showing impaired cell shape and multiple division sites. White arrow indicates aggregated cells that failed to segregate; red arrows indicate cells with distorted cell shape; yellow arrows indicate cells with formation of multiple division rings. Bar scale indicated at the bottom right corner of each image; (D) Comparison of cell lengths for *E. faecalis* strains: JH2-2 (n=141), MK0 (n=165, harboring pMSPEA), MK12 (n=127) and MJ26 (n=174). *E. faecalis* strains JH2-2 and MK0 served as control strains. "n" represents the number of cells counted for each sample; * represents two-tail *p* value from t-test for each group set (i.e. $p < 0.05$); NS- non-significant. The error bars represent 1 standard deviation.

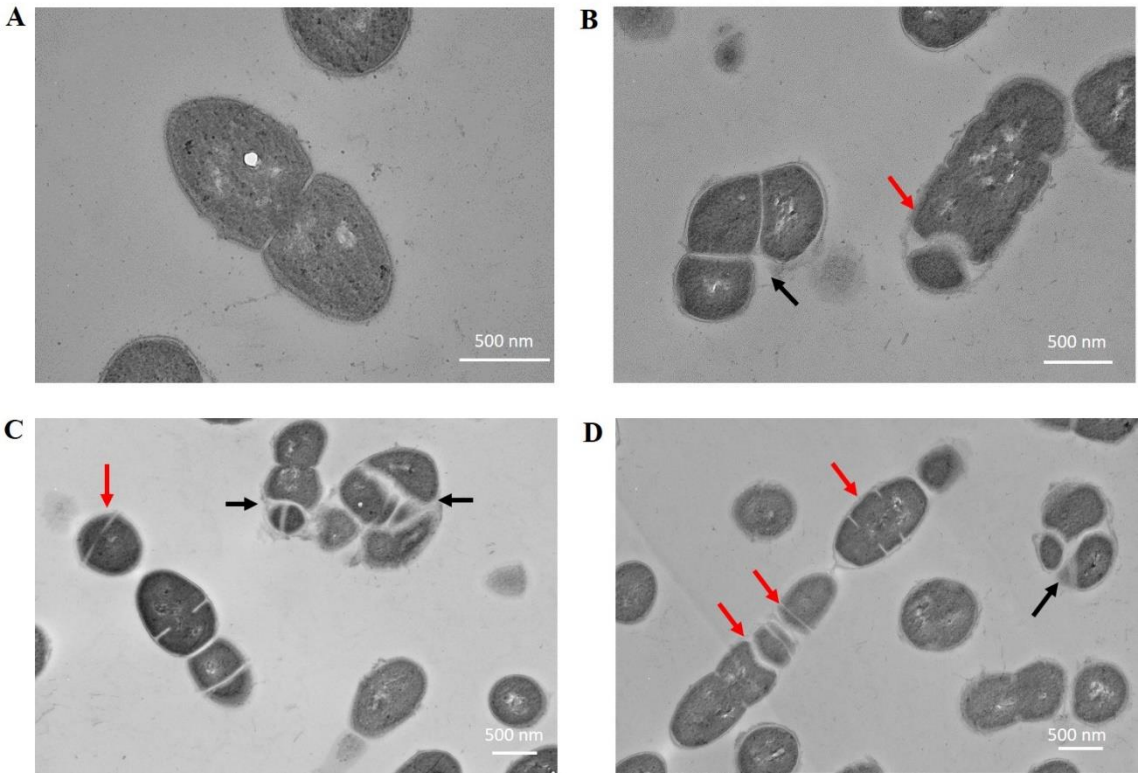

Figure 2.6. *E. faecalis* MJ26 cells showed impaired cell division. Transmission electron micrographs showing (A) wild-type *E. faecalis* JH2-2 lancet-shaped cells; (B, C and D) *E. faecalis* MJ26 cells with aggregated cells that failed to segregate and impaired septation leading to unequal daughter cells. Black arrows indicate aggregated cells that failed to segregate; red arrows indicate septa formation at random sites within the cells. Bar scale indicated at the bottom right corner of each image.

2.4.5. Overexpression of *EF1025* in *E. faecalis* and *E. coli* induces cell elongation

E. faecalis MK23 was created in which *EF1025* is expressed from its native promoter both from the chromosome and from pMSPEF1025A. In order to ensure that *EF1025* could be expressed from its native promoter *in trans*, *E. faecalis* MK24 was constructed (contains pMSPEF1025-flag) and the protein detected in whole cell extract by Western blot using a monoclonal anti-flag antibody (Fig. S8A. Lane 3). Expression of EF1025-flag was not detected in *E. faecalis* JH2-2 or MK23 cell extracts (Fig S8A, Lanes 1 and 2). This confirmed expression of an extra chromosomal copy of EF1025 in *E. faecalis* MK24 when electroporated with pMSPEF1025-flag. This shows that *E. faecalis* MK23 is overexpressing EF1025 due to the presence of an extra chromosomal copy of EF1025. When anti-EF1025 antibody was used to identify the expression levels of EF1025, the overexpression of EF1025 in *E. faecalis* MK23 and *E. faecalis* MK24 was observed as determined by densitometric quantification of band intensities, as compared to its expression in *E. faecalis* JH2-2 (Fig. S8B and C).

SEM analysis showed a statistically significant ($p<0.05$) increase in cell length (1.37 ± 0.21 µm, n=202; Fig. 2.7B and C) in *E. faecalis* MK23 as compared to wild type *E. faecalis* JH2-2 cells (1.16 ± 14 µm, n=141; Fig. 2.7A and C).

Seventy per cent of cells (63/89) overexpressing *EF1025* in *E. coli* PB103 (i.e. *E. coli* MK23) were filamentous (Fig. S9B) as compared none of the cells being filamentous in controls comprising *E. coli* cells with pUC18 and cells overexpressing $prgX_{Ef}$, a transcriptional regulator encoding gene (Christie and Dunny, 1986; Bae et al., 2000) in the same vector.

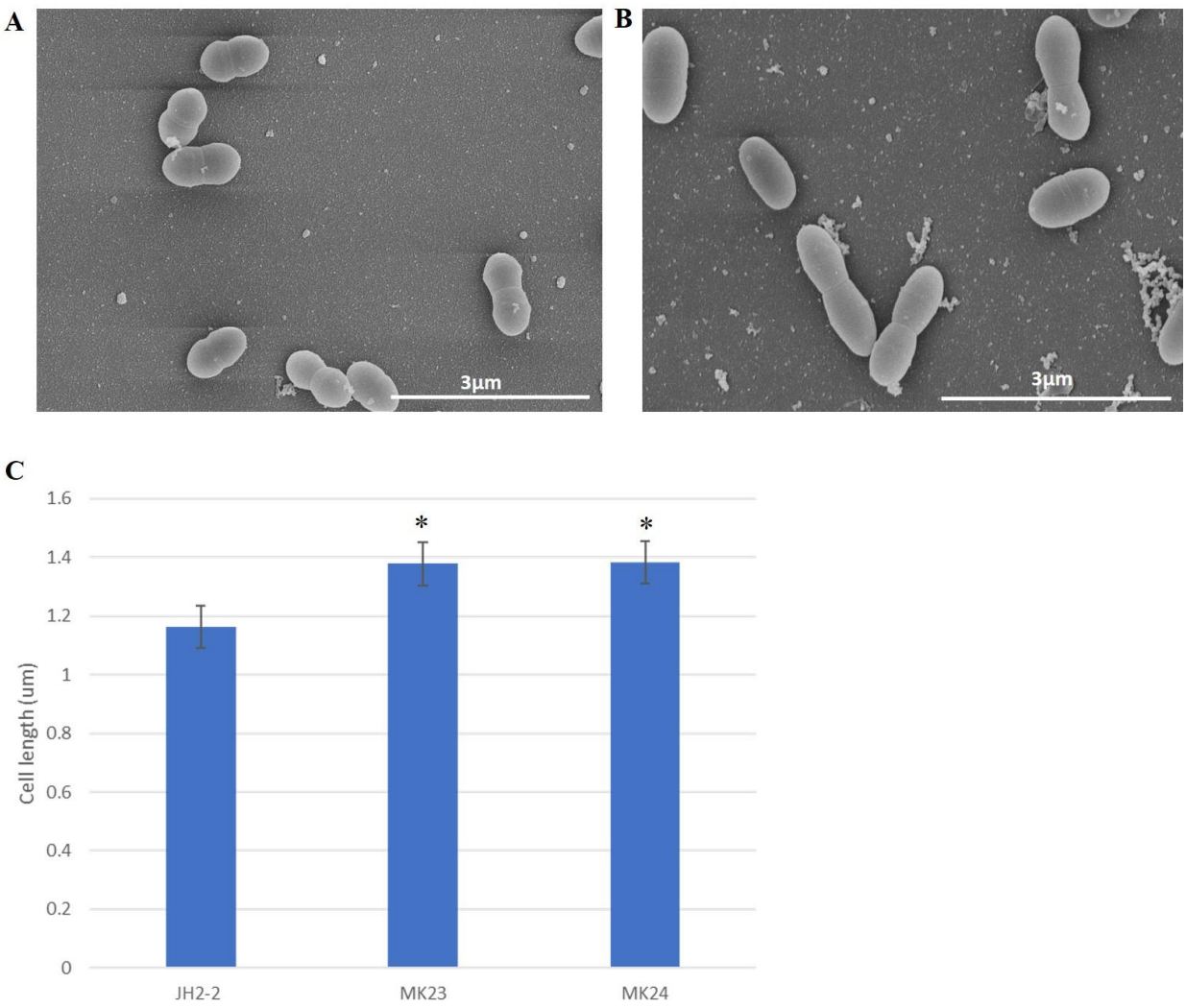

Figure. 2.7. EF1025 overexpression in *E. faecalis* JH2-2 cells causes cell elongation. Scanning electron micrographs showing (A) *E. faecalis* JH2-2 lancet-shaped cells; (B) *E. faecalis* MK23 cells harbouring pMSPEF1025A, showing elongated cell morphology. 3µm bar scale at the bottom right corner of each image establishes the comparison in cell length for *E. faecalis* JH2-2 and MK23; and (C) Comparison of cell lengths of *E. faecalis* strains: JH2-2 (n=141), MK23 (n=202) and MK24 (n=226) where "n" represents a number of cells counted for each sample. * represents two-tail *p* value from t-test for each group set (i.e. $p < 0.05$). The error bars represent 1 standard deviation.

2.4.6. EF1025 localizes at the septum and cell poles in *E. faecalis*

Immunofluorescence studies of *E. faecalis* JH2-2 cells with anti-DivIVA$_{Ef}$ or anti-EF1025 polyclonal antibody were performed to determine their localization patterns during cell division. Cell division that entailed 5 stages (273 cells counted for DivIVA$_{Ef}$ and 281 for EF1025 localization). During Stage 1, as the cell started to divide and the chromosome started to segregate, DivIVA$_{Ef}$ (20.5%, 56/273 cells) localized at the poles and along the length of the cell. In this stage, EF1025 (23.1%, 65/273 cells) was dispersed along the inner membrane (Fig. 2.8, Stage 1). In Stage 2, EF1025 (14.9%, 42/281) localized along the length of the cell in contrast with DivIVA$_{Ef}$ (36.7%, 100/273) that remained localized at the poles and the midcell (Fig. 2.8, Stage 2). At Stage 3, EF1025 (36%, 104/281 cells) and DivIVA$_{Ef}$ (16.1%, 44/273) localized similarly, i.e. to the cell poles and midcell. In Stage 4, as the cells progressed towards completion of cell division, EF1025 (13.2%, 37/281) and DivIVA$_{Ef}$ (16.8%, 46/273) localized as disks and bands along the cell length and septum. With one completed round of cell division (i.e. Stage 5), EF1025 (11.7%, 33/281 cells) was redistributed along the inner membrane before another round of cell division, while DivIVA$_{Ef}$ (9.9%, 27/73) once again localized as dots at the cell poles of the newly formed daughter cells (Fig. 2.8, Stage 5), like Stage 1 cells. The coiled-coil region of DivIVA$_{Ef}$ facilitates oligomerization and is essential for its biological functioning (Rigden et al., 2008). *E. faecalis* MWMR16 which contains point mutations in the coiled-coil region of DivIVA$_{Ef}$ (Rigden et al., 2008) exhibited loss of DivIVA$_{Ef}$ localization at the cell poles and midcell position (Fig. S10). The signal was observed to be dispersed all along the membrane. The different stages of cell division were missing for *E. faecalis* MWMR16.

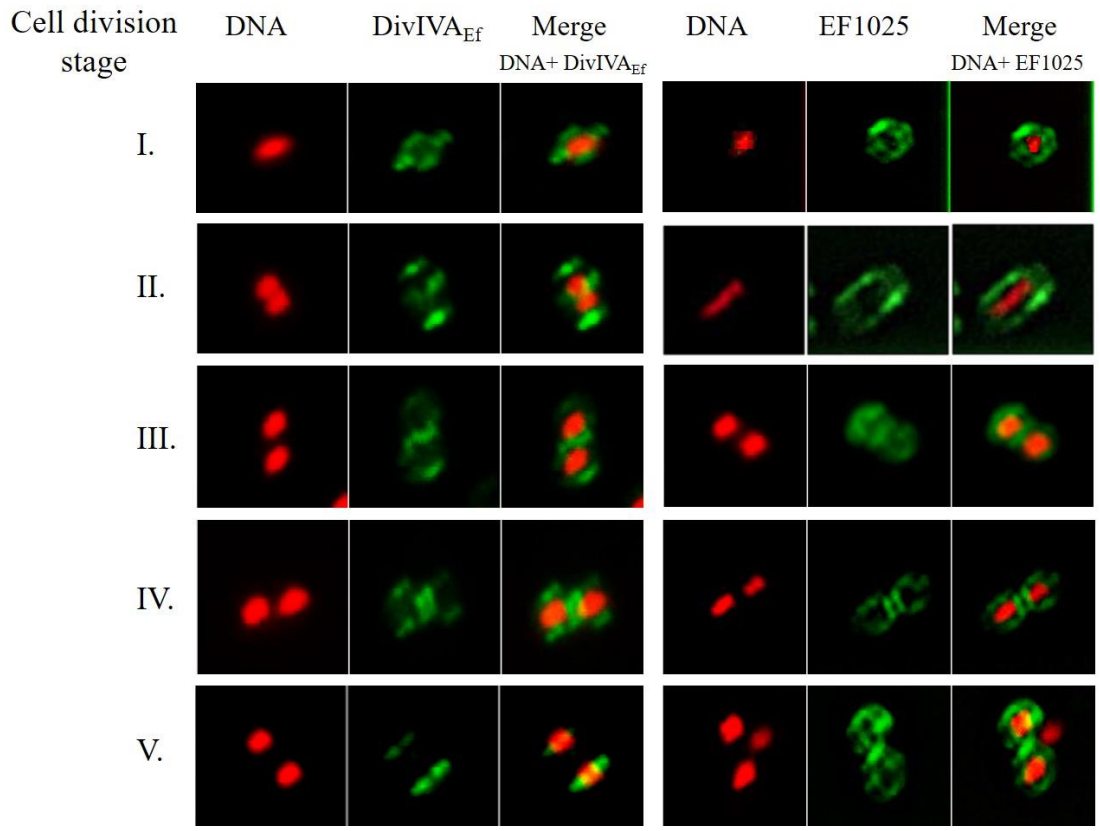

Figure 2.8. DivIVA$_{Ef}$ and EF1025 localizes similarly in the later stages of cell division in *E. faecalis* JH2-2 cells. Averaged images and fluorescence intensity traces of *E. faecalis* JH2-2 cells grown to mid-exponential phase in BHI broth and dual-stained with DAPI and Alexa-Fluor 488 as described in the methodology section. Cells were segregated into five division Stages, and images from the indicated number of cells (n) were acquired using the InVitro 3 and ImagePro 6.0 softwares (Media Cybernetics) as described in Methodology. EF1025 localized at the cell poles and the septa in *E. faecalis* JH2-2 cells similar to DivIVAEf localization. Column 1 and 4, nucleoid localization from DAPI labelling; Column 2 and 5, DivIVA and EF1025 localization, respectively, in immunofluorescence microscopy; Column 3 and 6, merged image of DAPI stained nucleoid and fluorescent DivIVA and EF1025, respectively.

2.5. Discussion

In the present study, we investigated a novel $DivIVA_{Ef}$ interacting protein, EF1025, from *E. faecalis*. EF1025 belongs to the CBS pair superfamily and is conserved in Firmicutes including *Bacillus, Streptococcus, Clostridium, Paenibacillus, Staphylococcus, Lactobacillus, Streptomyces* and *Listeria*. Surprisingly, EF1025 homologues in the Firmicutes *S. pneumoniae, S. pyogenes and L. lactis* did not belong to the CBS pair superfamily as they contained an N-terminal HTH domain, but no CBS domains and their sequence similarities ranged from 40-44%. We also determined bioinformatically that EF1025 homologues, with uncharacterized functions and different combinations of CBS and HTH domains, may be present in species of the *Proteobacteria* and *Euryarcheota* such as *Vibrio, Campylobacter, Burkholderia, Acinetobacter, Fusobacterium, Methanosarcina* and *Methanoculleus*. Proteins containing CBS domains are present in organisms ranging from archaea to humans and were originally identified in *Methanococcus jannaschii* as sequence motifs of approximately 60 amino acids (Bateman, 1997). Although several crystallographic studies have been carried out on CBS domains from bacteria, their precise function remains unexplained (Baykov et al., 2011). It has been postulated that CBS domains may act as allosteric "internal inhibitors" of the functional domains of proteins (Aravind and Koonin, 1999; Biemans-Oldehinkel et al., 2006). Proteins with CBS domains can form dimers through the interaction of these domains. For example, TM0935 of *Thermotoga maritima* self-interacts through its two CBS domains forming a dimer (Miller et al., 2004). An Mg^{2+} transporter from *E. faecalis*, MgtE, also contains two CBS domains but the precise function of these CBS domains remains unelucidated (Ragumani et al., 2010). Our experiments show the importance of the two CBS domains in EF1025 self-interaction. The absence of one CBS domain resulted in the loss of EF1025 self-interaction.

DivIVA, a topological factor in Gram-positive bacteria, interacts with a variety of proteins in various bacteria (Muchová et al., 2002; Halbedel and Lewis, 2019). The range of DivIVA interacting partners changes from one genus to another (Kaval and Halbedel, 2012). In *Listeria monocytogenes* (Lm), $DivIVA_{Lm}$, performs a variety of functions through its interaction with different proteins (i.e. MinCD and SecA2), including precise positioning of the septum at midcell, assistance in the secretion of autolysins, enabling swarming motility (Kaval et al., 2014, 2017). In *Streptococcus suis* (Ss) serotype 2, Ser/Thr kinases (STK) directly phosphorylate $DivIVA_{Ss}$ thereby affecting cell growth and division (Nováková et al., 2010). DivIVA from *S. aureus* (Sa)

associates with various divisome proteins ($FtsZ_{Sa}$, $FtsA_{Sa}$, $EzrA_{Sa}$, $DivIC_{Sa}$, $DivIB_{Sa}$, $PBP1_{Sa}$ and $PBP2_{Sa}$) to ensure cell division and chromosome segregation (Bottomley et al., 2017). The molecular chaperone, DnaK, interacts and stabilizes $DivIVA_{Sa}$ in *S. aureus* (Bukau and Walker, 1989; Bottomley et al., 2017). Bottomley et al., 2017 also reported an indirect function of $DivIVA_{Sa}$ in chromosomal segregation by its interaction with the chromosome segregation protein, SMC (Bottomley et al., 2017). In *Mycobacterium smegmatis* (Ms) and *M. tuberculosis* (Mt), the DivIVA homologue is Wag31 (Nguyen et al., 2007; Kang et al., 2008; Meniche et al., 2014). $Wag31_{Mt}$ interacts with the penicillin-binding protein, PBP3 (Mukherjee et al., 2009) as well as and ParB (Donovan et al., 2012) and $Wag31_{Ms}$ interacts with ParA (Donovan et al., 2012; Ginda et al., 2013). DivIVA from *E. faecalis* is essential for cell viability and growth, proper cell division and chromosome segregation (Ramirez-Arcos, 2005). Rigden et al. (2008) showed that the oligomerization of $DivIVA_{Ef}$ is mediated by two centrally located coiled coils that are important for its proper biological functioning (Rigden et al., 2008). *E. faecalis* $DivIVA_{Ef}$ mutant, *E. faecalis* MWMR16, contained a disrupted coiled coil region, failed to interact with EF1025 in a B2H assay due to the loss of a functional coiled-coil region in $DivIVA_{Ef}$ (Rigden et al., 2008; Hedlin, 2009). Our research addressed the essentiality, localization and function of EF1025 during cell division.

Immunostaining showed that EF1025 localized in a pattern comparable to $DivIVA_{Ef}$ in *E. faecalis*. Previously, Fadda et al 2007 showed DivIVA localization to the mid-cell septa and poles in *S. pneumoniae* using similar methods (Fadda et al., 2007). EF1025 localized laterally along the cell length in Stages 1 and 2 and a pattern comparable to $DivIVA_{Ef}$ in Stages 3, 4 and 5 of cell division. This localization progression may assist proper cell segregation required for cell division during the later stages of cell division when these two proteins interact. GpsB, an essential protein which determines the ellipsoidal shape in *S. pneumoniae*, localized in a similar but not identical manner to FtsZ and is implicated in determining cell shape by septal ring closure (Land et al., 2013). There is a possibility that the localization of EF1025 (a cytosolic protein) to the lateral cell regions could be facilitated by $DivIVA_{Ef}$ association. Different domains of $DivIVA_{Bs}$ have been reported to interact with different partners that are membrane proteins as well as cytosolic proteins (Perry and Edwards, 2006; Bramkamp et al., 2008; Patrick and Kearns, 2008; Briley et al., 2011; dos Santos et al., 2012; Baarle et al., 2013; Halbedel et al., 2014; Schumacher, 2017; Halbedel and Lewis, 2019). Membrane localization of cytosolic proteins enhances the interaction

abilities of interacting partners during processes such as cell division which involves multi-protein complex formation (Yogurtcu and Johnson, 2018).

We postulate that *EF1025* may be an essential gene since, during our attempts to delete or insertionally inactivate the gene, we were never able to recover viable cells. When these strains were complemented with EF1025 (i.e. *E. faecalis* MJ26 and MK12) they grew more slowly with a longer log phase as compared to the *E. faecalis* JH2-2. This most likely occurred because the rescue plasmids (i.e. pMSPEF1025-pro and pMSPEF1025A) failed to provide full complementation. This failure also led to altered cell shape and length. In *S. pneumoniae,* depletion of GpsB, caused cessation of growth and substantial cell elongation (Chastanet and Carballido-Lopez, 2012; Land et al., 2013). Based on the localization pattern of EF1025 and the elongated and aberrant phenotypes exhibited by *E. faecalis* MK12 cells, and the similarity of their localization patterns, we postulate that EF1025 could be one of the members of the septal machinery in *E. faecalis*, which has an unstudied GpsB homologue.

An interesting EF1025 homologue (41% identity) in *B. subtilis,* named CcpN (control catabolite protein of gluconeogenic genes), has two CBS domains and an HTH domain (Servant et al., 2005). CcpN plays a negative regulatory role in the transcription of the gluconeogenic genes *gapB* (one of the GAPDH-encoding genes) and *pckA* (encodes PEP carboxykinase), which are required in carbon catabolite repression pathways (Licht et al., 2005; Servant et al., 2005; Tännler et al., 2008; Licht and Brantl, 2009). Transcription regulation by CcpN has been attributed to its HTH domain which binds to the conserved upstream promoter regions of *gapB* and *pckA* (Licht et al., 2005; Servant et al., 2005; Tännler et al., 2008; Licht and Brantl, 2009). We detected strong interactions between CcpN and $DivIVA_{Bs}$ by B2H and GST-pull down assay (paper in preparation). We observed that *gapB* from *B. subtilis* shared 48% homology with *type I gap* from *E. faecalis* while *pckA* from *B. subtilis* and *E. faecalis* showed 20% homology. *E. faecalis* was observed to have *type I* and *type II gap* as two homologues of *gapB*. Our preliminary sequence searches indicate that the conserved upstream promoter sequences from *B. subtilis* are absent in *E. faecalis* for *type I gapB* and *pckA* (unpublished data). This suggests that even though CcpN and EF1025 belong to the same superfamily, they possibly regulate the expression of different genes. CcpN is not an essential gene in contrast to EF1025 (Servant et al., 2005; Tännler et al., 2008); this may be because each protein may regulate different genes.

In conclusion, this research presents the first evidence of a $DivIVA_{Ef}$ interacting protein, EF1025, in *E. faecalis* that affects cell viability, cell length and shape. Using immunofluorescence, we showed that the localization patterns of EF1025 and $DivIVA_{Ef}$ during the later stages of cell division in *E. faecalis* were similar. Our inability to insertionally inactivate or delete *EF1025* without in trans complementation of the gene indicates that gene is important for viability. Different microscopy methods showed cell elongation, aggregation and impaired cell division in complemented cells with a deleted or inactivated chromosomal gene.

2.6. Supplemental information

2.6.1. Strains, plasmids and growth conditions

Plasmid DNA was purified using Plasmid Mini-prep or Plasmid Midi-prep Kits (Qiagen Inc., CA). Reading frame conservation and gene integrity of all plasmids was confirmed by DNA sequencing [Core DNA Synthesis and Sequencing Facility, Centre for Research in Biopharmaceuticals and Biotechnology, University of Ottawa, (UOCDSSF), the Plant Biotechnology Institute (PBI), National Research Council of Canada, Saskatoon, Saskatchewan] or Eurofins Canada. Primers (Table S3) were synthesized at the UOCDSSF and Invitrogen (Thermo Scientific; Waltham, MA), and were used for PCR and DNA sequencing reactions. PCR reactions were carried out using Q5 DNA polymerase (New England BioLabs Ltd., ON, Canada) in a Perkin Elmer GenAmp PCR System 9600 Thermocycler (Perkin Elmer, Inc., Woodbridge, ON, USA).

2.6.2. Cloning and screening an *E. faecalis* genomic DNA library by Y2H assay

An *E. faecalis* JH2-2 genomic DNA library was created in the Y2H system (Clontech) using the vector pGAD424 of the Clontech Matchmaker GAL4 Two-Hybrid System (Clontech) (Table S2C). *E. faecalis* JH2-2 genomic DNA was prepared using the Wizard Genomic DNA Purification Kit according to the manufacturer's instructions (Promega, Madison, WI USA). Approximately 10 µg genomic DNA was partially digested with Sau3AI and size-fractionated by agarose gel electrophoresis. DNA fragments ranging between 0.2- to 1.5-kb were excised from the gel and purified using PCR Purification Kit (Qiagen). Purified DNA fragments were then ligated to pre-cleaved *Bam*HI-pGAD424. The ligation mixture was transformed into *E. coli* DH5α competent cells and transformants were selected on LB plates supplemented with Amp 100 µg/ml (LB-Amp). Colonies were harvested by washing the plates with LB-Amp broth. Approximately 1×10^5 colonies were collected in 50 ml LB-Amp broth which was incubated at 37°C for 2 hrs, followed by centrifugation to collect pelleted cells. Plasmid DNA was purified using Midi-prep Kit (Qiagen) and was named pGAD424-Lib (Table S2C). Colony counts were estimated by serially diluting an aliquot of the cell suspension in LB-Amp broth.

To determine the ratio of colonies harbouring a plasmid with an inserted DNA fragment and sizes of the inserts, 30 individual colonies were randomly selected from the original library

and were sub-cultured on LB-Amp broth. Plasmid DNA was purified and double digested with EcoRI/BglII followed by electrophoresis on 1% agarose gels. 77% (23/30) of the recombinant clones carried inserts of sizes ranging between ~350 bp to ~2 kb. To determine the quality of the library, an aliquot of the purified library plasmid DNA (pGAD424-Lib) or the parental vector pGAD424 DNA was digested with SnaBI/PstI. The digested library DNA (pGAD424-Lib) exhibited DNA fragments of various sizes that were bigger than 1.5 kb, indicating that the majority of the library plasmid DNA carried inserts (data not shown).

To screen the library, the previously constructed plasmid pSRBD-Div was used to express the bait protein, $DivIVA_{Ef}$ (Table S2C; (Ramirez-Arcos 2005)). Plasmids pSRBD-Div and pGAD424-Lib were co-transformed into *S. cerevisiae* SFY526 according to the manufacturer's instructions (Clontech). Transformants were selected on complete synthetic medium lacking leucine and tryptophan (SD-leu-trp) (Clontech). After 3-4 days of incubation at 30°C, blue-coloured clones were screened in the presence of 5-Bromo4-chloro-3-indolyl-β-D-galactopyranoside (X-Gal, Sigma-Aldrich; St. Louis, MS) by a colony–lift filter assay (Clontech). Positive clones were streaked on SD-leu-trp medium plates (Clontech). A spectrophotometric assay for β-galactosidase activity, using the substrate o-nitrophenyl β-$_D$-galactopyranoside (ONPG liquid assays), was performed to confirm the results of the colony-lift assay (Ramirez-Arcos, 2005). Transformation efficiency was monitored by plating 50 µL of diluted transformants on SD-leu-trp medium plates followed by counting the number of colonies produced.

In a positive clone, pGAD424-Lib plasmid was separated from a pSRBD-Div by sub-culturing the yeast cells of the positive clone in SD-leu-trp broth for 2-4 days at 30°C. Cells were harvested by centrifugation and the cell pellet was re-suspended in 250 µL of Qiagen buffer P1 (Qiagen plasmid mini-prep kit) with 10 µL glass beads (Sigma), followed by vigorous vortexing for 3 min. P2 buffer (250 µL, Qiagen) was added to the lysate, and plasmid DNA was purified. To isolate plasmid pGAD424-Lib, the aforementioned purified plasmid DNA was transformed into *E. coli* DH5α cells and the resulting *E. coli* colonies were examined for plasmid content in a cracking assay (Ramirez-Arcos, 2005). The size of released supercoiled plasmid DNA was determined by electrophoresis on 1 % agarose gels. The difference in the size of pSRBD-Div (6.2 kb) and pGAD424-Lib (≥6.6 kb) allowed easier separation from each other. The plasmid of interest (i.e. pGAD424-Lib) was then purified from *E. coli* transformants and analyzed by restriction endonuclease digestion with EcoRI/PstI. Purified plasmid DNA was sequenced at the

UOCDSSF using primers AD424F and AD424R (Supplementary Materials, Table S3C) to generate DNA sequences of the inserts in pGAD424-Lib for bioinformatic identification of the discovered genes.

2.6.3. Reverse transcriptase PCR (RT-PCR)/qPCR

Total RNA from *E. faecalis* JH2-2 and MJ26 was isolated using the Qiagen RNeasy Total RNA kit (Qiagen) for RT-PCR assay which was performed as previously described (Fadda et al., 2003). cDNA was created from total isolated RNA by incubating ~0.1 µg RNA, 0.5 unit reverse transcriptase (Promega) and 2 µl random primer mix at 42°C for 30 min. This cDNA was used to amplify *EF1026* from JH2-2 and MJ26 using primers EF26aF/R, EF26bF/R (Table S3E). The housekeeping gene, *gdh* (encoding glucose dehydrogenase) was used as a positive control and was PCR amplified using primers HKaF/R, HKbF/R (Table S3E). PCR amplification of genomic DNA using primers EF26aF/R served as a positive control whereas PCR amplification of total RNA using primers EF26aF/R served as a negative control. PCR products were separated by electrophoresis on 1.5% agarose gel for further analysis. For qPCR, cDNA from *E. faecalis* JH2-2 was used to create standards using primers EF26aF/R (Table S3E) and was used to identify EF1026 levels in *E. faecalis* MJ26. Each reaction was performed in triplicate and contained 2X SYBR-Green master mix (Cat # 4472912, Life Technologies Inc.), 0.25 µL of each primer (10 µM), 1 µL of DNA (50 ng/µL), and 3.5 µL PCR-grade water in a total 10 µL reaction volume.

2.6.4. Expression of *EF1025* in *E. coli* PB103

To express *EF1025* in *E. coli* PB103, *EF1025* was PCR-amplified from *E. faecalis* JH2-2 and cloned into pUC18 (Amersham), resulting in plasmid pUCHisEF1025 (Table S2F). For controls, *prgX*, a transcriptional regulator of itself and PrgB (cell wall aggregation substance) (Bhatty et al., 2015; Bae et al., 2000), was PCR-amplified from pSR-X (Table S2F; Bae et al., 2000; Rigden et al., 2008) and cloned into pUC18, resulting in plasmid pUCHisPrgx, which encodes 6×His tagged PrgX (Table S2F). Each plasmid was individually transformed into *E. coli* PB103 and transformants were selected on LB medium supplemented with Amp100 creating strains *E. coli* PB MK23 and *E. coli* PB MK25, respectively (Table S1). Expression of 6×His-EF1025 or 6×His-PrgX was determined by Western blot assays using anti-6×His monoclonal antibodies (Biorad).

2.6.5. Atomic force microscopy

For atomic force microscopy, cell suspensions from overnight grown cultures of *E. faecalis* were deposited onto Cell-Tak (LifeTechnologies) coated coverslips for 30 min, fixed with formalin, and air-dried prior to AFM imaging (Bhat et al., 2015). Samples were imaged with silicon nitride cantilevers (HYDRA6R-200NG; Nanosensors, Neuchatel, Switzerland) with calibrated spring constants ranging from 0.03 to 0.062 N/m. QI™ images and force curves (JPK software) at each pixel of a 128×128 raster scan were collected using a Z-length of 0.926 um and a scan rate of 95 um/s. Surface roughness was calculated according to Bhat et al. (2015) from multiple 200 x 200 nm squares along the centre of the cell from QI™ height images for at least 10 cells each from three biological replicates.

The morphology of *E. coli* PB103 harboring pUCHisEF1025 was ascertained using an Olympus BX61 microscope (Olympus Canada Inc.), as described previously (Ramirez-Arcos et al., 2001). At least 30 fields were examined each containing a minimum of 40 cells.

2.6.6. Statistical analysis

All studies were conducted in triplicates and GraphPad Prism was used for statistical analysis unless otherwise indicated. The results were reported as mean ± standard deviation (SD), differences assessed using a two-tailed unpaired t-test and ANOVA for which $p < 0.05$ was considered statistically significant.

Table S1. Bacterial strains used in the study.

Strains	Relevant characteristics	Resources or references
E. coli XL1-Blue	*recA1 endA1 gyrA96 thi-1 hsdR17 supE44 relA1 lac* [F´ *proAB lacI*q*Z_M15*Tn*10* (Tetr)]	Strategene
E. coli DH5α	*endA*1 hsdr17 ($r_k^- m_k^+$) *supE*44 *thi*-1 *recA*1 *gyrA*96 *relA*1 Δ(*arg*F-*lac*ZYA) *U*169 *deoR* [ø80d *lac* Δ(*lacZ*) M15)	Gibco-BRL
E. coli C41 (DE3)	F^- *ompT hsdS*$_B$ (*r*$_B$-*m*$_B$-) *gal dcm Δ(srl-recA)* 306::Tn*10* (*tet*^{R}) *(DE3)*	Miroux et al., 1996
E. coli PB103	*dadR1 trpE61 trpA62 tna-5 purB*$^+$	de Boer et al., 1988
E. coli R721	71/18 *glpT*::O-P434/P22*lacZ*	Di Lallo et al., 2001, 2003
E. faecalis JH2-2	Rif^R, Fus^R; plasmid free	Jacob & Hobbs, 1974
S. cerevisiae SFY526	*MATa ura3-52 his3-200 ade2-101 lys2-801 trp1-901 leu2-3 112 can*^{r} *gal4-542 gal80-538 URA3::GAL1*$_{UAS}$- *GAL1*$_{TATA}$ *–lacZ*	Clontech Laboratories, CA
E. faecalis MK0	*E. faecalis* JH2-2 carrying pMSP3545A	This study
E. faecalis MK23	*E. faecalis* JH2-2 carrying pMSPEF1025A (P$_{EF1025}$-*EF1025*) for expressing *EF1025 in trans* under its native promoter. Ery^R (125 µg/mL)	This study
E. faecalis MK24	*E. faecalis* JH2-2 carrying pMSPEF1025-flag (P$_{EF1025}$-*EF1025-flag*) for expressing *EF1025*-flag *in trans* under its native promoter. Ery^R (125 µg/mL)	This study
E. faecalis MJ26	Derived from *E. faecalis* JH2-2 with insertionally inactivated *EF1025* (*EF1025::kan*^{R}). *E. faecalis* MJ26 carried pMSPEF1025-Pro (P$_{EF1025}$-*EF1025*) for expressing *EF1025 in trans* under its native promoter. Kan^R (500 µg/mL) and Ery^R (125 µg/mL)	This study
E. faecalis MK12	Derived from *E. faecalis* JH2-2 with deletion of *EF1025* (Δ*EF1025::cat*^{R}). *E. faecalis* MK12 carried pMSPEF1025A (P$_{EF1025}$-*EF1025*) for expressing *EF1025 in trans* under its native promoter. Cat^R (5 µg/mL) and Ery^R (125 µg/mL).	This study
E. coli PB MK23	Derived from *E. coli* PB103 for overexpressing *EF1025* using pUCHisEF1025. Amp^R (100 µg/mL)	This Study
E. coli PB MK25	Derived from *E. coli* PB103 for overexpressing *prgX* using pUCHisPrgx. Amp^R (100 µg/mL).	This Study

Table S2. Plasmids used in this study

Plasmid	Relevant characteristics	Sources or references
(A) Plasmids for bacterial two-hybrid assays		
pcI434	Kan^R, bacterial two-hybrid vector	Di Lallo et al., 2001
pcIp22	Amp^R, bacterial two-hybrid vector	Di Lallo et al., 2001
pcIp22-L	pcI_{P22} derivative carrying a linker with multiple cloning sites	This study
pcI434-L	pcI_{434} derivative carrying a linker with multiple cloning sites	This study
pdivIVA22	pcI_{P22} derivative carrying *E. faecalis divIVA*	This study
pdivIVA434	pcI_{434} derivative carrying *E. faecalis divIVA*	This study
pEF1025434	$pcI_{P434}L$ derivative carrying *EF1025*	This study
p22CBS1CBS2	$pcI_{P22}L$ derivative carrying *EF1025* fragment coding AA80-204	This study
p434CBS1CBS2	$pcI_{434}L$ derivative carrying *EF1025* fragment coding AA80-204	This study
(B) Plasmids for GST pull-down assays and 6×His tagged protein expression		
pGEX-2T	Amp^R P_{lac}*::gst*	Amersham Bioscience
pGST-Div	Amp^R P_{lac}*::gst*, GST-$DivIVA_{Ef}$	This study
pET30a(+)	Kan^R P_{T7}::*6xhis*	Novagen
pETEF1025	Kan^R P_{T7}, 6xHis-EF1025	This study
pETEF1025CBS12	Kan^R P_{T7}, 6xHis-EF1025 with CBS1 and CBS2 domains	This study
(C) Plasmids for EF1025 self-interaction studies		

pGAD424	Amp^R P_{ADH1}*::gal4* (AD)	Clonetech, CA
pGBT9	Amp^R P_{ADH1}*::gal4* (DBD)	Clonetech, CA
pGADEF1025CBS12	Amp^R P_{ADH1}*::gal4* (AD), AD-EF1025 with CBS1 and CBS2 domains (AA80-204)	This study
pGBDEF1025CBS12	Amp^R P_{ADH1}*::gal4* (DBD), DBD- EF1025 with CBS1 and CBS2 domains (AA80-204)	This study
pGADEF1025NCBS1	Amp^R P_{ADH1}*::gal4* (AD), AD-EF1025 with N-terminal and CBS1 domains (AA1-137)	This study
pGBDEF1025NCBS1	Amp^R P_{ADH1}*::gal4* (DBD), DBD-EF1025 with N-terminal and CBS1 domains (AA1-137)	This study
pGADEF1025CBS2	Amp^R P_{ADH1}*::gal4* (AD), AD-EF1025 with CBS2 domain (AA137-204)	This study
pGBDEF1025CBS2	Amp^R P_{ADH1}*::gal4* (DBD), DBD- EF1025 with CBS2 domain (AA137-204)	This study
pGADEF1025-N	Amp^R P_{ADH1}*::gal4* (AD), AD-EF1025 with N-terminal domain (AA1-50)	This study
pGBDEF1025-N	Amp^R P_{ADH1}*::gal4* (DBD), DBD- EF1025 with N-terminal domain (AA1-50)	This study
pGADEF1025	Amp^R P_{ADH1}*::gal4* (AD), AD-EF1025 (AA1-209)	This study
pGBDEF1025	Amp^R P_{ADH1}*::gal4* (DBD), DBD-EF1025 (AA1-209)	This study
pSRBD-Div	Amp^R P_{ADH1}*::gal4* (DBD), DBD-$DivIVA_{Ef}$	(Ramirez-Arcos, 2005)
pGAD424-Lib	*E.faecalis* genomic DNA library constructed in pGAD424 vector	This study
(D) Plasmids for construction of an *EF1025* insertion or deletion strain and plasmids to overexpress *EF1025* in *E. faecalis* JH2-2		
pMSP3545	Ery^R P_{nisA}*::nisA*	Callegan et al., 1999

pcDNA3.1(+)	Amp^R Neo^R, P_{lac}, P_{SV40} and P_{T7}*::flag*	Invitrogen
pMSP3545A	Ery^R, Amp^R, P_{nisA}*::nisA*	This study
pMSPEF1025A	Ery^R, Amp^R P_{EF1025}*::EF1025* for *EF1025*expression under its native promoter	This study
pMSPEF1025-flag	Ery^R, Amp^R P_{EF1025}*::EF1025* for *EF1025* expression under its native promoter with flag tag on C-terminus	This study
pMSPEF1025-pro	Ery^R P_{mljd}*::mljd1* for *EF1025* expression under its native promoter	This study
p3ERMEF1025::Kan	p3ERM Δ*Hind*III, *EF1025::Kan*	This study
p3ERMΔEF1025::Cat	p3ERM Δ*Hind*III, Δ*EF1025::Cat*	This study
pUC18	Amp^R P_{lac}*::lacZ*	Amersham Biosciences
pUCEF1025-N	N-terminus of EF1025 ligated in pUC18	This study
pTCV-lac	Kan^R::*lacZ*	Poyart & Trieu-Cuot, 1997
pUCEF1025-N-Kan	N-*EF1025* (5')-kan^R	This study
pUCEF1025::Kan	*EF1025::*kan^R	This study
pLEMO	Cat^R, P_{T7}, pACYC184 derivative carrying *lysY*	New England Biolabs
(E) Plasmids for heterologous expression of *EF1025* in *E. coli*		
pUCHisEF1025	Amp^R P_{lac}, 6xHis-EF1025	This study
pSR-X	Amp^R P_{lac}, PrgX	This study
pUCHisPrgx	Amp^R P_{lac}, 6xHis-Prgx	This study

Table S3. Primers used in this study

Primer	**Sequence (5’ to 3’)**
(A) Primers for B2H experiments	
EF1025-F	GCGTCGAC TTATCTGTTTTGTGCG
EF1025-R	GCGGATCCCTACGTAATATAGGTTAAAATTTTCGT
EF1025C-F	GCGTCGACGGAGATCATGAGTCCACCA
EF1025C-R	GCGGATCCCTACGTAATATAGGTTAAAATTTTCGT
CBdivIVA-F	GCGTCGACTATGGCATTAAC
CBdivIVA-R	GCGGATCCCTATTTTGATTC
(B) Primers for GST pull-down assays	
IVA-5	GCGCGGATCCATGGCATTAACTCCATTAGA
IVA-11	GCGCGAATTCTTACTATTTTGATTCTTCTTCAA
EF1025F-F	CGCTTAAGTTATCTGTTTTGTGCG
EF1025F-R	CGGGATCCATGAAATTAAGTAAACG
EF1025-CF	CGCGGATCCCCACCATTGATGGTTGCCCAAGAC
EF1025-CR	GCCCTCGAGCCCTTATCTGTTTTGTGCGGCTTC
(C) Primers for EF1025 self-interaction studies and other Y2H assays	
AD424F	ACCACTACAATGGATGAT

AD424R	ACAGTTGAAGTGAACTTG C
CBSDPF	GCCGGAATTCATGAAATTAAGTAAACG AC
CBSDPR2	AAACTGCAGTTATCTGTTTTGCGGC
CBSAA80F	CGGGATCCATGAGTCCACCAT TG
CBSAA137R	AAACTGCAGTTAATTTAAAGAGGC
CBSAA137F	CGGAATTCAATACAAATATTGATGGC
DEORR	AAACTGCAGTTAAACTTTCGGACTTGC
AD424F	ACCACTACAATGGATGAT
AD424R	ACAGTTGAAGTGAACTTG C
(D) Primers for construction of an *EF1025* knockout strain and plasmids to overexpress *EF1025* in *E. faecalis* JH2-2	
AmpF	GGAGTCTAGAGCTACCATGGATCCGTGCGCGGAACCCCTATTTG
AmpR	GAACGAGATCTGTCTGACGCTCAGTGGAACG
LinkA	GGTGTCAACGATATCCTCC
LinkB	AATTGGAGGATATCGTTGACACCTTC
EF1025npF	GAGCCCATGGCGTGACCTCCGTTTAATATGTG
EF1025npR	GGGTCTAGATTAAGCTCCCTTATCTGTTTTGTG
CBSDPF	GCCGGAATTCATGAAATTAAGTAAACG AC
CBS55-R-Hind	CCCAAGCTTAACTTTCGGACTTGC

KanF	CCCAAGCTTGTGGTTTCAAAATCG
KanR	TCCCCCGGGTTAGGTACTAAAACA
CBS55-F-Sma	TCCCCCGGGGCAAGTCCGAAAGTTG
EF1025-R-BamHI	CGGGATCCTTATCTGTTTTGTGCGGC
Mut-F	CTCTTTACCTTCATTGTGTG
ProF	AACTGCAGCAAAATTTCTGATTGTAAGTG
CBSDPR	AAACTGCAGTTATCTGTTTTGCGGC
ppdKF	GAGGGATCCAGCACCGCTGCGAACGGAAACTAAG
ppdKR	CCAGTGATTTTTTTCTCCATCATTTCCTCCTCAATTCCTC
1026F	GAGTGGCAGGGCGGGGCGTAAGGGAGCTTAATTATGAAAAAAGAG
1026R	GAGGAATTCTACATACTGACTGGCGTCTTTGAGG
CatF	GAGGAATTGAGGAGGAAATGATGGAGAAAAAAATCACTGGATATAC
CatR	CTTTTTTCATAATTAAGCTCCCTTACGCCCCGCCCTGCCACTC
FlagF	GATCTTTATAATCACCGTCATGGTCTTTGTAGTCG
FlagR	GAGATCTAGACTACTTGTCATCGTCATCCTTG
(E) Primers used for RT-PCR	
EF25aF	CGCATTTCGGACATACTAGC
EF25aR	TTGGGCAACCATCAATGGTG

EF26aF	TCAAGCGAAAGCCGGAGTAG
EF26aR	ACTGACTGGCGTCTTTGAGG
EF26bF	CAGTCGGTTGGCTTCCTTAG
EF26bR	CACTGGGATGCCATACTTCG
HKaF	TGGTGCAGCTACGGGTTTAG
HKaR	CTTTAGGCAGCTCACCGACA
HKbF	CTGGTGCAGCTACGGGTTTA
HKbR	GCTCACCGACATAGTCAGCA
(F) Primers used for the construction of plasmids to express *EF1025* in *E. coli* PB103	
HisEF1025F3	CGGAATTCGCACCATCATCATCATCATATGAA
EF1025-R-BH	CGGGATCCTTATCTGTTTTGTGCGGC
HisPrgxF2	CGGAATTCGCACCATCATCATCATCATATGAC
PrgxR2	GCTCTAGATTAGTTTAAGATAGGTTC

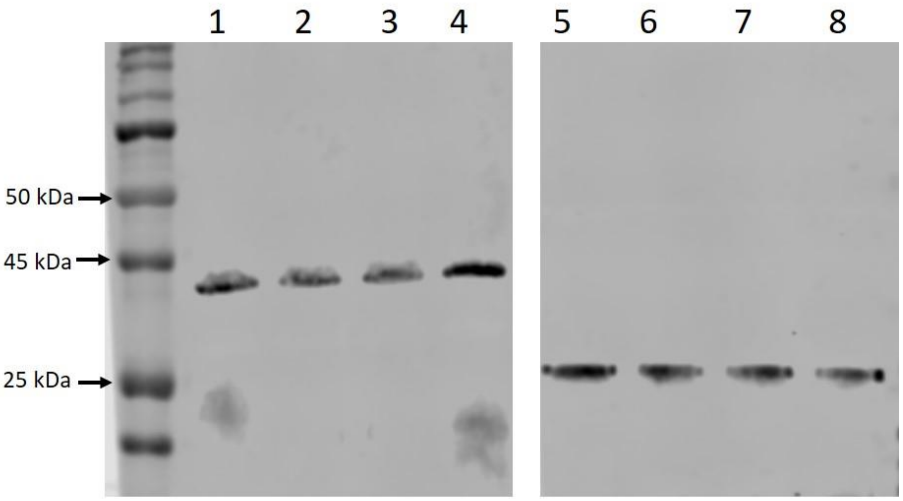

Figure S1. Western blot exhibiting specificity of anti-DivIVA$_{Ef}$ and anti-EF1025 antibody for DivIVA$_{Ef}$ and EF1025. An *E. faecalis* whole cell lysate was probed with anti-DivIVA$_{Ef}$ (Lanes 1-4), and anti-EF1025 (Lanes 5-8). A protein ladder confirmed the presence of protein bands of sizes corresponding to DivIVA$_{Ef}$ (40 kDa) or EF1025 (27 kDa).

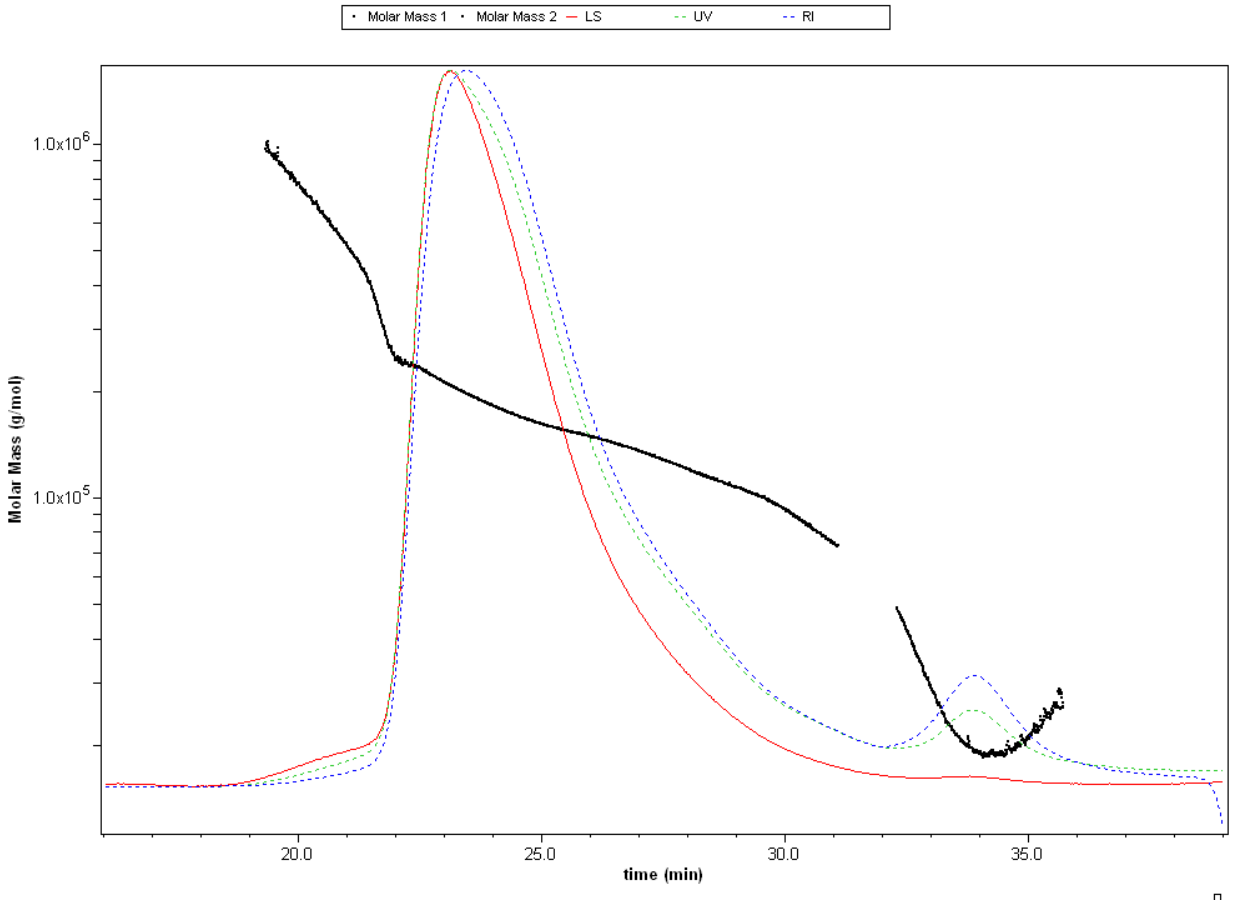

Figure S2. Light scattering (LS) data and measured molar mass for EF1025 by SEC-MALS. Separated by SEC and detected using the μDAWN and UT-rEX (red) detected with the Wyatt TREOS and Optilab T-rEX (blue). The plot shows the chromatograms as a function of elution time. The average molecular weight calculated was 222 kDa for the complex. Black line shows the aggregation profile of the protein.

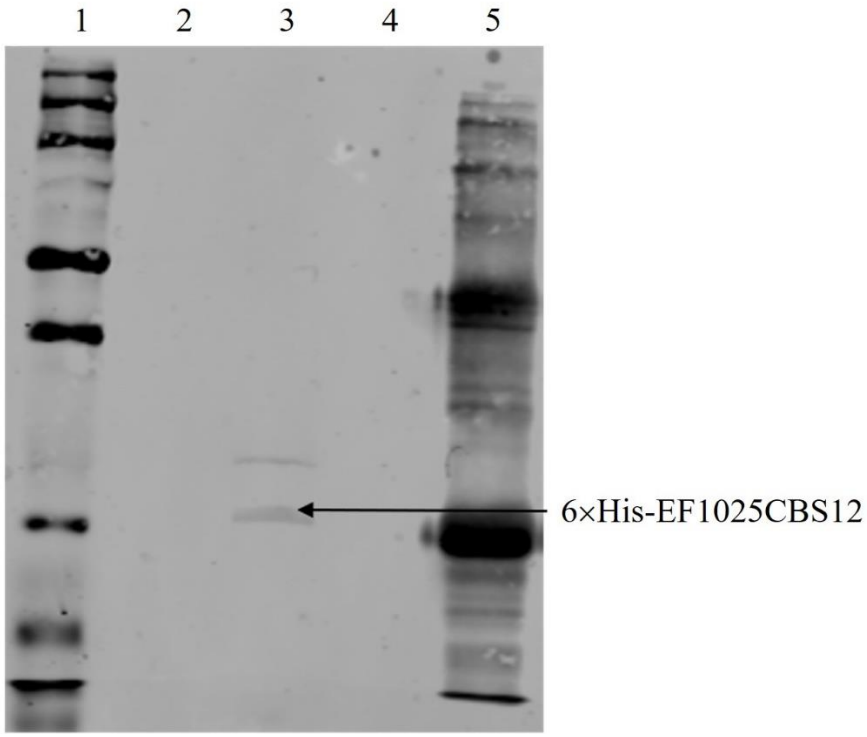

Figure S3. EF1025CBS12 interacts with $DivIVA_{Ef}$ in GST pull-down assay. Shown is a Western blot probed with an anti-6xHis EF1025 monoclonal antibody. Lane 1: Protein Ladder; Lane 2: GST bound beads; Lane 3: GST-$DivIVA_{Ef}$ bound beads; Lane 5: *E. faecalis* extracts representing 10% input of EF1025CBS12.

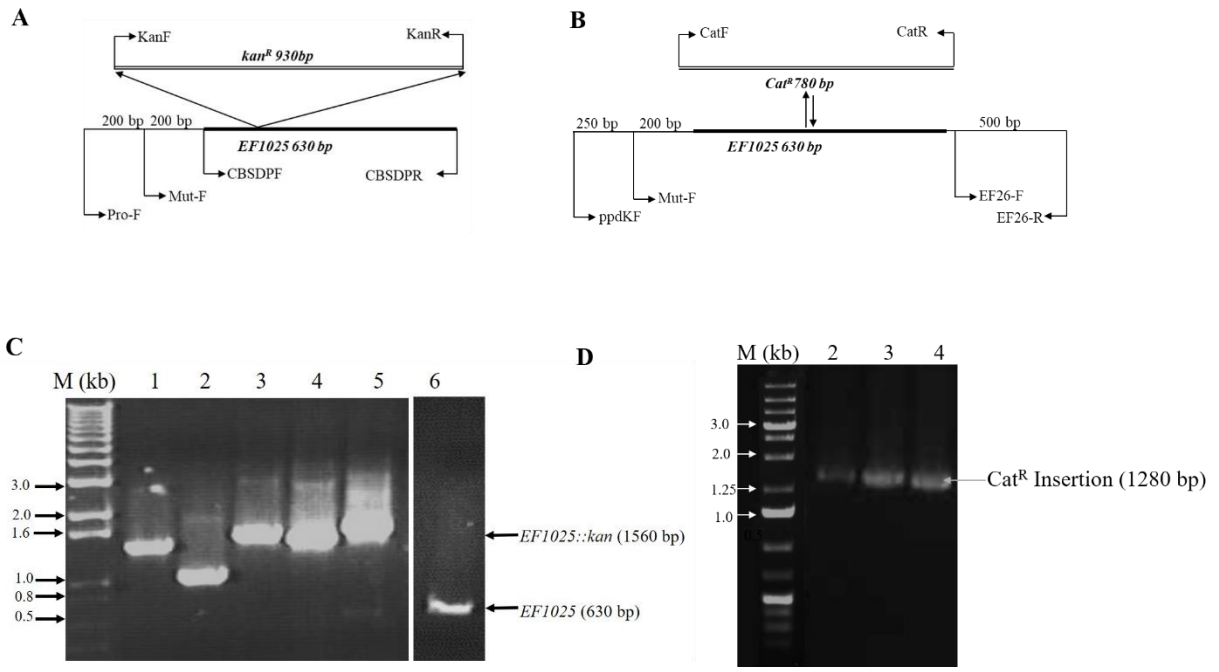

Figure S4. PCR Confirmation for creation of *E faecalis* MJ26 and *E faecalis* MK12. (A) Schematic presentation of genomic insertional inactivation of *EF1025* in *E. faecalis*. A *kan*^{R} cassette was inserted at the nt151 position of *mljd1*. Arrows indicated primers used for PCR amplification to confirm Kan^R insertion in the *E. faecalis* genomic DNA; (B) Schematic presentation of deletion of *EF1025* in *E. faecalis*. (C) PCR confirmation of insertional mutation. PCR was performed on *E. faecalis* MJ26 genomic DNA using primer pairs Mut-F/Kan-R (Lane 1- 1300 bp), Kan-F/Kan-R (Lane 2- 930 bp), Pro-F/Kan-R (Lane 3- 1500 bp), Kan-F/CBSDPR (Lane 4- 1409 bp) and CBSDPF/CBSDPR (Lane 5- 1560 bp and 630 bp). M: 1kb plus DNA ladder. Presence of wild type *EF1025* was due to the presence of co-transformed plasmid pMSPEF1025-Pro (Lane 5). Lane 6: cropped lane from same gel with amplified wild type *EF1025*; (D) PCR confirmation of *EF1025* deletion using primer pairs ppdKF/EF26b-R (Lane 2- 1780 bp), mutF/EF26b-R (Lane 3- 1480 bp), catF/1026R (Lane 4- 1280 bp).

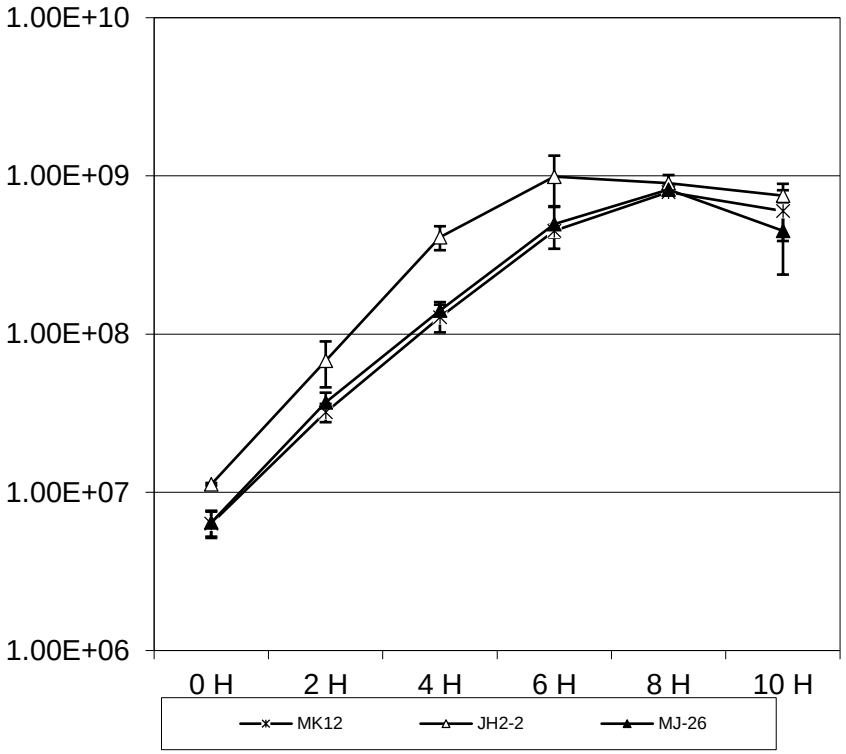

Figure S5. *E. faecalis* MJ26 and MK12 grew slower than *E. faecalis* JH2-2 cells. Viability curve of *E. faecalis* MJ26 cells. Growth was measured by OD at 600nm and normalised for each sample. *E. faecalis* MJ26 cells were subcultured on BHI containing appropriate antibiotics. Samples were withdrawn for plating every 2 hours. X- axis: Viable counts (CFU/ml), Y- axis- time (hours). X marked line- *E. faecalis* MK12; Open triangle line- *E. faecalis* JH2-2; Closed triangle line- *E. faecalis* MJ26. The error bars represent 1 standard deviation.

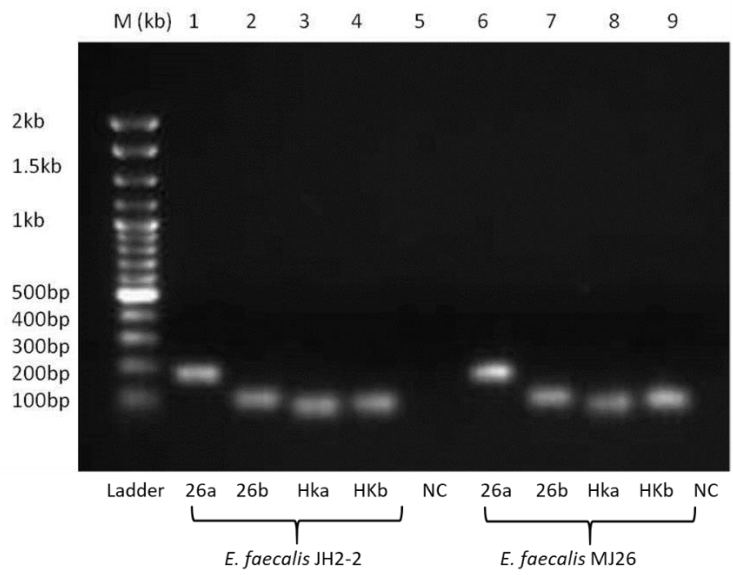

Figure S6. Figure S6. RT-PCR of EF1026 in *E. faecalis* JH-2-2 and MJ26 showing absence of polar effect. PCR amplified products corresponding to EF1026 from JH-2-2 and MJ26. Lanes 1 and 2: EF_1026 from *E. faecalis* JH-2-2, Lanes 3 and 4: *gdh* from *E. faecalis* JH-2-2, Lane 5: negative control E. *faecalis* JH-2-2 with no reverse transcriptase; Lanes 6 and 7: EF_1026 from *E. faecalis* MJ26, Lanes 8 and 9: *gdh* from *E. faecalis* MJ26, Lane 10: negative control from *E. faecalis* MJ26 with no reverse transcriptase. *gdh*- glucose dehydrogenase (housekeeping gene).

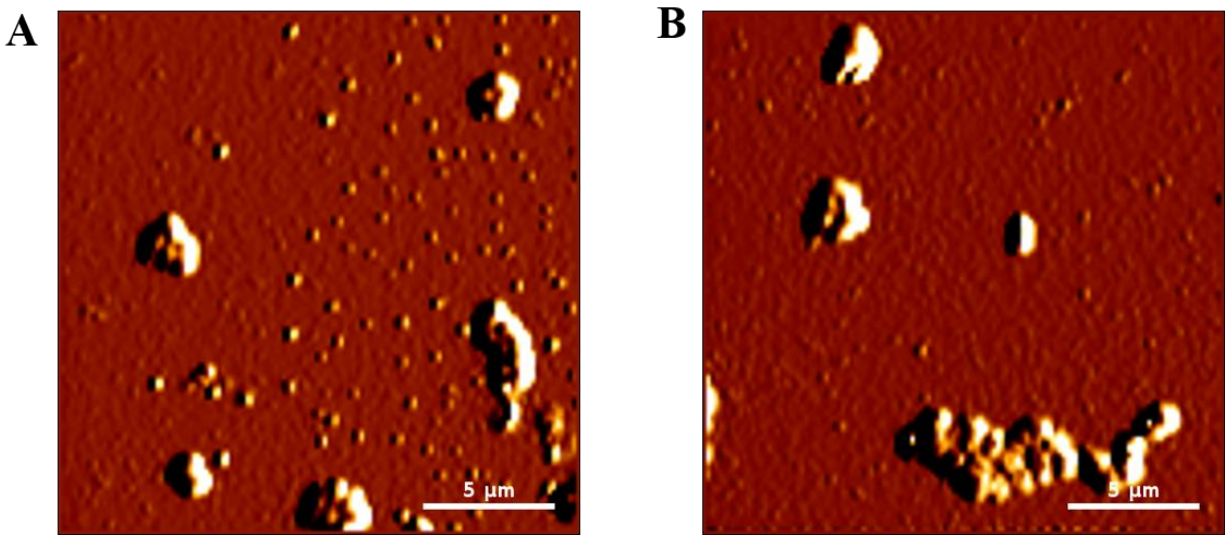

Figure S7. *E. faecalis* MK12 cells exhibit larger aggregates than JH2-2. Representative AFM error images of *E. faecalis* JH2-2 (A) and *E. faecalis* MK12 (B) collected in QI mode with a resolution of 128×128 pixels per image. Both JH2-2 and MK12 form relatively frequent cell aggregates that are larger for MK12. Since these clusters had irregular shapes and cell numbers, sizes could not be accurately estimated. Bar scale (5 µm) indicated at the bottom right corner of each image.

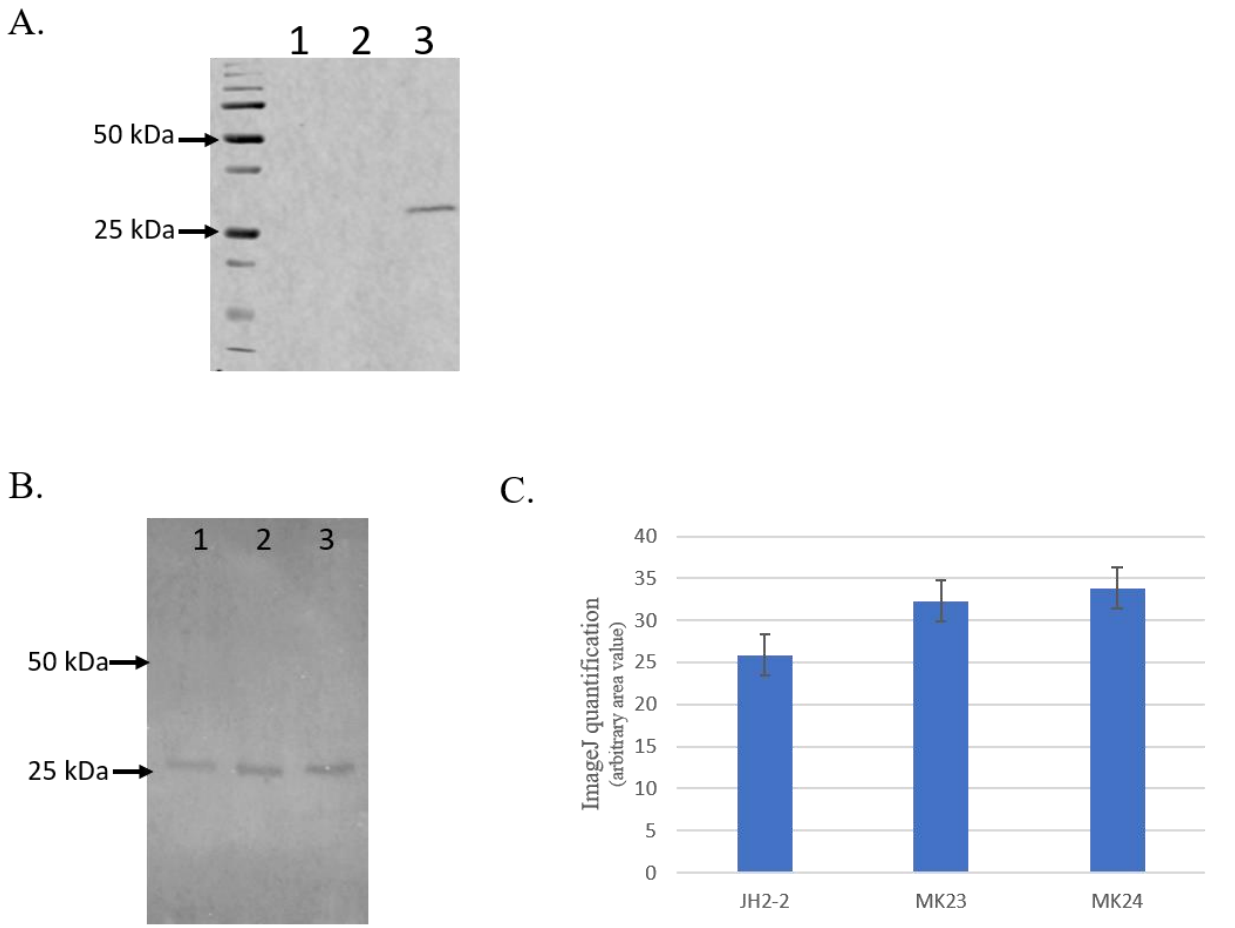

Figure S8. Shown are (A) Western blot probed with anti-Flag antibody to detect the presence of EF1025-flag in *E. faecalis* MK24. (B) Representative Western blot probed with anti-EF1025 to detect the presence of EF1025. Whole cell extract from: Lane 1: *E. faecalis* JH2-2; Lane 2: *E. faecalis* MK23; and Lane 3: *E. faecalis* MK24. (C) Densitometric quantification of band intensities corresponding to EF1025 from strains *E. faecalis* JH2-2, *E. faecalis* MK23, and *E. faecalis* MK24.

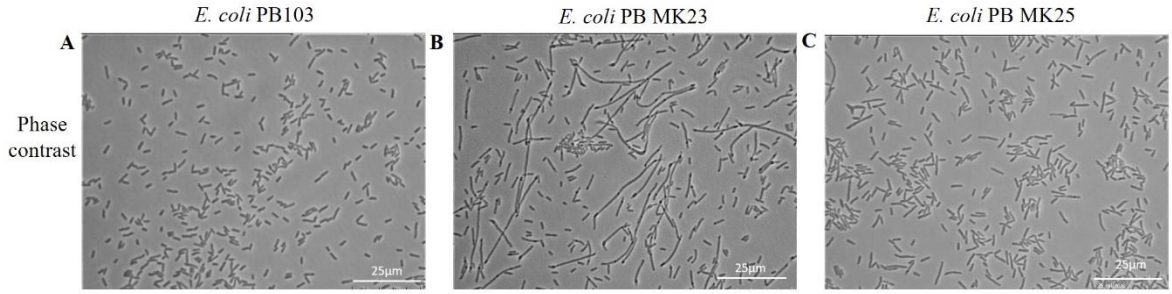

Figure S9. Overexpression of *EF1025* in *E. coli* PB103 leads to severe cell elongation. Phase contrast microscopy of *E. coli* PB103 cells. (A) *E. coli* PB103 cells; (B) filamentous *E. coli* PB MK23 (>15 µm) cells transformed with pUCHisEF1025, and (C) *E. coli* PB MK25 overexpressing $prgX_{Ef}$. Scale bars represent 25 µm; n=89.

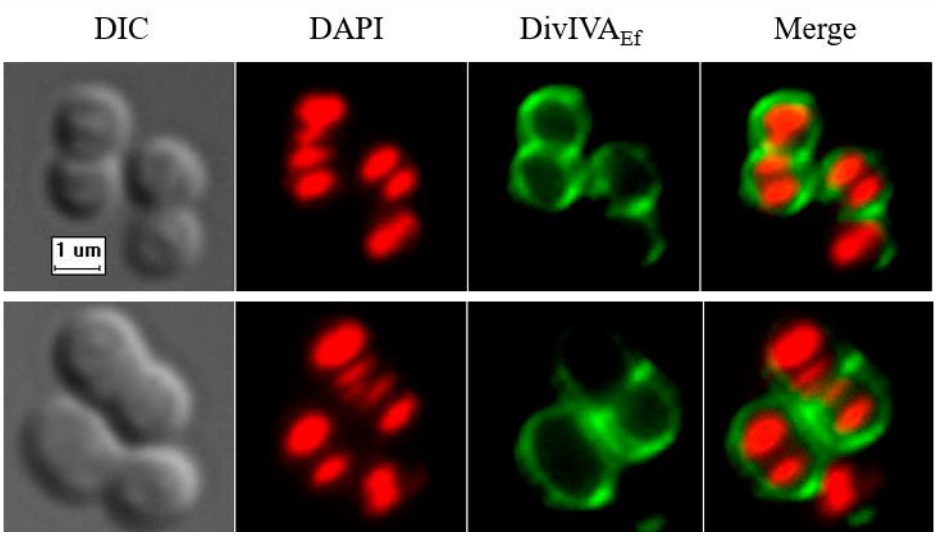

Figure S10. DivIVA$_{Ef}$ exhibited loss of localization at the cell poles and midcell position in *E. faecalis* MWMR16 cells. Averaged images and fluorescence intensity traces of *E. faecalis* MWMR16 cells grown to mid-exponential phase in BHI broth and dual-stained with DAPI and Alexa-Fluor 488 as described in the methodology section and images were acquired using the InVitro 3 and ImagePro 6.0 softwares (Media Cybernetics) as described in Methodology. DivIVA$_{Ef}$ with coiled-coil disrupted region localized along the cell membrane.

Chapter 3. CcpN: a moonlighting protein regulating catabolite repression of gluconeogenic genes in *Bacillus subtilis* also affects cell length and interacts with DivIVA

Kusum Sharma[1], Taranum Sultana[2], Tanya E S Dahms[2] and Jo-Anne R Dillon[1,3*]

[1] kus601@mail.usask.ca

Department of Biochemistry, Microbiology and Immunology, College of Medicine, University of Saskatchewan, 107 Wiggins Road, Saskatoon, Saskatchewan, Canada S7N 5E5.

[2] taranum.sultana@uregina.ca

Ph.D., Department of Chemistry and Biochemistry[3], 3737 Wascana Parkway, University of Regina, Regina, Saskatchewan, Canada S4S 0A2.

[2] tanya.dahms@uregina.ca

Professor, Department of Chemistry and Biochemistry[3], 3737 Wascana Parkway, University of Regina, Regina, Saskatchewan, Canada S4S 0A2.

Phone: 306-585-4246

[3] j.dillon@usask.ca

*Corresponding author:

Distinguished Professor, Department of Biochemistry, Microbiology and Immunology, College of Medicine, Research Scientist, Vaccine and Infectious Disease Organization, University of Saskatchewan, 120 Veterinary Road, Saskatoon, Saskatchewan, Canada S7N 5E3.

Phone: 306-966-1535

Submitted to: **Canadian Journal of Microbiology**

Keywords: Gluconeogenesis, Enterococcus faecalis, DivIVA, protein-protein interaction, Bacillus subtilis, CcpN

Author contribution:

We are grateful to Cherise Hedlin (University of Saskatchewan) for creating *B. subtilis ccpN* knockout (i.e. Bs KS1685). Thank you to Jared Price and Henrique Cardoso Batista Brandão (University of Regina) for their help in collecting the AFM images. Kusum Sharma performed all interaction studies (i.e. B2H and GST-pull down assays), microscopy experiments and statistical analysis pertaining to SEM and AFM experiments.

3.1. Abstract

CcpN is a transcriptional repressor in *Bacillus subtilis* that binds to the promoter region of *gapB* and *pckA*, downregulating their expression in the presence of glucose. CcpN also represses *sr1*, which encodes a small non-coding regulatory RNA that suppresses the arginine biosynthesis gene cluster. CcpN has homologues in other Gram-positive bacteria including *Enterococcus faecalis*. We report the interaction of CcpN with DivIVA of *B. subtilis* as determined using Bacterial two-hybrid and GST pull-down assays. Insertional inactivation of CcpN leads to cell elongation and formation of straight chains of cells. These findings suggest that CcpN is a moonlighting protein involved in both gluconeogenesis and cell elongation.

3.2. Introduction

DivIVA is a highly conserved cell division protein in Gram-positive bacteria which interacts with a variety of different proteins in various species (Cha and Stewart, 1997; Fadda et al., 2003; Pinho and Errington, 2004; Ramirez-Arcos, 2005). In *Bacillus subtilis* (Bs), DivIVA ($DivIVA_{Bs}$) acts as a temporal regulator for FtsZ-inhibiting MinCD proteins, restricting their activity to the cell's polar and septal areas and prevents cell division in the chromosome-free areas near the poles as well as in the vicinity of the active Z-ring (Cha and Stewart, 1997; Edwards and Errington, 1997; Marston et al., 1998; Marston and Errington, 1999; Edwards et al., 2000; Karoui and Errington, 2001; Harry and Lewis, 2003). $DivIVA_{Bs}$ is also involved in the segregation of chromosomes during sporulation by positioning the *oriC* region of the chromosome to the cell poles through its association with RacA, which acts as a bridge between the *oriC* region and the cell poles (Thomaides et al., 2001; Ben-Yehuda et al., 2003). $DivIVA_{Bs}$ also binds to Maf, a protein involved in cell division arrest in competent cells (Briley et al., 2011). As well, DivIVA is involved in apical growth and cell polarity control by establishing hyphal branching sites and cell wall growth both in *B. subtilis* (Flärdh, 2010) as well as *Streptomyces coelicolor* (Flärdh, 2003). In *S. pneumoniae,* DivIVA interacts with several divisome proteins including FtsZ, FtsA, ZapA, FtsK, FtsI, FtsB, FtsQ and FtsW (Fadda et al., 2007). We recently reported that DivIVA from *E. faecalis* interacts with a newly reported protein, EF1025, and affects cell length (Sharma et al., 2020).

The EF1025 homologue in *B. subtilis* is CcpN, a transcriptional regulator of gluconeogenic genes (Servant et al., 2005). While the majority of genes involved in carbon catabolite repression are regulated by CcpA-dependent catabolite control, three genes, *gapB, pckA* and *sr1*, are downregulated by CcpN in the presence of glucose (Licht et al., 2005; Servant et al., 2005). During glycolysis, *gapB* and *pckA*, enzymes which are involved in gluconeogenesis (i.e. NADPH-dependent glyceraldehyde-3-P dehydrogenase, and PEP carboxykinase) are repressed (Servant et al., 2005). The other gene repressed by CcpN is *sr1*, which encodes a small non-coding regulatory RNA that inhibits the translation of *ahrC* (Licht et al., 2005). *ahrC* encodes a transcriptional regulator that activates arginine catabolism in *rocABC* and *rocDEF* operon and suppresses the arginine biosynthesis gene cluster (Heidrich et al., 2006, 2007). CcpN in *B. subtilis* controls central

carbon fluxes; and disruption of CcpN led to mutant growth phenotype caused by ATP dissipation via extensive futile cycling (Tännler et al., 2008).

The $DivIVA_{Ef}$ interacting protein, EF1025, from *Enterococcus faecalis*, shares 41% homology with CcpN from *B. subtilis* (Sharma et al., 2020). EF1025 is essential for cell viability and affects the cell length and shape of *E. faecalis*. Because the EF1025/CcpN protein is highly conserved in Gram-positive bacteria, we hypothesized that CcpN would also interact with $DivIVA_{Bs}$. We report a unique interaction between CcpN and DivIVA from *B. subtilis*, using bacterial-two hybrid and GST-pull down assays. A heterologous interaction was also determined between EF1025 and $DivIVA_{Bs}$ in a GST-pull down assay. Insertional inactivation of *ccpN* leads to cell elongation and changes in cell surface roughness in *B. subtilis*, suggesting a possible function for CcpN during the cell elongation process. Our research expands the knowledge of $DivIVA_{Bs}$ interacting partners and highlights a dual function for CcpN in *B. subtilis*.

3.3. Materials and methods:

3.3.1. Strains and growth conditions

Bacterial strains and plasmids used in this study are shown in Table 3.1. *E. coli* XL1-Blue or DH5α were used for cloning, *E. coli* C41 (DE3) was used to overexpress cloned proteins and *E. coli* R721 was the host (Di Lallo et al., 2001, 2003) for bacterial-two hybrid assays. *B. subtilis* 168 genomic DNA was used to amplify *ccpN* and *divIVA* to create constructs for B2H and GST pull-down assays. *E. coli* and *B. subtilis* strains were grown in Luria-Bertani (LB) broth (Difco, Franklin Lakes, NJ, USA) at 37°C and the following antibiotics (Sigma, CA) were added to the medium as required: ampicillin, kanamycin, erythromycin and chloramphenicol.

3.3.2. Bioinformatic analysis

The EF1025 homologue in *B. subtilis*, CcpN, was identified using BLASTp (https://blast.ncbi.nlm.nih.gov/Blast.cgi?PAGE=Proteins) against the non-redundant protein sequences database for which the EF1025 protein sequence was used as a query. The deduced amino acid sequence was analyzed using the ProtParam tool (http://us.expasy.org/tools/protparam.html). The CcpN sequence was also analyzed by PROSITE (Sigrist et al., 2010) (https://www.ncbi.nlm.nih.gov/Structure/cdd/cdd.shtml) to identify functional domains. Transmembrane motifs were predicted using the TMbase program (https://embnet.vital-it.ch/software/TMPRED_form.html) and potential coiled-coil structures in CcpN were predicted using the COILS program (http://www.ch.embnet.org/software/COILS_form.html).

Table 3.1. Bacterial strains used in the study.

Strains	Relevant characteristics	Resources or References
Escherichia coli XL1-Blue	*recA1 endA1 gyrA96 thi-1 hsdR17 supE44 relA1 lac* [F´ *proAB lacI*q*Z_M15*Tn*10* (Tetr)]	Strategene
E. coli DH5α	*endA*1 hsdr17 ($r_k^- m_k^+$) *supE*44 *thi*-1 *recA*1 *gyrA*96 *relA*1 Δ(*arg*F-*lac*ZYA) *U*169 *deoR* [ø80d *lac* Δ(*lacZ*) M15)	Gibco-BRL
E. coli C41 (DE3)	F¯*ompT hsdS*$_B$ *(r*$_B$*-m*$_B$*-) gal dcm Δ(srl-recA)* 306*::*Tn*10 (tet*^{R}*) (DE3)*	Miroux et al., 1996
E. coli R721	71/18 *glpT*::O-P434/P22*lacZ*	Di Lallo et al., 2001, 2003
E. coli pETEF1025	*E. coli* C41 (DE3) with pETEF1025 for 6×His-EF1025 overexpression	Sharma et al., (2020)
B. subtilis 168	*trpC2*; plasmid free	*B. subtilis* Genetic Stock Center (BGSC)
B. subtilis KS1685	*trpC2 ccpN'*:: pMUTIN4	This study
B. subtilis GM1620	*trpC2 ccpN'*:: pMUTIN2	Servant et al., 2005
B. subtilis PS1622	*trpC2amyE*'::P*gapB*::*lacZ-cat ccpN*'::pEC23	Servant et al., 2005
B. subtilis PS1649	*trpC2 amyE*'::P*pckA*::*lacZ-cat*	Servant et al., 2005

3.3.3. CcpN-DivIVA interactions in the Bacterial Two-Hybrid assays (B2H)

The B2H system of Di Lallo et al. (2001) was employed to investigate interactions between CcpN and $DivIVA_{Bs}$. To facilitate cloning, B2H vectors pcI434 and pcIp22 (Di Lallo et al., 2001) were modified by inserting a linker containing multiple endonuclease restriction sites, resulting in plasmids pcI434-L and pcIp22-L (Table 3.2). *ccpN* and $divIVA_{Bs}$ were PCR-amplified from *B. subtilis 168* using primers CcpNF/CcpNR and $DivIVA_{Bs}F$/$DivIVA_{Bs}R$, respectively (Table 3.3). Amplicons were cloned into the B2H vectors pcI434-L and pcIp22-L, resulting in plasmids pcIp22CcpN, pcI434CcpN, pcIp22divIVA and pcI434divIVA (Table 3.2). B2H plasmids were transformed into *E. coli* R721 either singly or in combination. B2H assays were modified (Di Lallo et al. 2001, 2003) as follows: freshly transformed single colonies of *E. coli* R721 cells, harbouring different combinations of plasmids pcIp22CcpN, pcI434CcpN, pcIp22divIVA and pcI434divIVA, were grown overnight in 4 mL LB medium supplemented with Chl 30 µg/ml, Amp 50 µg/ml and Kan 25 µg/ml. Cells were diluted 1:100 in fresh LB medium containing the same antibiotics for ~1 hour (OD600 ~0.1) at 34°C, followed by the addition of 0.1 mM isopropyl β-D-1-thiogalactopyranoside (IPTG). Cells were further cultured to mid-log phase (OD600=~0.5) at 34°C, harvested, and tested for β-galactosidase activity as previously described (Di Lallo et al., 2001). *E. coli* R721 cells were used as the baseline control for the calculation of the percentage residual β-galactosidase activity (Table 3.1). A value of less than 50% residual β-galactosidase activity as compared to the *E. coli* R721 cells, was defined as positive for protein interactions. Each experiment was performed in triplicate, and an average of the percentage residual β-galactosidase activity and the standard deviation was determined.

Table 3.2. Plasmids used in the study.

Plasmids	Relevant Characteristics	Resources/References
pcI434	Kan^R, bacterial two-hybrid vector	Di Lallo et al., 2001
pcIp22	Amp^R, bacterial two-hybrid vector	Di Lallo et al., 2001
pcIp22-L	pcI_{P22} derivative carrying a linker with multiple cloning sites	Sharma et al., (2020)
pcI434-L	pcI_{434} derivative carrying a linker with multiple cloning sites	Sharma et al., (2020)
pcIp22CcpN	pcI_{P22} derivative carrying the *B. subtilis ccpN* gene	This study
pcIp434CcpN	pcI_{434} derivative carrying the *B. subtilis ccpN* gene	This study
pcI22divIVA	pcI_{P22} derivative carrying the *B. subtilis divIVA* gene	This study
pcI434divIVA	pcI_{434} derivative carrying the *B. subtilis divIVA* gene	This study
pGEX-2T	Amp^R P_{lac}*::gst*	Amersham Bioscience
pGST-Div	Amp^R P_{lac}*::gst*, GST-$DivIVA_{Bs}$	This study
pET30a(+)	Kan^R P_{T7}*::6xhis*	Novagen
pETCcpN	Kan^R P_{T7}, 6×His-CcpN	This study
pMUTIN4	Integration vector Em^R, Amp^R, LacZ	*B. subtilis* Genetic Stock Center (BGSC)
pMUTccpN	Integration vector Em^R, Amp^R, *LacZ*::*ccpN*	This study

Table 3.3. Primers used in the study.

Primer name	Sequence 5’ to 3’
CcpNF	GCGGTCGACT GTGAGTACGATCGAACTAAA
CcpNR	GCCCGGATCCA TTATAGGATTTCATTTTCAG
$DivIV_{Bs}F$	GAGGGATCCTATGCCATTAACGCCAAATGATATTC
$DivIV_{Bs}R$	GCGAGATCTTTTATTCCTTTTCCTCAAATACAGCGTC
BsDivIVF	GAGGGATCCATGCCATTAACGCCAAATGATATTC
BsDivIVR	GCGCTCGAGTTATTCCTTTTCCTCAAATACAGCGTC
BsCcpNF	GCGCCATATGAGTACGATCGAACTAAATAAAC
BsCcpNR	GCGCGGATCCTAGGATTTCATTTTCAGATAAACTGAC
KOCcpN-F	GCGCGAATTCGTGAGTACGATCGAACTAAATAAAC
KOCcpN120	GCGCGAATTCGCGCCCGGATTTAGCCATAC
KOCcpN-R	GCGCGGATCCTTATAGGATTTCATTTTCAGATAAACTGAC
KOCcpN318	GCGCGGATCCTTATTCTAAAAACATGGTGCAAATCGCATC
EryF	CGGGTCAGCACTTTACTATTG
EryR	GGACCTACCTCATAGACAAG
LacZR	TTATTTTTGACACCAGACC

3.3.4. GST pull-down assays

To create a GST-DivIVA$_{Bs}$ fusion, *divIVA$_{Bs}$* was PCR-amplified from *B. subtilis* 168 using primers BsDivIVF/BsDivIVR (Table 3.3). The amplicon was cloned into the GST vector pGEX-2T, generating plasmid pGST-Div (Table 3.2). *ccpN* was PCR-amplified using primers BsCcpNF/BsCcpNR (Table 3.3B) and cloned into the 6×His tag vector pET30a(+), resulting in plasmid pETCcpN (Table 3.2). GST-DivIVA$_{Bs}$ or 6×His-CcpN fusions were overexpressed in *E. coli* C41 (DE3) as described in Rigden et al. (2008). GST-DivIV$_{Bs}$ was purified and bound to GST affinity beads according to the manufacturer's instructions (GST-Bind Kit, Novagen, USA). Soluble 6×His-CcpN was extracted from 200 mL log-phase growth cells of *E. coli* C41 by sonication in 5 ml Interaction Buffer (IB, 20 mM Tris/HCl pH 7.5, 10% glycerol, 50 mM KCl, 0.5 mM EDTA, 1% Triton X100, 1 mM DTT). The cell lysate was centrifuged and the supernatant (50µl) was incubated with 20 µL GST-DivIVA$_{Bs}$ bound beads pre-equilibrated with IB buffer, at 4˚C for 2 hours. Beads were washed with cold IB buffer three times. Protein retained on the beads was eluted using 40 µL 1×SDS loading buffer and heating at 95˚C for 10 min. Eluted protein was separated by SDS-PAGE, followed by Western blot analysis using anti-6×His and anti-GST monoclonal antibody (Genscript, USA) at a concentration of 0.3 µg/mL. Purified GST protein was used as a control and was produced in *E. coli* C41 (DE3) from plasmid pGEX2T, as previously described (Zou et al., 2017).

To study the heterologous interaction between EF1025 and DivIVA$_{Bs}$, pGST-Div was overexpressed in *E. coli* C41 (DE3)(Ramirez-Arcos, 2005) (Table 3.1 and 3.2B). The GST-DivIVA$_{Bs}$ fusion protein was purified using GST affinity beads (GST-Bind Kit, Novagen, USA) and was used to study its interaction with 6×His-EF1025, which was purified from *E. coli* pETEF1025, as previously described (Sharma et al., 2020). SDS-PAGE and Western blot were developed formed as described previously (Ramirez-Arcos, 2005; Rigden et al., 2008). Monoclonal anti-GST antibody was used for detecting GST-DivIVA$_{Ef}$ (Genscript, USA) at 0.3 µg/mL. The 6×His tagged proteins were probed with anti-6×His monoclonal antibodies (0.25 µg/mL) according to the manufacturer's instructions (Genscript, USA).

3.3.5. Insertional inactivation of *ccpN*

B. subtilis ccpN was disrupted by insertional mutagenesis by constructing an integration plasmid as follows: a 120 bp fragment of the N-terminal coding sequence of *ccpN* was PCR-amplified from *B. subtilis* 168 using primers KOCcpN-F/KOCcpN120 (Table 3.3). A fragment from the C-terminal was amplified using primers KOCcpN-R/KOCcpN318 (Table 3.3). These amplicons were digested with BamHI and EcoRI and ligated to predigested pMUTIN4 resulting in pMUTccpN (Table 3.2). pMUTccpN carried the N-terminal and C-terminal fragments of *ccpN* flanking either end of the *LacZ* and P_{Spec} of pMUTIN4. pMUTccpN was transformed into competent *E. coli* DH5α and selected for ampicillin resistance. pMUTccpN was electroporated into electrocompetent *B. subtilis* 168 cells creating *B. subtilis* KS1685 and cells were selected for erythromycin resistance (Bron and Venema, 1972), creating *B. subtilis* KS1685. Correct clones were confirmed using PCR amplification of the upstream and downstream regions of pMUTIN4 using primer sets LacZR/KOCcpN-R, KOCcpN-F/EryF, KOCcpN-F/LacZR, and EryF/KOCcpN-R to ensure the integration of pMUTIN4 into *B. subtilis* 168 genome (Table 3.3).

3.3.6. Microscopy

A SU8010 Cold Field Emission Ultra-High-Resolution scanning electron microscope (SEM) (WCVM, University of Saskatchewan, Saskatoon, Saskatchewan) was used to image *B. subtilis* strains 168, KS1685 (this study), GM1620, PS1622 and PS1649 (Dr. Stephane Aymerich, Director, Micalis Institute, Paris, kindly provided *B. subtilis* strains GM1620, PS1622 and PS1649, Table 3.1). Cells were cultured in LB medium with or without appropriate antibiotics, without agitation at 37°C either overnight (~20 h) or to stationary phase. Cells were fixed on poly-L-lysine coverslips, sequentially dehydrated in ethanol, critical point dried, sputter coated with gold and imaged (Ramirez-Arcos et al., 2001). The percentage of elongated cells were calculated measuring the length of 90-105 cells.

For atomic force microscopy (AFM), coverslips were coated with Cell-Tak (LifeTechnologies) to which cell suspensions from overnight cultures were deposited. Cells were fixed with formalin, air dried (Bhat et al., 2015) and imaged with silicon nitride cantilevers (HYDRA6R-200NG; Nanosensors, Neuchatel, Switzerland) with calibrated spring constants ranging from 0.03 to 0.062 N/m. QI™ images were collected (Z-length = 0.926 um; scan rate =

95 um/s; 128 × 128 pixel raster scan) and generated force curves (JPK software) at each pixel (Sharma et al., 2020). Height, length and surface roughness were calculated from QI™ height images according to Bhat et al. (2015), the latter from multiple squares (200 × 200 nm) along the centre of at least 10 cells each from 3 biological replicates.

3.3.7. Statistical analysis

AFM and SEM studies were conducted in triplicate and analyzed using Microsoft Excel or Graph Pad Prism respectively unless otherwise indicated. The results were reported as mean ± standard deviation (SD), differences assessed using a two-tailed unpaired t-test and ANOVA for which $p < 0.05$ was considered statistically significant.

3.4. Results

3.4.1. Bioinformatics analysis

CcpN, a protein comprising 212 amino acids (AA) with an estimated molecular weight of ~24 kDa and a theoretical isoelectric point of 6.97, contains no transmembrane motifs or coiled-coil regions. CcpN contains an N-terminal helix-turn-helix (HTH) DNA binding domain (AA 11-60), and two Cystathionine β-Synthase (CBS) domains (i.e. CBS1, AA 82-148 and CBS2, AA 155-206). The CBS1 domain is centrally located whereas the CBS2 domain is located at the C-terminus of CcpN.

3.4.2. CcpN interacts with DivIVA *in vitro* and *in vivo*

CcpN shares 41 % homology with EF1025 from *E. faecalis*. Since EF1025 interacts with $DivIVA_{Ef}$, and because many firmicutes have homologues of this protein, we investigated whether such an interaction is unique to *E. faecalis*. In the B2H system used to assess the interaction between CcpN and $DivIVA_{Bs}$, less than 50% residual β-galactosidase activity is considered as a positive interaction (Di Lallo et al., 2001, 2003). A positive interaction was observed between DivIVA and CcpN (Fig. 3.1, 32%) when *E.coli* R721 cells harbouring plasmids pdivIVA22 and pCcpN434 together (Table 3.2) were measured for residual β-galactosidase activity. The reverse combination of these plasmids i.e. pCcpN22 and pdivIVA434 together also resulted in a positive interaction (24%). As a positive control, FtsA and FtsZ proteins from *Neisseria gonorrheae* were measured for residual β-galactosidase activity (28%). *E. coli* R721 cells (Table 3.1) served as a control baseline β-galactosidase activity control.

The *in vitro* interaction between CcpN and $DivIVA_{Bs}$ was ascertained by GST-pull down assay, in which 6×His-CcpN was pulled down by GST-$DivIVA_{Bs}$ (45 kDa). GST alone acted as a negative control and did not interact with 6×His-CcpN (Fig. 3.2A, Lane 3). A Western blot using monoclonal anti-His antibody revealed the presence of a 25 kDa band corresponding to 6×His-CcpN (Fig. 3.2A, Lane 5).

In a heterologous interaction, the *in vitro* interaction between EF1025 and $DivIVA_{Bs}$ was ascertained by GST-pull down assay in which 6×His-EF1025 was pulled down by GST-$DivIVA_{Bs}$ (45 kDa). GST alone acted as a negative control and did not interact with 6×His-EF1025 (Fig.

3.2B, Lane 3). A Western blot using an anti-EF1025 antibody (Sharma et al., 2020) revealed the presence of a 25 kDa band corresponding to 6×His-EF1025 (Fig. 3.2B, Lane 5).

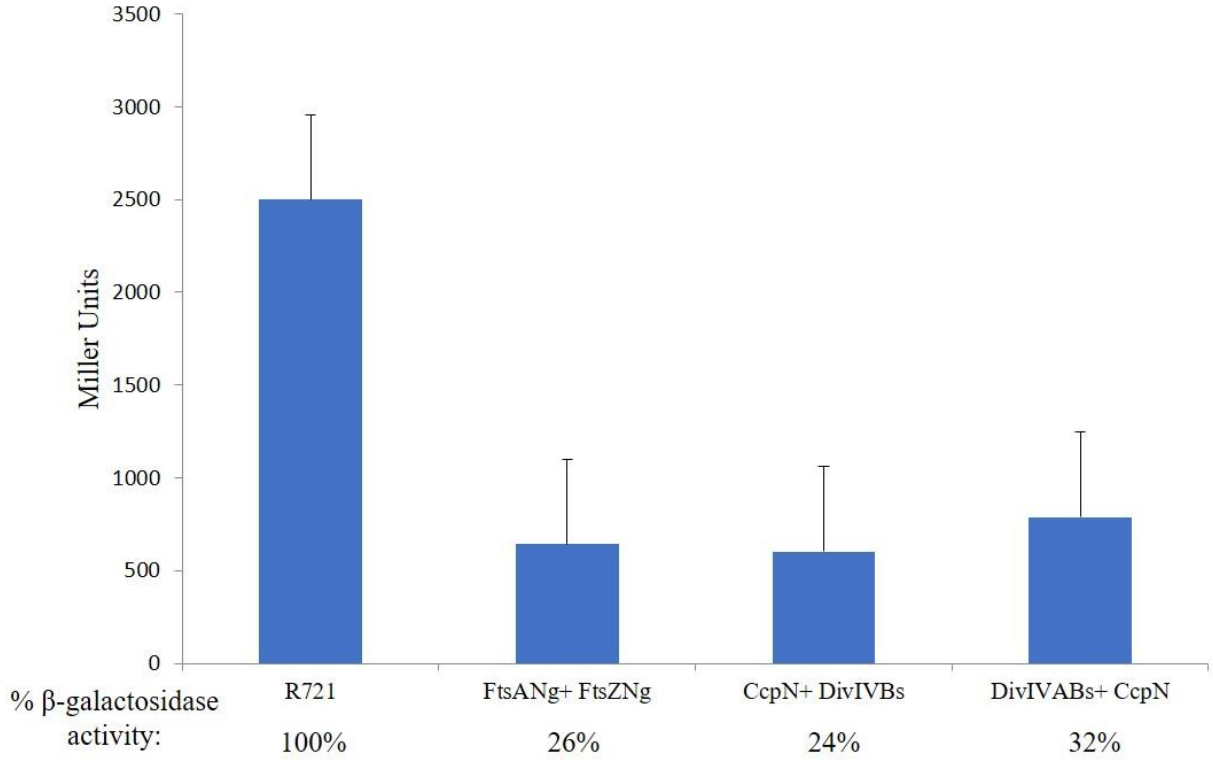

Figure 3.1. CcpN interacts with $DivIVA_{Bs}$ in B2H assay. The β-galactosidase activity was expressed in Miller Units (y-axis). The x-axis shows the combination of B2H plasmids used and the percentage Miller Units. Average values were obtained from three independent assays in triplicate. Values of less than 50% indicate a positive interaction. The error bars represent 1 standard deviation.

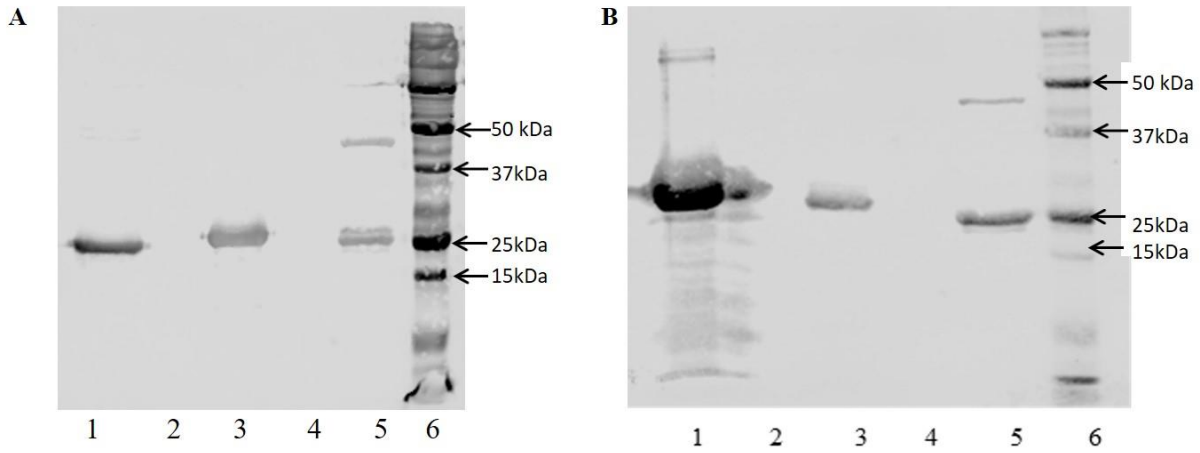

Figure 3.2. $DivIVA_{Bs}$ interacts with CcpN and EF1025 in GST pull-down assay. (A) Western blot probed with anti-6×His and anti-GST monoclonal antibody. Lane 1: overexpressed and purified CcpN (25 kDa); Lane 2 and 4: empty; Lane 3: GST (25 kDa); Lane 5: pulled down GST-$DivIVA_{Bs}$ (45 kDa) along with CcpN (25 kDa); Lane 6: Protein ladder. (B) Western blot probed with anti-6×HisEF1025 polyclonal antibody and anti-GST monoclonal antibody. Lane 1: overexpressed 6×His-EF1025 (25 kDa) containing supernatant representing 10% input; Lane 2 and 4: empty; Lane 3: GST (25 kDa); Lane 5: pulled down GST-$DivIVA_{Bs}$ (45 kDa) bound beads along with 6×His-EF1025 (25 kDa); Lane 6: Protein ladder.

3.4.3. *ccpN* insertional inactivation leads to cell elongation

Insertional inactivation of *EF1025* in *E. faecalis* affects cell length and cell septation, phenotypes (Levin et al., 1992; Varley and Stewart, 1992; Abhayawardhane and Stewart, 1995; Chung et al., 2004). We proposed that disruption of *ccpN* could also produce a similar phenotype in *B. subtilis*. *ccpN* was insertionally inactivated by introducing an erythromycin cassette using the plasmid pMUTIN4 in *B. subtilis* KS1685 (Tables 3.1 and 3.2). Using scanning electron microscopy (SEM), *B. subtilis* KS1685 cells were compared with wild type *B. subtilis* 168 cells. *B. subtilis* 168 cells showed rod-shaped cells with normal division (Fig. 3.3A). *B. subtilis* KS1685 cells were elongated and grew in straight chains of connected cells (Fig. 3.3C). These cells failed to segregate and detach distinctively from one another (Fig. 3.3D). We compared the morphology of *B. subtilis* KS1685 cells with *B. subtilis* GM1620 and PS1622 strains developed by Servant et al., 2005 (Fig. 3.3E and 3.3F) which contain *ccpN* disrupted by pMUTIN2 through single/multiple integration events (Table 3.1). *B. subtilis* GM1620 and PS1622 cells were also elongated and failed to segregate. Another control strain i.e. *B. subtilis* PS1649 (Table 3.1), developed by Servant et al., 2005, containing disrupted *pckA*, exhibited rod-shaped cells with a normal division like *B. subtilis* 168 (Fig. 3.3B).

The lengths of wild type *B. subtilis* 168 cells (2.6 ± 0.94 µm, n= 102), *B. subtilis* KS1685 (6.16 ± 1.2 µm, n= 92), *B. subtilis* GM1620 (6.67 ± 2.13 µm, n= 92) and PS1622 (6.88 ± 2.51 µm, n= 97) cells were compared. *B. subtilis* KS1685 (6.16±1.2 µm, n=92), *B. subtilis* GM1620 (6.67±2.13 µm, n=92) and PS1622 (6.88±2.51 µm, n=97) strains with *ccpN* disruption were significantly ($p < 0.05$) longer (Fig. 3.4) as determined by SEM. Control strain, *B. subtilis* PS1649 (Table 3.1), had a cell length (2.51 ± 0.54 µm, n= 97) similar ($p > 0.05$) to wild type *B. subtilis* 168 cells (2.6 ± 0.94 µm, n= 102) (Fig. 3.3B and 3.4).

Analysis of the cells by AFM showed that wthe cell length of *B. subtilis* 168 (3.08 ± 0.56 µm) was similar ($p= 0.36$) to that of PS 1649 (3.24 ± 0.74 µm). These lengths were statistically different ($p < 0.05$) from *B. subtilis* KS 1685 (4.71 ± 0.58 µm), PS 1622 (4.05 ± 0.39 µm) and GM 1620 (5.33 ± 0.86 µm) cells which were longer (Fig. 3.5). The cell heights measured by AFM for *B. subtilis* 168 (0.36 ± 0.044 µm), PS 1649 (0.36 ± 0.01 µm) and GM 1620 (0.038 ± 0.048 µm)

were statistically identical but were statistically different ($p < 0.05$) from both *B. subtilis* KS 1685 (0.31 ± 0.01 µm) and *B subtilis* PS 1622 (0.32 ± 0.01 µm).

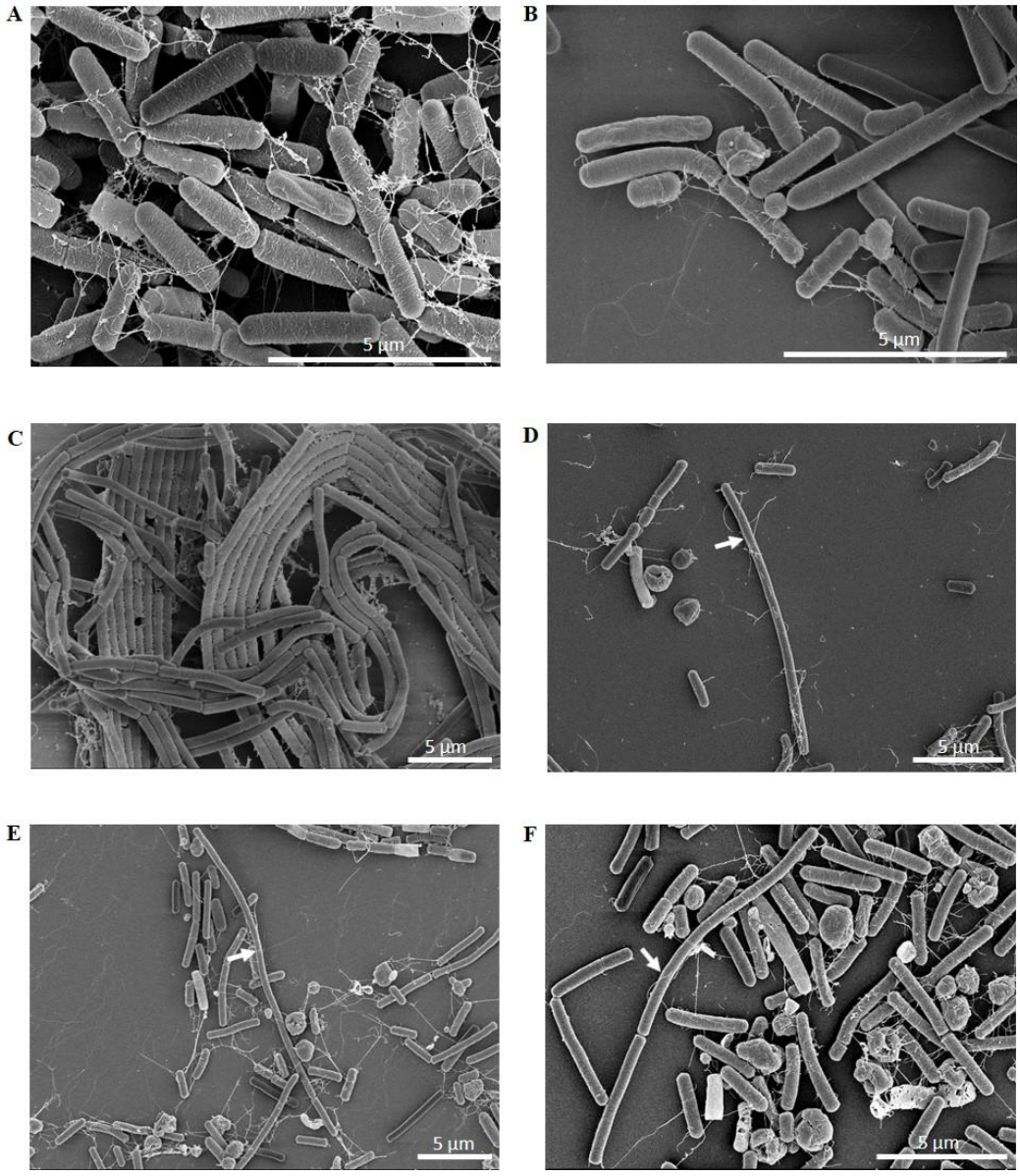

Figure 3.3. Insertional inactivation of *ccpN* leads to cell elongation and failed segregation in *B. subtilis* KS 1685 (this study), PS 1622 and GM1620. Scanning electron micrographs showing (A) Normal *B. subtilis* 168 cells; (B) *B. subtilis* PS 1649 cell exhibiting normal cell length and morphology; (C and D) *B. subtilis* KS 1685 cells; (E and F) *B. subtilis* PS 1622 and GM 1620 cells, respectively, showing elongated cells with impaired segregation. White arrow indicates failed segregation in rod-shaped cells. Bar scale indicated at the bottom right corner of each image.

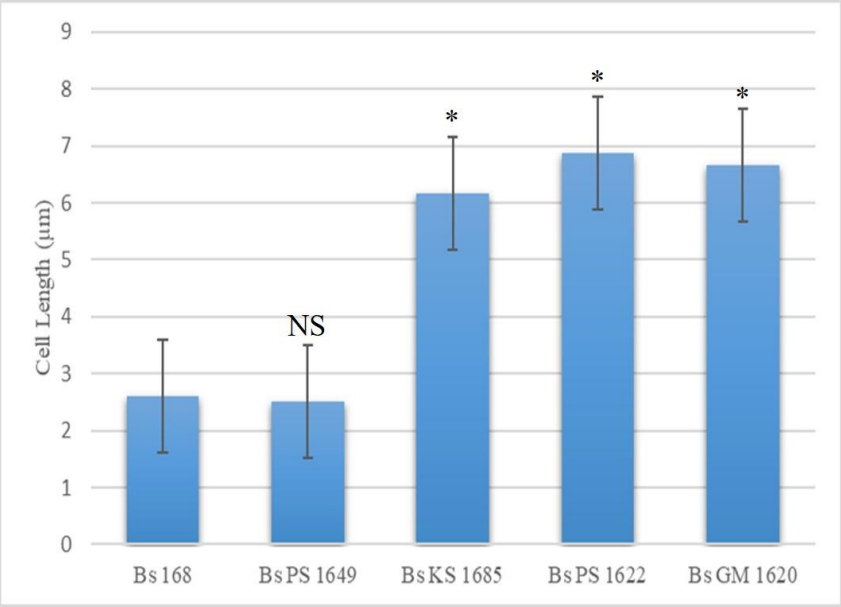

Figure 3.4. Comparison of cell lengths for *B. subtilis* strains: 168 (n= 102), PS 1649 (n= 97), KS 1685 (n= 92), PS 1622 (n= 97) and GM 1620 (n= 92). *B. subtilis* strains 168 and PS 1649 served as control strains. "n" represents the number of cells counted for each sample; * represents two-tail *p* value from t-test for each group set ($p < 0.05$); NS- non-significant. The error bars represent 1 standard deviation.

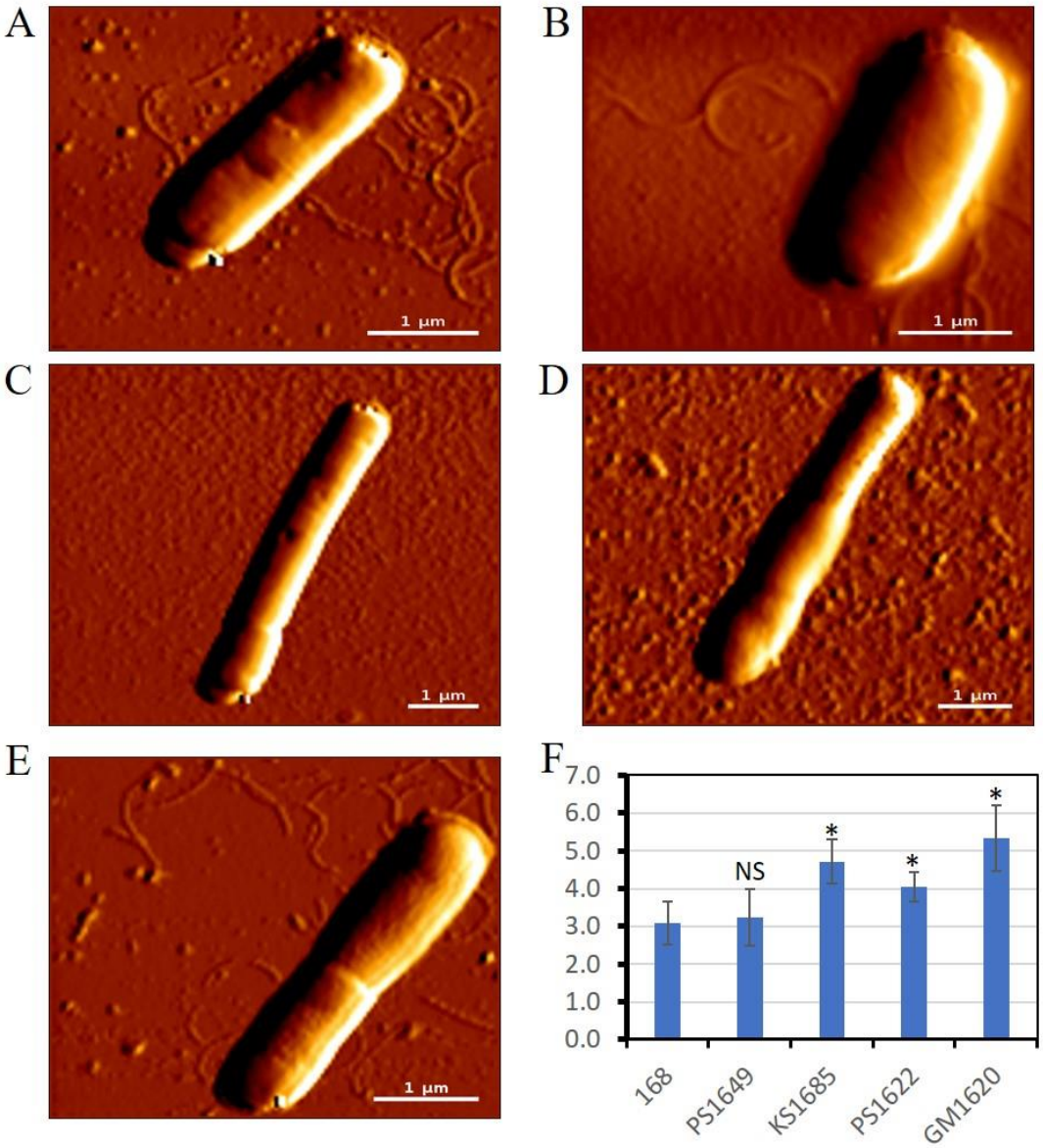

Figure 3.5. *B. subtilis* KS1685 cells exhibited cell elongation. Representative AFM images of (A) *B. subtilis* 168; (B) *B. subtilis* PS1649; (C) *B. subtilis* KS1685; (D) *B. subtilis* GM1620; (E) *B. subtilis* PS1622 collected in QI mode with a resolution of 128×128 pixels per image. Bar scale (1 µm) indicated at the bottom right corner of each image; and (F) Comparison of cell lengths for *B. subtilis* strains: 168 (n= 43), PS 1649 (n= 43), KS 1685 (n= 32), PS 1622 (n= 34) and GM 1620 (n= 37). All data was analyzed by t-test where * indicates $p < 0.05$; NS- non-significant. The error bars represent 1 standard deviation.

3.5. Discussion

Studies of protein-protein interactions between various proteins have been mostly studied using two-hybrid systems or other biochemical methods like GST-pull down and Co-immunoprecipitation (Ishikawa et al., 2006). The *in vivo* Bacterial two-hybrid assay shows a novel interaction between CcpN and DivIVA in *B. subtilis*. This interaction was confirmed using an *in vitro* GST pull-down assay. We also observed a positive heterologous interaction between EF1025, a CcpN homologue in *E. faecalis*, and $DivIVA_{Bs.}$ These data suggest that the interaction between DivIVA and CcpN homologues is probably conserved among Gram-positive microorganisms. EF1025 interacts with $DivIVA_{Ef}$ and affects cell length and shape (Sharma et al., 2020). The two CBS domains of EF1025 independently interacted with EF1025 in B2H and GST pull-down assays. While the function of the HTH domain of CcpN in gluconeogenesis has been previously discussed by Servant et al. (2005), the function of the two CBS domains in CcpN remains to be answered.

We investigated whether CcpN in *B. subtilis* might play a similar role as its homologue, EF1025 in *E. faecalis* (Sharma et al., 2020). CcpN affects the cell length in *B. subtilis* (Servant, Le Coq and Aymerich 2005; Sharma et al., 2020). *B. subtilis* 1685 cells containing disrupted *ccpN* were significantly longer than the wild-type *B. subtilis* 168 cells. We observed the same degree of elongation in *B. subtilis* GM1620 and PS1622. *B. subtilis* PS1649, with disrupted *pckA* (one of the genes regulated by CcpN), showed no change in cell length and behaved like the wild-type *B. subtilis* 168 cells. This shows that the cell elongation phenotype is exclusive to the strains containing a disruption of *ccpN* expression, and that *ccpN* is involved in determining cell length in *B. subtilis*. Interestingly, unlike EF1025, disruption of ccpN proved to be non-essential.

B. subtilis cells have a distinctive elongated cylindrical tube morphology with hemispherical poles. Growth occurs through elongation along the cell's long axis with division occurring when a cell doubles in length (Errington and Wu, 2017). In *B. subtilis*, cell shape is determined and maintained by the action of "cytoskeletal" proteins of the MreB family such as MreB, Mbl, MreBH and RodA that are structurally and biochemically related to eukaryotic actins (Henriques et al., 1998; Carballido-Lopez, 2006). A degree of remodelling or active movement of the filaments occurs during cell elongation (Carballido-López and Errington, 2003; Defeu Soufo and Graumann, 2004). *B. subtilis* cells with mutations in *mreB* exhibited enhanced diameter and

grew in “straight rows” (Carballido-Lopez, 2006). MreB associates with elongation-specific peptidoglycan-synthesizing complexes that include MreC, MreD, RodA, Penicillin Binding Proteins (PBPs), and peptidoglycan hydrolases (Carballido-López and Formstone, 2007; White et al., 2010). CcpN may be another member of the category of proteins that determine cell length in *B. subtilis*. The cells were longer and failed to segregate in the *ccpN* mutants *B. subtilis* 1685, GM1620 and PS1622, in which cells remained closely attached to one another and grew in straight rows. Taken together, these results suggest that CcpN affects cell length and enables timely cell segregation in *B. subtilis*. This also suggests that CcpN has two different functions in the cell i.e. controlling cell length and expression of *gapB* and *pckA* in the presence or absence of glucose (Servant et al., 2005).

Many proteins, called “moonlighting proteins” perform multiple, apparently unrelated, functions that have not resulted from gene fusions, RNA splicing, or pleiotropic impacts, and they are found throughout the evolutionary tree (Jeffery, 1999). By using only one polypeptide chain, moonlighting proteins govern different functions and interacting partners possibly due to the minor differences in amino acid sequence (Jeffery, 2016). For example, CbtA (formerly known as YeeV) of *E. coli* alters cell shape by inhibiting both cell division and cell elongation. CbtA is the toxin component of the CbtA/CbeA chromosomal toxin-antitoxin system in *E. coli* that targets both FtsZ and MreB. CbtA interacts independently with FtsZ and MreB affecting cell shape (Heller et al., 2017) by a simultaneously blocking cell division and cell elongation pathways. Both of these interactions are functionally important, independently contributing both to toxicity and cell-shape disturbances (Heller et al., 2017).

Very often two protein species with a high degree of amino acid sequence identity share the same function. However, there have been many cases reported in which two proteins have different functions resulting from subtle differences in amino acid sequence (Jeffery, 2016). EF1025 and CcpN share 41% homology at the protein level, and both contain one N-terminal helix-turn-helix domain and two CBS domains, one located centrally and the other at the C-terminus. Since CBS domains in EF1025 are responsible for interaction with $DivIVA_{Ef}$, we propose that different domains of CcpN may govern different cellular functions. The disparate cellular functions, namely gluconeogenesis and determination of cell shape, could be attributable to different domains of CcpN (Servant et al. 2005). Here we report another novel function of CcpN

from *B. subtilis*. CcpN interacts with $DivIVA_{Bs}$ like its homologue, EF1025 from *E. faecalis*. *ccpN* is a non-essential gene for cell viability but it regulates cell length and the ability to segregate after successful division.

Chapter 4. Unique cell division interactome of *E. faecalis*

Manuscript under preparation for submission to **Canadian Journal of Microbiology**

Author contribution:

We are grateful to Kristen Pedrizet and Monica Wang for performing B2H assays using $FtsZ_{Ef}$, $FtsA_{Ef}$, $FtsQ_{Ef}$, $FtsL_{Ef}$, $FtsI_{Ef}$, and $DivIVA_{Ef}$. Kusum Sharma performed B2H assays using $FtsB_{Ef}$ and analyzed all the results received from all of the above mentioned B2H assays.

4.1. Abstract

Bacterial cell division, an essential process, is orchestrated by the coordinated interaction of key cell division proteins forming a macromolecular complex called the divisome, spanning the cytoplasmic membrane during cell division. Key cell division proteins like FtsZ, FtsA, FtsQ/DivIB, FtsL, FtsW, FtsB/DivIC, FtsI and FtsK are relatively conserved. Using *in vivo* and *in vitro,* biochemical techniques cell division protein-protein interaction networks have been established for only four bacterial species i.e. *E. coli*, *N. gonorrhoeae*, *S. aureus* and *S. pneumoniae*. *E. faecalis* contains homologues of divisome proteins FtsZ, FtsA, FtsK, FtsQ, FtsL, FtsI and FtsB, however, the cell division interactome of *E. faecalis*, by contrast, is not presently known. In this research article, we are reporting the unique interactome of *E. faecalis* divisome proteins (i.e. $FtsZ_{Ef}$, $FtsA_{Ef}$, $FtsQ_{Ef}$, $FtsL_{Ef}$, $FtsI_{Ef}$, $FtsW_{Ef}$, $DivIVA_{Ef}$, and $FtsB_{Ef}$), established using Bacterial-two hybrid system. We also used EF1025, a $DivIVA_{Ef}$ interacting protein, to test for potential interactions with *E. faecalis* divisome proteins. EF1025 did not interact with any divisome protein except $DivIVA_{Ef}$.

4.2. Introduction

Bacterial cells are critically dependent for growth, development, and reproduction on their ability to divide. Cell division is a complex mechanism orchestrated at the division site by a multi-protein macromolecular complex called the divisome (Margolin, 2000; Gamba et al., 2009). The genes encoding these proteins are located in a highly conserved cluster known as "division cell wall (*dcw*)" cluster (Ayala et al., 1994; Tamames et al., 2001). The proteins encoded by the *dcw* genes are involved in cell division and peptidoglycan synthesis and are mostly essential for cell division (Boyle and Donachie, 1998; Kobayashi et al., 2003). Although the organization of various genes within the *dcw* cluster varies in different bacterial species as found in *E. coli*, *B. subtilis*, *Staphylococcus aureus*, *Streptococcus pyogenes*, *Enterococcus faecalis*, and *S. pneumoniae* (Fig. 1.1; Massidda et al., 1998; Francis et al., 2000; Snyder et al., 2001; Fadda et al., 2003; Ramirez-Arcos, 2005; Real and Henriques, 2006), the proteins involved in the process of cell division are comparatively conserved (Lutkenhaus et al., 2012; Haeusser and Margolin, 2016).

The context of the divisome varies in different bacteria. For example, in *B. subtilis*, divisome assembly follows a concerted or cooperative mode, because most divisome proteins are interdependent for septal localization (Gamba et al., 2004). Over 13 proteins form the core divisome (i.e. $FtsZ_{Bs}$, $FtsA_{Bs}$, $SepF_{Bs}$, $ZapA_{Bs}$, $EzrA_{Bs}$, $GpsB_{Bs}$, $FtsL_{Bs}$, $FtsB_{Bs}$, $FtsQ_{Bs}$, $FtsW_{Bs}$, $PBP1_{Bs}$, $PBP2B_{Bs}$ and $DivIVA_{Bs}$) in *B. subtilis* (Gamba et al., 2009; Halbedel and Lewis, 2019). $FtsZ_{Bs}$ assembles forming single-stranded protofilaments at the mid-cell where it is tethered to the membrane by the "early" divisome proteins $FtsA_{Bs}$ or $SepF_{Bs}$ (Jensen et al., 2005; Hamoen et al., 2006; Peters et al., 2007; Gamba et al., 2009). Sequentially, $ZapA_{Bs}$ and $EzrA_{Bs}$ then interact with the Z-ring facilitating FtZ_{Bs} polymerization (Levin et al., 1999; Gueiros-Filho and Losick, 2002; Singh et al., 2007; Cleverley et al., 2014). The complex comprised of $FtsZ_{Bs}$-$FtsA_{Bs}$-$SepF_{Bs}$-$ZapA_{Bs}$-$EzrA_{Bs}$ then recruits the 'late' cell division proteins i.e. $FtsW_{Bs}$, $PBP1_{Bs}$, $PBP2B_{Bs}$, $DivIB_{Bs}$, $DivIC_{Bs}$ and $FtsL_{Bs}$, $DivIVA_{Bs}$ and $GpsB_{Bs}$ (Perry and Edwards, 2004; Tavares et al., 2008; Gamba et al., 2009; Lenarcic et al., 2009; den Blaauwen, 2018; Taguchi et al., 2019). These proteins do not directly interact with $FtsZ_{Bs}$ and are mainly cytosolic proteins or membrane proteins (Ishikawa et al., 2006). In *E. coli*, over 10 proteins ($FtsZ_{Ec}$, $FtsA_{Ec}$, $FtsL_{Ec}$, $FtsW_{Ec}$, $FtsB_{Ec}$, $ZipA_{Ec}$, $FtsI_{Ec}$, $FtsK_{Ec}$, $FtsQ_{Ec}$, and $FtsN_{Ec}$) constitute the core divisome because of their essentiality during the process of cell division (Haeusser and Margolin, 2016). In *E. coli*, "early" divisome proteins ($FtsZ_{Ec}$, $FtsA_{Ec}$ and $ZipA_{Ec}$) locate to the septum forming a dynamic ring

structure, called as the proto-ring, at an early stage in cell division which acts as an assembly stage for the remaining proteins (Erickson et al., 2010; Rico et al., 2013; Ortiz et al., 2016). This is followed by the recruitment of the "late" proteins ($FtsK_{Ec}$, $FtsQ_{Ec}$, $FtsL_{Ec}$, $FtsB_{Ec}$, $FtsW_{Ec}$, $FtsI_{Ec}$ and $FtsN_{Ec}$) that are involved in remodelling of the peptidoglycan layer and chromosome segregation (Aarsman et al., 2005).

Using *in vivo* and *in vitro,* biochemical techniques such as bacterial two-hybrid (B2H) assay, GST-pull down assay, Co-immunoprecipitation (Co-IP) and Surface Plasmon Resonance (SPR), cell division protein-protein interaction networks have been established for four bacterial species i.e. *E. coli* (Di Lallo et al., 2003; Karimova et al., 2005), *N. gonorrhoeae* (Zou et al., 2017), *S. aureus* (Steele et al., 2011) and *S. pneumoniae* (Fadda et al., 2007; Maggi et al., 2008). In Gram-negative *E. coli*, sixteen interactions between ten cell division proteins (i.e. including $FtsZ_{Ec}$, $FtsA_{Ec}$, $ZipA_{Ec}$, $FtsK_{Ec}$, $FtsQ_{Ec}$, $FtsB_{Ec}$, $FtsL_{Ec}$, $FtsI_{Ec}$, $FtsW_{Ec}$, and $FtsN_{Ec}$) were identified (Di Lallo et al., 2003; Karimova et al., 2005). Zou et al. (2017) characterized nine interactions among eight cell division proteins i.e. $FtsZ_{Ng}$, $FtsA_{Ng}$, $ZipA_{Ng}$, $FtsK_{Ng}$, $FtsQ_{Ng}$, $FtsI_{Ng}$, $FtsW_{Ng}$, and $FtsN_{Ng}$, from *Neisseria gonorrhoeae* that defined the cell division interactome.

Using two different approaches i.e. bacterial two-hybrid (B2H) system and co-immunoprecipitation (Co-IP), a total of 37 homo and/or hetero-dimeric interactions were observed among nine *S. pneumoniae* cell division proteins that included $FtsZ_{Sp}$, $FtsA_{Sp}$, $FtsK_{Sp}$, $DivlB_{Sp}$, $DivlC_{Sp}$, $FtsL_{Sp}$, $FtsW_{Sp}$, and $PBP2x_{Sp}$ (Maggi et al., 2008). In a B2H assay, Fadda et al. (2007) showed that $DivIVA_{Sp}$ interacts with several divisome proteins, including $FtsZ_{Sp}$, $FtsA_{Sp}$, $ZapA_{Sp}$, $FtsK_{Sp}$, $FtsI_{Sp}$, $FtsB_{Sp}$, $FtsQ_{Sp}$ and $FtsW_{Sp}$ in *S. pneumoniae* (Fadda et al., 2007). Using the same method, Steele et al. (2011) reported around 49 homo-and/or hetero-dimeric protein interactions between thirteen divisome proteins (i.e. $FtsZ_{Sa}$, $FtsA_{Sa}$, $EzrA_{Sa}$, $GpsB_{Sa}$, $SepF_{Sa}$, $Pbp1_{Sa}$, $Pbp2_{Sa}$, $Pbp3_{Sa}$, $DivIB_{Sa}$, $DivIC_{Sa}$, $FtsL_{Sa}$, $FtsW_{Sa}$ and $RodA_{Sa}$) in *S. aureus*.

The *E. faecalis dcw* cluster contains homologues of divisome proteins FtsZ, FtsA, FtsK, FtsQ (DivIB), FtsL, FtsI and probably FtsB (DivIC), EzrA and ZapA (Pucci et al., 1997; Duez et al., 1998; Massidda et al., 1998) but the interaction network for these cell division proteins in *E. faecalis*, by contrast, is not presently known. To investigate the network of cell divisome proteins that forms a divisome in *E. faecalis*, protein-protein interactions between eight *E. faecalis* divisome proteins were studied using a B2H assay. Sixteen homo/hetero-dimer interactions were

identified among *E. faecalis* divisome proteins that included $FtsZ_{Ef}$, $FtsA_{Ef}$, $FtsQ_{Ef}$, $FtsL_{Ef}$, $FtsI_{Ef}$, $FtsW_{Ef}$, $DivIVA_{Ef}$, and $FtsB_{Ef}$. EF1025, a $DivIVA_{Ef}$ interacting protein, failed to interact with any divisome protein members, therefore, is not a part of *E. faecalis* divisome. B2H assay results reflect the existence of unique interactome for *E. faecalis* when compared with interactomes from *E. coli*, *N. gonorrhoeae*, *S. aureus*, and *S. pneumoniae*.

4.3. Materials and methods

4.3.1. Strains, plasmids and growth conditions

Bacterial strains and plasmids used in this study are listed in Table 4.1. *E. coli* DH5α was used for cloning and *E. coli* R721 for B2H assays (Di Lallo et al., 2001). *E. coli* DH5α and *E. coli* R721 were grown at 37 °C in Luria-Bertani (LB) medium (BD Difco™, Sparks, MD) with appropriate antibiotics in the following concentrations as required: ampicillin (Amp) 50 μg/mL, kanamycin (Kan) 30 μg/mL and chloramphenicol (Chl) 33 μg/mL, for 6-8 hours. During B2H assays, *E. coli* R721 was grown in LB medium for the duration required and incubated at 34°C, as previously described (Di Lallo et al., 2001). *E. faecalis* JH2-2 (Jacob and Hobbs, 1974), was used for the preparation of genomic DNA and was cultured at 37°C without aeration in Brain Heart Infusion (BHI) broth (Difco, Detroit, MI). Genomic DNA was prepared from *E. faecalis* JH2-2 using QIAamp DNA Mini Kit as per manufacturer instructions (Qiagen, CA).

Table 4.1. Bacterial strains used in the study.

Strain	Relevant Genotype	Source
Escherichia coli XL1 Blue	*hsdR17*, *supE44*, *recA1*, *endA1*, *gyrA46*, *thi* *relA1*, *lac*/F' [*proAB*$^{+}$, *lacI*^{q}, *lacZ*DM15::Tn*10*(Tet^{r})]	Stratagene
Escherichia coli R721	71/18 *glpT* :: O-$_{P434/P22}$ *lacZ*	Di Lallo *et. al.* 2001
Enterococcus faecalis JH2-2	wild type, Rif^{R}, Fus^{R}	Jacob & Hobbs, 1974

4.3.2. Divisome protein interactions in the Bacterial Two-Hybrid assays (B2H)

The B2H system (Di Lallo et al., 2001) was employed to investigate potential interactions between eight different *E. faecalis* divisome proteins i.e. $FtsZ_{Ef}$, $FtsA_{Ef}$, $FtsQ_{Ef}$, $FtsL_{Ef}$, $FtsB_{Ef}$, $FtsI_{Ef}$, $DivIVA_{Ef}$, and $FtsW_{Ef}$. EF1025, a $DivIVA_{Ef}$ -interacting protein, was also tested for its potential interactions with *E. faecalis* divisome proteins. The B2H and a quantitative β-galactosidase activity assay were performed as previously described (Miller and Lee, 1984; Di Lallo et al., 2003). To facilitate cloning, modified B2H vectors pcI434-L and pcIp22-L (Di Lallo et al., 2001; Zou et al., 2017) that contained linkers were used. *ftsA, ftsZ, ftsQ, ftsI, ftsW, ftsB, divIVA, EF1025* and *ftsL* were PCR amplified from *E. faecalis* JH2-2 genomic DNA using primer pairs A1/2, Z1/2, Q1/2, I1/2, W1/2, B1/2, D1/2, EF10251/2, and L1/2 (Table 4.3). Amplicons were cloned into the B2H vectors pcI434-L and pcIp22-L, respectively, resulting in plasmids pcIp22-A, pcIp22-Z, pcIp22-Q, pcIp22-I, pcIp22-W, pcIp22-B, pcIp22-D, pcIp22-E1025, pcIp22-L, pcI434-A, pcI434-Z, pcI434-Q, pcI434-I, pcI434-W, pcI434-B, pcI434-D, pcI434-E1025 and pcI434-L (Table 4.2). These plasmids were transformed into *E. coli* R721 either singly or in combination for B2H assays (Di Lallo et al., 2001, 2003; Greco-Stewart et al., 2007). Freshly transformed single colonies of *E. coli* R721 cells, harbouring different combinations of plasmids, were grown overnight in 4 mL of LB medium containing appropriate antibiotics. Cells were then diluted at 1:50 in fresh LB medium supplemented with the same antibiotics and incubated for ~1 hr at 34°C, followed by the addition of 0.1 mM isopropyl β-D-1-thiogalactopyranoside (IPTG). At mid-log phase (OD600= 0.6), cells were centrifuged and tested for β-galactosidase activity as previously described (Di Lallo et al., 2001).

Table 4.2. Plasmids used in the study.

Plasmid	Genotype	Source
pCI_{p22L}	pCI_{p22} derivative carrying a linker	(Di Lallo et al., 2001; Zou et al., 2017)
pCI_{434L}	pCI_{434} derivative carrying a linker	(Di Lallo et al., 2001; Zou et al., 2017)
pcIp22-Z	pCI_{p22L} derivative carrying *ftsZ*	This study
pcI434-Z	pCI_{434L} derivative carrying *ftsZ*	This study
pcIp22-W	pCI_{p22L} derivative carrying *ftsW*	This study
pcI434-W	pCI_{434L} derivative carrying *ftsW*	This study
pcIp22-Q	pCI_{p22L} derivative carrying *ftsQ*	This study
pcI434-Q	pCI_{434L} derivative carrying *ftsQ*	This study
pcIp22-L	pCI_{p22L} derivative carrying *ftsL*	This study
pcI434-L	pCI_{434L} derivative carrying *ftsL*	This study
pcIp22-I	pCI_{p22L} derivative carrying *ftsI*	This study
pcI434-I	pCI_{434L} derivative carrying *ftsI*	This study
pcIp22-A	pCI_{p22L} derivative carrying *ftsA*	This study
pcI434-A	pCI_{434L} derivative carrying *ftsA*	This study
pcIp22-D	pCI_{p22L} derivative carrying *divIVA*	This study
pcI434-D	pCI_{434L} derivative carrying *divIVA*	This study
pcI434-B	pCI_{434L} derivative carrying *ftsB*	This study
pcIp22-B	pCI_{p22L} derivative carrying *ftsB*	This study
pcIp22-EF1025	pCI_{p22L} derivative carrying *EF1025*	This study
pcI434-EF1025	pCI_{434L} derivative carrying *EF1025*	This study

Table 4.3. Primers used in the study.

Primer	**Sequence (5'-3')[1]**	**Restriction Endonuclease site**
A1	GGCAGATCTCATGGCAAAAACAGGAATG	BglII
A2	CCGGATCCTTAGTCGAAAATGTTCGAGA	BamHI
L1	GCGGGTCGACGATGGCTGAATTGAAGAAAGT	SalI
L2	GCGGGATCCTTATTTAAACAGTCCTAACATT	BamHI
Q1	GCCGTCGACAGTGTGGAAGATTAGTAACGA	SalI
Q2	CGGGATCCTTATTCTGCTTGTTGCACTTC	BamHI
I1	GCCCGTCGACCATGATGAAAAGACATAAAT	SalI
I2	CCCAGATCTTTATTCTGTGCCTTCTAAAG	BglII
Z1	GCGCGTCGACCATGGAATTTTCATTAGAC	SalI
Z2	CGGGATCCTTATCGTTTTCTGCGGAAAA	BamHI
W1	GCCCGTCGACCTTGCCAAACAAAGTAAAGAAAC	SalI
W2	GCGGGATCCTTATTGGTTCTGTTCTAAAGATA	BamHI
B1	GCCGTCGACCATGGGAAAGAATGAAAAAAACTC	SalI
B2	GCGGGATCCTTATTCAGCTGAAGACTTAGTTGTT	BamHI
D1	GCGTCGACTATGGCATTAAC	SalI
D2	GCGGATCCCTATTTTGATTC	BamHI
EF10251	GCGTCGAC TTATCTGTTTTGTGCG	SalI
EF10252	GCGGATCCCTACGTAATATAGGTTAAAATTTTCG	BamHI

E. coli R721 cells with no plasmid were used as the baseline control for β-galactosidase production while *E. coli* R721 with single plasmid transformants served as a negative control for the calculation of the percentage residual β-galactosidase activity (Table 4.1). A percentage decrease in residual β-galactosidase activity was compared to the *E. coli* R721 cells, where a value of less than 50% was defined as positive for protein interactions. B2H studies were conducted in triplicate and analyzed using Graph Pad Prism respectively and an average of the percentage residual β-galactosidase activity and the standard deviation was determined.

4.4. Results

4.4.1. *E. faecalis* divisome protein interactions

The B2H assay (Di Lallo et al., 2001), was used to detect pairwise interactions between the proteins ($FtsZ_{Ef}$, $FtsA_{Ef}$, $FtsQ_{Ef}$, $FtsL_{Ef}$, $FtsI_{Ef}$, $FtsW_{Ef}$, $DivIVA_{Ef}$, and $FtsB_{Ef}$) from *E. faecalis* whose homologues have been reported to be implicated in divisome formation in *S. pneumoniae*, *B. subtilis* and *S. aureus* (Fadda et al., 2007; Maggi et al., 2008; Gamba et al., 2009; Steele et al., 2011; Halbedel and Lewis, 2019). EF1025, a $DivIVA_{Ef}$ interacting protein from *E. faecalis*, was also tested for potential interactions with *E. faecalis* divisome proteins.

We identified twelve homo/hetero-dimer interactions among seven divisome proteins including $FtsZ_{Ef}$, $FtsA_{Ef}$, $FtsQ_{Ef}$, $FtsL_{Ef}$, $FtsI_{Ef}$, $FtsW_{Ef}$, and $FtsB_{Ef}$. Proteins like $FtsZ_{Ef}$, $FtsQ_{Ef}$, $FtsW_{Ef}$, and $FtsB_{Ef}$ were identified to homo-dimerize by displaying lower than 50% residual β-galactosidase activity which indicated a positive interaction (Table 4.4). The self-interaction of $FtsZ_{Ef}$ served as a positive control in all B2H assays. Strong interaction was observed between $FtsZ_{Ef}$-$FtsA_{Ef}$ (30%), $FtsZ_{Ef}$-$FtsL_{Ef}$ (37%), $FtsZ_{Ef}$-$FtsI_{Ef}$ (41.6%), $FtsW_{Ef}$-$FtsA_{Ef}$ (35.5%), $FtsW_{Ef}$-$FtsI_{Ef}$ (42.1%), $FtsB_{Ef}$-$FtsQ_{Ef}$ (43.9%), and $FtsB_{Ef}$-$FtsL_{Ef}$ (42%) while $FtsI_{Ef}$-$FtsA_{Ef}$ displayed relatively weaker interaction i.e. 47.2% residual β-galactosidase activity. The interaction between $FtsB_{Ef}$ and $FtsW_{Ef}$ showed borderline (i.e. 50.9%) residual β-galactosidase activity.

pcIp22 / pcI434	FtsZ	FtsA	FtsQ	FtsL	FtsI	FtsW	FtsB
FtsZ	24.1%						
FtsA	30.0%	57.5%					
FtsQ	96.2%	84.4%	37.2%				
FtsL	37%	54.1%	62.1%	72.3%			
FtsI	41.6%	47.2%	56.4%	80.1%	69.3%		
FtsW	52.3%	35.5%	99.2%	86.8%	42.1%	42.1%	
FtsB	71.4%	78.4%	43.9%	42.1%	68.2%	50.9%	48.5%

Table 4.4. Interactions between seven cell division proteins from *E. faecalis* as determined by B2H assay. The β-galactosidase activity was expressed in percentage Miller Units. Average values were obtained from three independent assays in triplicates. Values of less than 50% indicate a positive interaction (indicated in a closed box). $FtsZ_{Ef}$ self-interaction was used as a positive control. The data are the mean values of averages of percentage β-galactosidase activity.

4.4.2. DivIVA$_{Ef}$ interaction with *E. faecalis* divisome proteins

DivIVA$_{Ef}$ was interpreted to interact with FtsZ$_{Ef}$ (47%), FtsQ$_{Ef}$ (47%), and FtsW$_{Ef}$ (39%) by displaying less than 50% residual β-galactosidase activity (Table 4.5). No interaction was observed between DivIVA$_{Ef}$-FtsA$_{Ef}$, DivIVA$_{Ef}$-FtsL$_{Ef}$, DivIVA$_{Ef}$-FtsI$_{Ef}$, and DivIVA$_{Ef}$-FtsB$_{Ef}$ as the residual β-galactosidase activity was observed to be higher than 50%. DivIVA$_{Ef}$ also interacted with EF1025, as is shown previously (Chapter 2).

Interacting Protein	% Residual β-galactosidase activity		
	pCI_{p22L}+$DivIVA_{Ef}$	pCI_{434L}+$DivIVA_{Ef}$	Average
FtsZ	54	40	**47**
FtsQ	52	42	**47**
FtsA	52	58	55
FtsL	77	74	76
FtsW	39	39	**39**
FtsI	53	64	59
FtsB	87	22	55

Table 4.5. $DivIVA_{Ef}$ interaction with other divisome proteins from *E. faecalis* as determined by B2H assays. The data are the averages of at least three independent assays in triplicates. Average values of less than 50% indicate a positive interaction- indicated in closed boxes.

4.4.3. EF1025 interaction with *E. faecalis* divisome proteins

EF1025 is a previously reported $DivIVA_{Ef}$ associating protein (Chapter 2) that affects cell length and shape in *E. faecalis*. To characterise whether EF1025 was a part of the divisome in *E. faecalis* or not, potential divisome interacting partners were identified in a B2H assay. EF1025 failed to interact with $FtsZ_{Ef}$, $FtsQ_{Ef}$, $FtsA_{Ef}$, $FtsL_{Ef}$, $FtsW_{Ef}$, $FtsI_{Ef}$, or $FtsB_{Ef}$. However, EF1025 showed positive interaction with $DivIVA_{Ef}$ (44%) in the B2H assay, consistent with previous reports (Table 4.6; Chapter 2).

Divisome Protein	% Residual β-galactosidase activity		
	pCI_{p22L}+EF1025	pCI_{434L}+EF1025	Average
FtsZ	78	85	82
FtsQ	93	97	95
FtsA	67	51	59
FtsL	64	52	58
FtsW	71	71	71
FtsI	65	78	72
FtsB	80	64	72
DivIVA	39	48	44

Table 4.6. Interaction of EF1025 with divisome proteins from *E. faecalis* as determined by B2H assay. The data are the averages of at least three independent assays in triplicates. Average values of less than 50% indicate a positive interaction- indicated in a box.

4.5. Discussion

Studying protein-protein interactions (PPIs) is important since identifying interaction partners for a protein can help in identifying its function (Rao et al., 2014). This has led to the development of interactomes for various cellular processes such as cell division. Techniques like Yeast-two hybrid (Y2H), GST (Glutathione S-transferase)-pull down, Co-immunoprecipitation (Co-IP), B2H, immunofluorescence microscopy (IFM), Surface Plasmon Resonance (SPR), and green fluorescent protein (GFP) fluorescence microscopy have been widely used to study binary PPIs and deduce cell division protein interactions (Harry et al., 1995; Ma et al., 1996; Karimova et al., 1998; Di Lallo et al., 2001; Fadda et al., 2007; Maggi et al., 2008; Rigden et al., 2008; Zou et al., 2017). Results from this study show for the first time, using B2H analysis, the presence of various interactions in the *E. faecalis* divisome proteins.

In total, 16 homo/hetero-dimer interactions were observed in proteins including $FtsZ_{Ef}$, $FtsA_{Ef}$, $FtsQ_{Ef}$, $FtsL_{Ef}$, $FtsI_{Ef}$, $FtsW_{Ef}$, $DivIVA_{Ef}$, and $FtsB_{Ef}$ where many divisome members like $FtsZ_{Ef}$, $FtsA_{Ef}$, $FtsL_{Ef}$, and $DivIVA_{Ef}$ had multiple interacting partners (Fig. 4.1). This indicates that multiple interactions tend to stabilize the multi-protein divisome complex during cell division. The interactions between FtsA and FtsZ, and FtsA and FtsI, are conserved not only in Gram-positive organisms like *S. pneumoniae* and *S. aureus* but in *E. coli,* a Gram-negative organism, as well (Karimova et al., 1998; Di Lallo et al., 2003; Maggi et al., 2008; Steele et al., 2011). This reflects the presence of a generic basic bacterial division multi-protein complex that is formed at the midcell. The homodimerization property of FtsZ, FtsB, FtsQ, and DivIVA has been reported in *S. pneumoniae*, and *S. aureus* also (Fadda et al., 2007; Maggi et al., 2008; Steele et al., 2011). Besides these, FtsA, FtsK, FtsL, and FtsL have been reported to homodimerize in *S. pneumoniae*, and *S. aureus* also (Fadda et al., 2007; Maggi et al., 2008; Steele et al., 2011). *E. coli* cell division interactome studies revealed homodimerization properties of $FtsZ_{Ec}$, $FtsA_{Ec}$, $FtsB_{Ec}$, $FtsQ_{Ec}$, $FtsK_{Ec}$, and $FtsL_{Ec}$ (Karimova et al., 1998; Di Lallo et al., 2003). Surprisingly, $FtsA_{Ef}$ was not found to self-interact in this study. DivIVA is a highly conserved, "late" cell division protein that is crucial for septum determination. Homologues of *B. subtilis* DivIVA are present in most Gram-positive bacteria, interacting with different partners and performing a variety of functions (Fadda et al., 2003; Kang et al., 2008; Rigden et al., 2008; Donovan et al., 2012; Massidda et al., 2013; Kaval et al., 2014; Bottomley et al., 2017; Ni et al., 2018; Halbedel and Lewis, 2019). Of all the

functionally characterized DivIVA interacting proteins, none is a divisome member. We observed similar findings since EF1025 failed to interact with any other *E. faecalis* divisome proteins except $DivIVA_{Ef}$.

When compared with cell division interactomes from Gram-negative bacteria, *E. faecalis* interactome shared four interactions i.e. FtsA-FtsI, FtsA-FtsZ, FtsB-FtsL and FtsB-FtsQ with *E. coli* divisome interactome (Karimova et al., 1998; Di Lallo et al., 2003), whereas *Neisseria gonorrhoeae* shared only one interaction between FtsA and FtsW (Zou et al., 2017). *E. faecalis* divisome interactome shared more number of key interactions with *S. pneumoniae*, and *S. aureus*, such as FtsZ-FtsA, FtsA-FtsL and FtsA-FtsI (Figure 4.1; Maggi et al., 2008; Steele et al., 2014). In comparison to *S. pneumoniae* interactome, the interaction of FtsZ with DivIVA and FtsL, and DivIVA interaction with FtsW and FtsQ are conserved (Fadda et al., 2007; Maggi et al., 2008). However, interactions like FtsA-FtsW, FtsL-FtsB, and FtsB-FtsQ were absent in *S. pneumoniae* but existed in *S. aureus* and *E. faecalis* (Maggi et al., 2008; Steele et al., 2011). Only one unique interaction i.e. $FtsZ_{Ef}$-$FtsI_{Ef}$ was identified in *E. faecalis* cell division interactome. This shows that although *E. faecalis* is a Gram-positive organism like *S. pneumoniae* and *S. aureus*, its interactome is unique.

B2H is a powerful genetic technique that studies a more integrated network of overlapping interactions in contrast to the genetic experiments that explain sequential recruitment of proteins during divisome assembly (Rowlett and Margolin, 2015). Nonetheless, like any two-hybrid assay, B2H is also prone to false positives and negatives. Therefore, B2H is often paired with other rigorous methods like Co-IP and GST-pull down assay (Maggi et al., 2008; Zou et al., 2017). Di Lallo et al. (2003) were the first to use B2H assay to deduce the cell division interactome network in *E. coli* using nine divisome proteins (i.e. $FtsZ_{Ec}$, $FtsA_{Ec}$, $ZipA_{Ec}$, $FtsK_{Ec}$, $FtsQ_{Ec}$, $FtsL_{Ec}$, $FtsI_{Ec}$, $FtsW_{Ec}$, and $FtsN_{Ec}$). Karimova et al. (2005) later on expanded on this knowledge using their own version of a B2H assay i.e. the bacterial adenylate cyclase two-hybrid (BACTH) system, which relies on the reconstruction of a cyclic AMP (cAMP) signalling cascade upon interaction (Karimova et al., 1998). They reconfirmed all the interactions showed by Di Lallo et al. (2003) and included FtsB for testing possible interactions with other cell division proteins. Collectively in *E. coli*, sixteen interactions between ten cell division proteins (i.e. including $FtsZ_{Ec}$, $FtsA_{Ec}$, $ZipA_{Ec}$, $FtsK_{Ec}$, $FtsQ_{Ec}$, $FtsB_{Ec}$, $FtsL_{Ec}$, $FtsI_{Ec}$, $FtsW_{Ec}$, and $FtsN_{Ec}$) were identified (Di Lallo et al., 2003; Karimova et al., 2005). Maggi et al. (2008) used B2H assay to test interactions between

eleven *S. pneumoniae* division proteins and reconfirmed nine interactions i.e. FtsA–FtsK, FtsA–FtsL, FtsZ–FtsW, FtsZ–FtsQ/DivIB, FtsZ–FtsL, FtsK–FtsW, FtsL–PBP2x, FtsZ–FtsB/DivIC and FtsW–FtsB/DivIC using Co-IP assay.

Co-IP is an excellent technique to study multi-protein complexes formed during cell division (Mackay et al., 2007). When coupled with mass spectrometry (MS), accurate detection of the complex components can be determined. However, producing an antibody against each protein in question with no cross-reactivity can be very expensive and time-consuming. Another robust technique to study co-complexes is tandem affinity purification-mass spectrometry (TAP-MS) which allows specific tagging and subsequent purification of the protein of interest along with its interacting partners (Berggård et al., 2007). TAP-MS can not only identify direct interaction but also indirect interactions between various proteins under the native conditions of the cell (Kaiser et al., 2008). Real-time imaging can also be performed to study the interaction of two cell division proteins using bimolecular fluorescence complementation (BIFC) (Pazos et al., 2013). BIFC relies on expressing the N-terminal and C-terminal fragments of a fluorescent protein which is non-fluorescent but fluoresces when brought together through PPI (Hu et al., 2002). Such imaging can also be performed using Forster resonance energy transfer (FRET) which depends on the transfer of energy from a donor fluorophore to receptor fluorophore when they are in proximity (between 1 and 8 nm), measured increase or decrease in donor emission reflects an interaction between two proteins (Sourjik and Berg, 2002).

In conclusion, the first cell division interactome of *E. faecalis* using B2H assay has been produced. In comparison with the published interactomes from *E. coli* (Karimova et al., 1998; Di Lallo et al., 2003), *S. aureus* (Steele et al., 2011), and *S. pneumoniae* (Fadda et al., 2007; Maggi et al., 2008), the interaction pair FtsA-FtsZ and FtsA-FtsI, was conserved. We observed only one unique interaction pair i.e. FtsZ-FtsI, which indicates that *E. faecalis* divisome requires different stabilizing members during the process of cell division. Future work needs to focus on confirming these interactions using a GST-pull down or Co-IP assay.

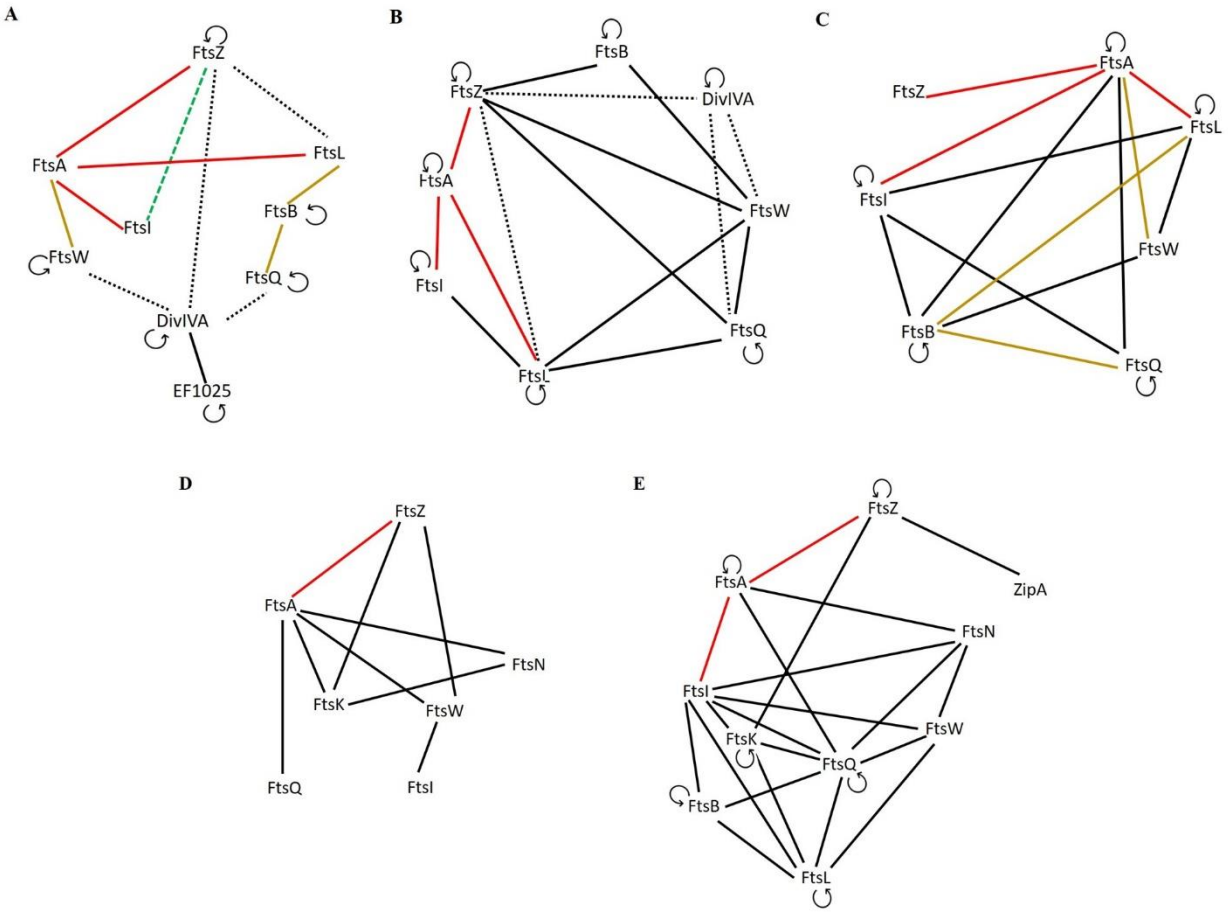

Figure 4.1. Cell division interactome of (A) *E. faecalis*, (B) *S. pneumoniae* (Fadda et al., 2007; Maggi et al., 2008), (C) *S. aureus* (Steele et al., 2011), (D) *N. gonorrhoeae* (Zou et al., 2017), (E) *E. coli* (Di Lallo et al., 2003; Karimova et al., 2005). Red lines- conserved interaction; Dotted black lines- conserved interaction between *E. faecalis* and *S. pneumoniae* interactomes; Yellow solid line- conserved interaction between *E. faecalis* and *S. aureus*; Green dotted line- unique interaction; Curved arrows show self-interaction of proteins in *E. faecalis*. Presented interactome for *S. pneumoniae* is a compilation of original interactomes reported by Fadda et al. (2007) and Maggi et al. (2008).

Chapter 5. General conclusion and future considerations

E. faecalis, well known for its multiple antibiotic resistance, is responsible for 70% of the hospital-acquired enterococcal infections worldwide (Cross and Jacobs, 1996; Hidron et al., 2008a). Due to its additional ability to form a biofilm, catheter-related urinary tract infections are difficult to treat with conventional antibiotics (Mohamed and Huang, 2007). All these added characteristics render Enterococci as an increasingly difficult problem for society with available therapeutic agents in the market today. New therapeutic targets and strategies are needed to combat enterococcal infections that ask for an in-depth understanding of enterococcal physiology and genetics.

B. subtilis served as a model organism for studying and understanding the process of cell division in Gram-positive bacteria for decades, and *E. coli* served the same role to Gram-negative bacteria. Researchers kept studying model organisms frequently for their convenience and made advancement in acquiring knowledge rapidly which resulted in the development of genetic tools, techniques and resources specifically for these organisms (Russell et al., 2017). As a result, studying model organisms surpassed studying non-model systems with time. Although major model organisms come with their convenience to study, aren't necessarily the best systems for all possible questions.

I present the first information about a $DivIVA_{Ef}$ interacting protein, EF1025, in *E. faecalis,* which is predominantly conserved in Gram-positive bacteria and affects cell length and shape. The interaction between $DivIVA_{Ef}$ and EF1025 was ascertained using *in vivo* and *in vitro* techniques. It was not possible to obtain viable cells after the deletion or insertional inactivation of *EF1025* without *in trans* expression of the gene. SEM and TEM images of the rescued cells displayed cell elongation and aberrant cell shape. My second study expanded the knowledge of the EF1025 homologue, CcpN, in *B. subtilis.* This research suggests that the interaction between DivIVA and CcpN homologues could be highly conserved among Gram-positive microorganisms. CcpN interacted with $DivIVA_{Bs}$ in B2H and GST-pull down assays and insertional inactivation of *ccpN* resulted in cell elongation. Finally, my third study reported the existence of a unique cell division interactome in *E. faecalis*. It also showed that EF1025 does not belong to *E. faecalis* divisome.

These findings collectively enhance knowledge of EF1025, a $DivIVA_{Ef}$ interacting protein, in *E. faecalis*, thereby contributing to the overall understanding of this pathogen.

5.1. EF1025 is a $DivIVA_{Ef}$ interacting protein from *E. faecalis*

Initially, DivIVA was proposed as the topological marker in *B. subtilis* where it was described as the replacement for MinE, a protein which provides the localization cues for targeting the MinCD complex to the cell poles (Cha and Stewart, 1997; Rowlett and Margolin, 2013). $DivIVA_{Bs}$ functions as a mid-cell determinant by attracting the MinC/MinD complex to the cell poles, therefore preventing cell division at the polar region (Cha and Stewart, 1997; Edwards et al., 2000; Edwards and Errington, 1997; Harry and Lewis, 2003; Karoui and Errington, 2001; Marston and Errington, 1999). $DivIVA_{Bs}$ was reported also to interact with sporulation proteins like RacA, Spo0J, and Soj (Ben-Yehuda et al., 2003; Wu and Errington, 2003). DivIVA interacts with different proteins in different Gram-positive bacterial species performing a wide variety of functions including synthesis of the cell wall (Nguyen et al., 2007; Kang et al., 2008), cell growth (Flärdh, 2010), chromosome segregation (Perry and Edwards, 2006; Fadda et al., 2007; Donovan et al., 2012; Bottomley et al., 2017), cell division (Bramkamp et al., 2008; Giefing et al., 2008; Patrick and Kearns, 2008; Mukherjee et al., 2009; Nováková et al., 2010; Ni et al., 2018), competence development (Briley et al., 2011; dos Santos et al., 2012), sporulation (Perry and Edwards, 2006; Lenarcic et al., 2009) and protein secretion (Nováková et al., 2010; Halbedel et al., 2012, 2014; Kaval et al., 2014; Ni et al., 2018). While there is a great deal of information about DivIVA interacting proteins in *B. subtilis, S. pneumoniae, S. suis, S. aureus, L. monocytogenes, C. glutamicum, M. tuberculosis, M. smegmatis* and *S. coelicolor,* there is no information available regarding DivIVA-associating proteins in *E. faecalis.*

EF1025 was found to affect cell length and shape of *E. faecalis* cells. The rod-shape of *B. subtilis* is determined and maintained by the action of "cytoskeletal" proteins of the MreB family i.e. MreB, MreC and MreD, that are also involved in cell elongation (Wachi et al. 1987; Levin et al. 1992; Varley and Stewart 1992; Abhayawardhane and Stewart 1995). Mutations in *mreB* exhibit enhanced diameter and grew in a straight row (Carballido-Lopez, 2006). MreC and MreD play important functions in lateral wall growth in *B. subtilis* and its depletion leads to slower growth (Leaver and Errington, 2005). MreB associates with elongation-specific peptidoglycan

(PG)-synthesizing complexes that include the morphogenetic determinants, MreC and MreD, flippase RodA, Penicillin Binding Proteins (PBPs), and peptidoglycan hydrolases (Carballido-López and Formstone, 2007; White et al., 2010). The other interacting partners included GpsB, a major PG synthesis regulator, and translation initiation factor EF-Tu (Soufo et al., 2010; Cleverley et al., 2019). Ovococcal species like *S. pneumoniae*, *L. lactis*, and *E. faecalis* do not produce MreB homologue but encodes MreC and MreD (Land and Winkler, 2011). MreC and MreD localized at the equator and septa of the dividing *S. pneumoniae* and their depletion results in cell rounding and lysis (Land and Winkler, 2011). The association of MreC and MreD with other possible members of the elongation machinery in *S. pneumoniae* is yet to be studied. *E. faecalis* also contains homologues of MreC and MreD, GpsB, RodA and various PBPs (unpublished work). Future work needs to focus on testing the interaction of EF1025 with these members of elongation-specific machinery in *E. faecalis* to achieve a better understanding of how cell elongation happens in this organism.

5.2. EF1025 homologue in *B. subtilis*, CcpN, also interacts with DivIVA$_{Bs}$

EF1025 is predominantly conserved in Gram-positive bacterial species. The EF1025 homologue in *B. subtilis*, CcpN, is a transcriptional regulator of gluconeogenic genes (Servant et al., 2005). EF1025 and CcpN share 41% homology and belongs to the CBS superfamily by possessing an HTH domain at N-terminal and two CBS domains at the central and C-terminal. CcpN has been extensively studied for its function in the downregulation of *gapB, pckA* and *sr1* in the presence of glucose (Licht et al., 2005; Servant et al., 2005). I report another interacting partner of DivIVA$_{Bs}$ and an additional novel function of CcpN in *B. subtilis*.

B2H and GST-pull down assays showed that CcpN interacted with DivIVA$_{Bs}$. Surprisingly, EF1025 also interacted with DivIVA$_{Bs}$ in a heterologous interaction. Such an observation shows that the interaction between DivIVA and EF1025 homologues might be highly conserved among Gram-positive microorganisms and are not species-specific. It would be interesting to study if such conserved interaction is due to the presence of the HTH and CBS domains among all EF1025 homologues or just the two CBS domains at the central and C-terminus. CcpN has been reported to utilize its HTH domain to bind to the conserved upstream promoter regions of *gapB* and *pckA*

for transcriptional regulation (Licht et al., 2005; Servant et al., 2005; Tännler et al., 2008; Licht and Brantl, 2009), but no research has focused on CBS domains in CcpN.

Insertional inactivation of *ccpN* was not lethal to *B. subtilis* (i.e. Bs 1685) in contrast to *EF1025* insertional inactivation of deletion in *E. faecalis*. *B. subtilis* 1685 cells were longer when observed using SEM or AFM. The strains developed by Servant et al. (2005) to study the effects of *ccpN* disruption in the transcription of *gapB* and *pckA* also reflected similar cell elongation. No elongation was observed in the control strain *B. subtilis* PS1649 with a disrupted *pckA.* This showed that the cell elongation phenotype was exclusive to the strains containing a disruption of *ccpN* expression. These strains also showed failed segregation and were observed to form long chains with closely attached cells. The failure to segregate was also observed in *E. faecalis* rescued cells (i.e. *E. faecalis* MJ26) with a complemented copy of *EF1025*. This shows that these phenotypes are specific to a function that might be played by CcpN in *B. subtilis*, and EF1025 in *E. faecalis*.

5.3. *E. faecalis* cell division interactome is unique

Bacterial divisomes are dynamic hyperstructures whose assembly is mediated by multiple protein interactions that exist between various cell division proteins (de Boer, 2010; Lutkenhaus et al., 2012; Egan and Vollmer, 2013). Using techniques like Y2H, GST-pull down, Co-IP, B2H, immunofluorescence microscopy (IFM), Surface Plasmon Resonance (SPR), and green fluorescent protein (GFP) fluorescence microscopy, binary protein-protein interactions among various cell division proteins have been studied (Harry et al., 1995; Ma et al., 1996; Karimova et al., 1998; Di Lallo et al., 2001; Fadda et al., 2007; Maggi et al., 2008; Rigden et al., 2008; Zou et al., 2017). This has lead to the development of cell division networks/interactomes for *E. coli* (Karimova et al., 1998; Di Lallo et al., 2003), *N. gonorrhoeae* (Zou et al., 2017), *S. aureus* (Steele et al., 2011), and *S. pneumoniae* (Fadda et al., 2007; Maggi et al., 2008).

Using B2H assay, protein-protein interactions among eight essential divisome proteins i.e. $FtsZ_{Ef}$, $FtsA_{Ef}$, $FtsQ_{Ef}$, $FtsL_{Ef}$, $FtsI_{Ef}$, $FtsW_{Ef}$, $DivIVA_{Ef}$, and $FtsB_{Ef}$, were tested to establish the very first cell division interactome of *E. faecalis*. The interaction between FtsZ and FtsA, and FtsA and FtsI was conserved when compared with interactomes from *E. coli*, *S. aureus*, and *S. pneumoniae.* However, *E. faecalis* and *N. gonorrhoeae* shared only interaction i.e. FtsZ-FtsA.

Proteins like $FtsZ_{Ef}$, $FtsQ_{Ef}$, $FtsB_{Ef}$, $FtsW_{Ef}$, and $DivIVA_{Ef}$ exhibited self-interaction. FtsZ has been reported to self-interact from all FtsZ homologue containing bacterial species. The self-interaction ability of FtsQ and FtsB has been reported from *E. coli*, *S. aureus*, and *S. pneumoniae* (Karimova et al., 1998; Maggi et al., 2008; Steele et al., 2011), but is absent for FtsW. *S. pneumoniae* and *E. faecalis* DivIVA has been also reported to self-interact but no such information is available for $DivIVA_{Sa}$ (Fadda et al., 2003; Ramirez-Arcos, 2005; Rigden et al., 2008). Surprisingly, the self-interaction of $FtsA_{Ef}$ was absent but have been reported for FtsA from *E. coli*, *S. aureus*, and *S. pneumoniae* (Karimova et al., 1998; Di Lallo et al., 2001; Maggi et al., 2008; Steele et al., 2011).

Using Co-IP, Buddelmeijer and Beckwin (2004) showed the formation of a trimeric complex by three membrane proteins i.e. FtsQ, FtsL, and FtsB, in *E. coli* and *B. subtilis* before their migration to the midcell position (Buddelmeijer and Beckwith, 2004). In *E. faecalis*, a positive interaction was observed between $FtsQ_{Ef}$-$FtsB_{Ef}$, and $FtsB_{Ef}$-$FtsL_{Ef}$ but no interaction between $FtsQ_{Ef}$ and $FtsL_{Ef}$ was observed. This could be because the interaction between $FtsQ_{Ef}$ and $FtsL_{Ef}$ is dependent on a stable interaction between $FtsB_{Ef}$ with either $FtsQ_{Ef}$ or $FtsL_{Ef}$. This observation was in line with Steele et al. (2011) where similar interactions were observed in *S. aureus*. Future studies can focus on investigating such ternary protein complexes using Co-IP, TAP-MS and bacterial three-hybrid systems. The interactome observed for *E. faecalis* cell divisome proteins was very different from *E. coli* cell division interactome. However, the *E. faecalis* divisome interactome exhibited a blend of conserved interactions among *S. pneumoniae* and *S. aureus* cell division proteins with only one unique interaction between $FtsZ_{Ef}$ and $FtsI_{Ef}$. This study also showed that EF1025 is not a member of the *E. faecalis* divisome. This reflects that the majority of the DivIVA interacting partners from various bacterial species are not a part of the divisome. $DivIVA_{Sp}$ has been reported to interact with $FtsZ_{Sp}$, $FtsQ_{Sp}$, and $FtsW_{Sp}$, however, the precise function of such interactions is yet to be explained (Fadda et al., 2007). To further validate this interactome more efficient and sensitive methods like GST-pull down, Co-IP, and SPR assays, need to be employed.

5.4. Limitations of this research

This research does not include the specific function of the distinct domains of EF1025 i.e. HTH domain and CBS domains. Although, the two CBS domains together interacted with $DivIVA_{Ef}$

and are responsible for the self-interaction property of EF1025, the precise function of CBS domains in EF1025 is unknown. EF1025 homologue in *B. subtilis*, CcpN, is a transcriptional regulator which utilizes its HTH domain to bind to the conserved upstream promoter regions of *gapB* and *pckA* (Licht et al., 2005; Servant et al., 2005; Tännler et al., 2008; Licht and Brantl, 2009). Preliminary bioinformatic searches have shown that the conserved upstream promoter sequences from *B. subtilis* are absent for its homologues in *E. faecalis* (i.e. *type I gapB* and *pckA*). This might reflect that EF1025 might be regulating the expression of a different set of genes. Thus, it is necessary to investigate the function of the HTH domain in *E. faecalis*. Future studies should also include studying the effects of *ccpN* overexpression on *B. subtilis* cell morphology. The cell division interactome of *E. faecalis* included eight divisome proteins (i.e. $FtsZ_{Ef}$, $FtsA_{Ef}$, $FtsQ_{Ef}$, $FtsL_{Ef}$, $FtsI_{Ef}$, $FtsW_{Ef}$, $DivIVA_{Ef}$, and $FtsB_{Ef}$) but did not include other divisome protein homologues of FtsK, EzrA and ZapA that are present in *E. faecalis*. Potential interactions of the *E. faecalis* FtsK, EzrA and ZapA with other divisome proteins can be examined using B2H and GST-pull down assay to obtain a complete divisome interactome for *E. faecalis*.

References

Aarsman, M. E. G., Piette, A., Fraipont, C., Vinkenvleugel, T. M. F., Nguyen-Distèche, M., and Blaauwen, T. den (2005). Maturation of the *Escherichia coli* divisome occurs in two steps. *Mol. Microbiol.* 55, 1631–1645. doi:10.1111/j.1365-2958.2005.04502.x.

Abhayawardhane, Y., and Stewart, G. C. (1995). *Bacillus subtilis* possesses a second determinant with extensive sequence similarity to the *Escherichia coli* mreB morphogene. *J. Bacteriol.* 177, 765–773. doi:10.1128/jb.177.3.765-773.1995

Al-Ahmad, A., Maier, J., Follo, M., Spitzmüller, B., Wittmer, A., Hellwig, E., et al. (2010). Food-borne enterococci integrate into oral biofilm: an in vivo study. *J. Endod.* 36, 1812–1819. doi:10.1016/j.joen.2010.08.011.

Al-Ahmad, A., Müller, N., Wiedmann-Al-Ahmad, M., Sava, I., Hübner, J., Follo, M., et al. (2009). Endodontic and salivary isolates of *Enterococcus faecalis i*ntegrate into biofilm from human salivary bacteria cultivated in vitro. *J. Endod.* 35, 986–991. doi:10.1016/j.joen.2009.04.013.

Anderson, D. E., Gueiros-Filho, F. J., and Erickson, H. P. (2004). Assembly dynamics of FtsZ rings in *Bacillus subtilis* and *Escherichia coli* and effects of FtsZ-regulating proteins. *J. Bacteriol.* 186, 5775–5781. doi:10.1128/JB.186.17.5775-5781.2004.

Aravind, L., and Koonin, E. V. (1999). Gleaning non-trivial structural, functional and evolutionary information about proteins by iterative database searches. *J. Mol. Biol.* 287, 1023–1040. doi:10.1006/jmbi.1999.2653.

Arias, C. A., and Murray, B. E. (2012). The rise of the Enterococcus: beyond vancomycin resistance. *Nat. Rev. Microbiol.* 10, 266–278. doi:10.1038/nrmicro2761.

Arias-Moliz, Mt., Baca, P., Ordonez-Becerra, S., Gonzalez-Rodriguez, Mp., and Ferrer-Luque, Cm. (2012). Eradication of enterococci biofilms by lactic acid alone and combined with chlorhexidine and cetrimide. *Med. Oral Patol. Oral Cirugia Bucal*. 17, 902–906. doi:10.4317/medoral.18133.

Ayala, J. A., Garrido, T., De Pedro, M. A., and Vicente, M. (1994). Molecular biology of bacterial septation. *New Compre Biochemi*, 73–101. doi:10.1016/S0167-7306(08)60408-1.

Baarle, S. van, Celik, I. N., Kaval, K. G., Bramkamp, M., Hamoen, L. W., and Halbedel, S. (2013). Protein-Protein Interaction Domains of *Bacillus subtilis* DivIVA. *J. Bacteriol.* 195, 1012–1021. doi:10.1128/JB.02171-12.

Bach, J. N., Albrecht, N., and Bramkamp, M. (2014). Imaging DivIVA dynamics using photo-convertible and activatable fluorophores in *Bacillus subtilis. Front. Microbiol.* 5, 59. doi:10.3389/fmicb.2014.00059.

Bae, T., Clerc-Bardin, S., and Dunny, G. M. (2000). Analysis of expression of prgX, a key negative regulator of the transfer of the *Enterococcus faecalis* pheromone-inducible plasmid pCF10. *J. Mol. Biol.* 297, 861–875. doi:10.1006/jmbi.2000.3628.

Barák, I., Muchová, K., and Labajová, N. (2019). Asymmetric cell division during *Bacillus subtilis* sporulation. *Future Microbio.* 14, 4. doi:10.2217/fmb-2018-0338.

Bateman, A. (1997). The structure of a domain common to archaebacteria and the homocystinuria disease protein. *Trends Biochem. Sci.* 22, 12–13. doi: 10.1016/s0968-0004(96)30046-7.

Baykov, A. A., Tuominen, H. K., and Lahti, R. (2011). The CBS domain: a protein module with an emerging prominent role in regulation. *ACS Chem. Biol.* 6, 1156–1163. doi:10.1021/cb200231c.

Beilharz, K., Nováková, L., Fadda, D., Branny, P., Massidda, O., and Veening, J.-W. (2012). Control of cell division in *Streptococcus pneumoniae* by the conserved Ser/Thr protein kinase StkP. *Proc. Natl. Acad. Sci.* 109, 905–913. doi:10.1073/pnas.1119172109.

Ben-Yehuda, S., Rudner, D. Z., and Losick, R. (2003). RacA, a bacterial protein that anchors chromosomes to the cell poles. *Science* 299, 532–536. doi:10.1126/science.1079914.

Berggård, T., Linse, S., and James, P. (2007). Methods for the detection and analysis of protein–protein interactions. *Proteomics.* 7, 2833–2842. doi:10.1002/pmic.200700131.

Bhat, S. V., Booth, S. C., Vantomme, E. A. N., Afroj, S., Yost, C. K., and Dahms, T. E. S. (2015). Oxidative stress and metabolic perturbations in *Escherichia coli* exposed to sublethal levels of 2,4-dichlorophenoxyacetic acid. *Chemosphere* 135, 453–461. doi:10.1016/j.chemosphere.2014.12.035.

Bi, E., and Lutkenhaus, J. (1991). FtsZ ring structure associated with division in *Escherichia coli*. *Nature* 354, 161–164. doi:10.1038/354161a0.

Biemans-Oldehinkel, E., Mahmood, N. A. B. N., and Poolman, B. (2006). A sensor for intracellular ionic strength. *Proc. Natl. Acad. Sci.* 103, 10624–10629. doi:10.1073/pnas.0603871103.

Bottomley, A. L., Liew, A. T. F., Kusuma, K. D., Peterson, E., Seidel, L., Foster, S. J., et al. (2017). Coordination of chromosome segregation and cell division in *Staphylococcus aureus*. *Front. Microbiol.* 8, 1575. doi:10.3389/fmicb.2017.01575.

Boyle, D. S., and Donachie, W. D. (1998). mraY Is an essential gene for cell growth in *Escherichia coli*. *J. Bacteriol.* 180, 6429–6432.

Bramkamp, M., Emmins, R., Weston, L., Donovan, C., Daniel, R. A., and Errington, J. (2008). A novel component of the division-site selection system of *Bacillus subtilis* and a new mode of action for the division inhibitor MinCD. *Mol. Microbiol.* 70, 1556–1569. doi:10.1111/j.1365-2958.2008.06501.x.

Briley, K., Prepiak, P., Dias, M. J., Hahn, J., and Dubnau, D. (2011). Maf acts downstream of ComGA to arrest cell division in competent cells of *B. subtilis*. *Mol. Microbiol.* 81, 23–39. doi:10.1111/j.1365-2958.2011.07695.x.

Brock, T. D., Peacher, B., and Pierson, D. (1963). Survey of the bacteriocines of enterococci. *J. Bacteriol.* 86, 702–707.

Bron, S., and Venema, G. (1972). Ultraviolet inactivation and excision-repair in *Bacillus subtilis* I. Construction and characterization of a transformable eightfold auxotrophic strain and two ultraviolet-sensitive derivatives. *Mutat. Res. Mol. Mech. Mutagen.* 15, 1–10. doi:10.1016/0027-5107(72)90086-3.

Bryan, E. M., Bae, T., Kleerebezem, M., and Dunny, G. M. (2000). Improved vectors for nisin-controlled expression in Gram-positive bacteria. *Plasmid* 44, 183–190. doi:10.1006/plas.2000.1484.

Buddelmeijer, N., and Beckwith, J. (2004). A complex of the *Escherichia coli* cell division proteins FtsL, FtsB and FtsQ forms independently of its localization to the septal region. *Mol. Microbiol.* 52, 1315–1327. doi:10.1111/j.1365-2958.2004.04044.x.

Bukau, B., and Walker, G. C. (1989). Delta dnaK52 mutants of *Escherichia coli* have defects in chromosome segregation and plasmid maintenance at normal growth temperatures. *J. Bacteriol.* 171, 6030–6038. doi:10.1128/jb.171.11.6030-6038.1989.

Butler, Y. X., Abhayawardhane, Y., and Stewart, G. C. (1993). Amplification of the *Bacillus subtilis* maf gene results in arrested septum formation. *J. Bacteriol.* 175, 3139–3145. doi: 10.1128/jb.175.10.3139-3145.1993

Carballido-Lopez, R. (2006). The bacterial actin-like cytoskeleton. *Microbiol. Mol. Biol. Rev.* 70, 888–909. doi:10.1128/MMBR.00014-06.

Carballido-López, R., and Errington, J. (2003). The bacterial cytoskeleton: in vivo dynamics of the actin-like protein Mbl of *Bacillus subtilis*. *Dev. Cell* 4, 19–28. doi:10.1016/S1534-5807(02)00403-3.

Carballido-López, R., and Formstone, A. (2007). Shape determination in *Bacillus subtilis*. *Curr. Opin. Microbiol.* 10, 611–616. doi:10.1016/j.mib.2007.09.008.

Cha, J.H., and Stewart, G. C. (1997). The divIVA minicell locus of *Bacillus subtilis*. *J. Bacteriol.* 179, 1671–1683. doi: 10.1128/jb.179.5.1671-1683.1997.

Chastanet, A., and Carballido-Lopez, R. (2012). The actin-like MreB proteins in *Bacillus subtilis*: a new turn. *Front. Biosci. Sch. Ed.* 4, 1582–1606. doi: 10.2741/s354.

Christie, P. J., and Dunny, G. M. (1986). Identification of regions of the *Streptococcus faecalis* plasmid pCF-10 that encode antibiotic resistance and pheromone response functions. *Plasmid* 15, 230–241. doi:10.1016/0147-619X(86)90041-7.

Chung, K.M., Hsu, H.H., Govindan, S., and Chang, B.-Y. (2004). Transcription regulation of ezrA and its effect on cell division of *Bacillus subtilis*. *J. Bacteriol.* 186, 5926–5932. doi:10.1128/JB.186.17.5926-5932.2004.

Claessen, D., Emmins, R., Hamoen, L. W., Daniel, R. A., Errington, J., and Edwards, D. H. (2008). Control of the cell elongation–division cycle by shuttling of PBP1 protein in *Bacillus subtilis*. *Mol. Microbiol.* 68, 1029-46. doi:10.1111/j.1365-2958.2008.06210.x.

Cleveland, J., Montville, T. J., Nes, I. F., and Chikindas, M. L. (2001). Bacteriocins: safe, natural antimicrobials for food preservation. *Int. J. Food Microbiol.* 71, 1–20. doi:10.1016/S0168-1605(01)00560-8.

Cleverley, R. M., Barrett, J. R., Baslé, A., Bui, N. K., Hewitt, L., Solovyova, A., et al. (2014). Structure and function of a spectrin-like regulator of bacterial cytokinesis. *Nat. Commun.* 5, 5421. doi:10.1038/ncomms6421.

Cleverley, R. M., Rutter, Z. J., Rismondo, J., Corona, F., Tsui, H.-C. T., Alatawi, F. A., et al. (2019). The cell cycle regulator GpsB functions as cytosolic adaptor for multiple cell wall enzymes. *Nat. Commun.* 10, 1–17. doi:10.1038/s41467-018-08056-2.

Cross, J. T., and Jacobs, R. F. (1996). Vancomycin-resistant enterococcal infections. *Semin. Pediatr. Infect. Dis.* 7, 162–169. doi:10.1016/S1045-1870(96)80004-5.

Dahlén, G., Blomqvist, S., Almståhl, A., and Carlén, A. (2012). Virulence factors and antibiotic susceptibility in enterococci isolated from oral mucosal and deep infections. *J. Oral Microbiol.* 4. doi:10.3402/jom.v4i0.10855.

Daniel, R. A., Drake, S., Buchanan, C. E., Scholle, R., and Errington, J. (1994). The *Bacillus subtilis* spoVD gene encodes a mother-cell-specific penicillin-binding protein required for spore morphogenesis. *J. Mol. Biol.* 235, 209–220. doi:10.1016/s0022-2836(05)80027-0.

de Boer, P. A., Crossley, R. E., and Rothfield, L. I. (1988). Isolation and properties of minB, a complex genetic locus involved in correct placement of the division site in *Escherichia coli*. *J. Bacteriol.* 170, 2106–2112. doi:10.1128/jb.170.5.2106-2112.1988.

de Boer, P. A. J. (2010). Advances in understanding *E. coli* cell fission. *Curr. Opin. Microbiol.* 13, 730–737. doi:10.1016/j.mib.2010.09.015.

Defeu Soufo, H. J., and Graumann, P. L. (2004). Dynamic movement of actin-like proteins within bacterial cells. *EMBO Rep.* 5, 789–794. doi:10.1038/sj.embor.7400209.

den Blaauwen, T. (2018). Is longitudinal division in rod-shaped bacteria a matter of swapping axis? *Front. Microbiol.* 9, 822. doi:10.3389/fmicb.2018.00822.

Di Lallo, G., Castagnoli, L., Ghelardini, P., and Paolozzi, L. (2001). A two-hybrid system based on chimeric operator recognition for studying protein homo/heterodimerization in *Escherichia coli*. *Microbiol. Read. Engl.* 147, 1651–1656. doi:10.1099/00221287-147-6-1651.

Di Lallo, G., Fagioli, M., Barionovi, D., Ghelardini, P., and Paolozzi, L. (2003). Use of a two-hybrid assay to study the assembly of a complex multicomponent protein machinery: bacterial septosome differentiation. *Microbiol. Read. Engl.* 149, 3353–3359. doi:10.1099/mic.0.26580-0.

Domínguez-Escobar, J., Chastanet, A., Crevenna, A. H., Fromion, V., Wedlich-Söldner, R., and Carballido-López, R. (2011). Processive movement of MreB-associated cell wall biosynthetic complexes in bacteria. *Science.* 333, 225–228. doi:10.1126/science.1203466.

Donczew, M., Mackiewicz, P., Wróbel, A., Flärdh, K., Zakrzewska-Czerwińska, J., and Jakimowicz, D. (2016). ParA and ParB coordinate chromosome segregation with cell elongation and division during *Streptomyces* sporulation. *Open Biol.* 6. doi:10.1098/rsob.150263.

Donovan, C., Schauss, A., Krämer, R., and Bramkamp, M. (2013). Chromosome segregation impacts on cell growth and division site selection in *Corynebacterium glutamicum*. *PLOS ONE.* 8, 55078. doi:10.1371/journal.pone.0055078.

Donovan, C., Sieger, B., Krämer, R., and Bramkamp, M. (2012). A synthetic *Escherichia coli* system identifies a conserved origin tethering factor in Actinobacteria. *Mol. Microbiol.* 84, 105–116. doi:10.1111/j.1365-2958.2012.08011.x.

dos Santos, V. T., Bisson-Filho, A. W., and Gueiros-Filho, F. J. (2012). DivIVA-mediated polar localization of ComN, a posttranscriptional regulator of *Bacillus subtilis*. *J. Bacteriol.* 194, 3661–3669. doi:10.1128/JB.05879-11.

Douzi, B. (2017). Protein–protein interactions: surface plasmon resonance. *Methods in Mol. Bio.* 257–275. doi:10.1007/978-1-4939-7033-9_21.

Duez, C., Thamm, I., Sapunaric, F., Coyette, J., and Ghuysen, J. M. (1998). The division and cell wall gene cluster of *Enterococcus hirae* S185. *DNA Seq.* 9, 149–161. doi:10.3109/10425179809072190.

Edwards, D. H., and Errington, J. (1997). The *Bacillus subtilis* DivIVA protein targets to the division septum and controls the site specificity of cell division. *Mol. Microbiol.* 24, 905–915. doi: 10.1046/j.1365-2958.1997.3811764.x.

Edwards, D. H., Thomaides, H. B., and Errington, J. (2000). Promiscuous targeting of *Bacillus subtilis* cell division protein DivIVA to division sites in *Escherichia coli* and fission yeast. *EMBO J.* 19, 2719–2727. doi:10.1093/emboj/19.11.2719.

Egan, A. J. F., and Vollmer, W. (2013). The physiology of bacterial cell division. *Ann. N. Y. Acad. Sci.* 1277, 8–28. doi:10.1111/j.1749-6632.2012.06818.x.

Eraso, J. M., Markillie, L. M., Mitchell, H. D., Taylor, R. C., Orr, G., and Margolin, W. (2014). The highly conserved MraZ protein is a transcriptional regulator in *Escherichia coli*. *J. Bacteriol.* 196, 2053–2066. doi:10.1128/JB.01370-13.

Erickson, H. P., Anderson, D. E., and Osawa, M. (2010). FtsZ in bacterial cytokinesis: cytoskeleton and force generator all in one. *Microbiol. Mol. Biol. Rev.* 74, 504–528. doi:10.1128/MMBR.00021-10.

Errington, J., and Wu, L. J. (2017). Cell Cycle Machinery in *Bacillus subtilis*. *Prokaryotic Cytoskeletons.* 67–101. doi:10.1007/978-3-319-53047-5_3.

Eswaramoorthy, P., Erb, M. L., Gregory, J. A., Silverman, J., Pogliano, K., Pogliano, J., et al. (2011). Cellular architecture mediates DivIVA ultrastructure and regulates min activity in *Bacillus subtilis. mBio.* 2, 00257-11. doi:10.1128/mBio.00257-11.

Eswaramoorthy, P., Winter, P. W., Wawrzusin, P., York, A. G., Shroff, H., and Ramamurthi, K. S. (2014). Asymmetric division and differential gene expression during a bacterial developmental program requires DivIVA. *PLoS Genet.* 10, 1004526. doi:10.1371/journal.pgen.1004526.

Fadda, D., Pischedda, C., Caldara, F., Whalen, M. B., Anderluzzi, D., Domenici, E., et al. (2003). Characterization of divIVA and other genes located in the chromosomal region downstream of the dcw cluster in *Streptococcus pneumoniae*. *J. Bacteriol.* 185, 6209–6214. doi:10.1128/JB.185.20.6209-6214.2003.

Fadda, D., Santona, A., D'Ulisse, V., Ghelardini, P., Ennas, M. G., Whalen, M. B., et al. (2007). *Streptococcus pneumoniae* DivIVA: localization and interactions in a MinCD-free context. *J. Bacteriol.* 189, 1288–1298. doi:10.1128/JB.01168-06.

Fisher, K., and Phillips, C. (2009). The ecology, epidemiology and virulence of Enterococcus. *Microbiology* 155, 1749–1757. doi:10.1099/mic.0.026385-0.

Flärdh, K. (2003). Essential role of DivIVA in polar growth and morphogenesis in *Streptomyces coelicolor* A3(2). *Mol. Microbiol.* 49, 1523–1536. doi:10.1046/j.1365-2958.2003.03660.x.

Flärdh, K. (2010). Cell polarity and the control of apical growth in *Streptomyces*. *Curr. Opin. Microbiol.* 13, 758–765. doi:10.1016/j.mib.2010.10.002.

Flemming, H.-C., and Wingender, J. (2010). The biofilm matrix. *Nat. Rev. Microbiol.* 8, 623–633. doi:10.1038/nrmicro2415.

Fleurie, A., Manuse, S., Zhao, C., Campo, N., Cluzel, C., Lavergne, J.-P., et al. (2014). Interplay of the Serine/Threonine-kinase StkP and the paralogs DivIVA and GpsB in pneumococcal cell elongation and division. *PLOS Genet.* 10, 1004275. doi:10.1371/journal.pgen.1004275.

Foulquié Moreno, M. R., Sarantinopoulos, P., Tsakalidou, E., and De Vuyst, L. (2006). The role and application of enterococci in food and health. *Int. J. Food Microbiol.* 106, 1–24. doi:10.1016/j.ijfoodmicro.2005.06.026.

Francis, F., Ramirez-Arcos, S., Salimnia, H., Victor, C., and Dillon, J.-A. R. (2000). Organization and transcription of the division cell wall (dcw) cluster in *Neisseria gonorrhoeae*. *Gene* 251, 141–151. doi:10.1016/S0378-1119(00)00200-6.

Franz, C. M. A. P., Stiles, M. E., Schleifer, K. H., and Holzapfel, W. H. (2003). Enterococci in foods- a conundrum for food safety. *Int. J. Food Microbiol.* 88, 105–122. doi:10.1016/s0168-1605(03)00174-0.

Gamba, P., Veening, J.-W., Saunders, N. J., Hamoen, L. W., and Daniel, R. A. (2009). Two-step assembly dynamics of the *Bacillus subtilis* divisome. *J. Bacteriol.* 191, 4186–4194. doi:10.1128/JB.01758-08.

Garner, E. C., Bernard, R., Wang, W., Zhuang, X., Rudner, D. Z., and Mitchison, T. (2011). Coupled, circumferential motions of the cell wall synthesis machinery and MreB filaments in *B. subtilis*. *Science* 333, 222–225.doi: 10.1126/science.1203285.

Gelsomino, R., Vancanneyt, M., Cogan, T. M., Condon, S., and Swings, J. (2002). Source of enterococci in a farmhouse raw-milk cheese. *Appl. Environ. Microbiol.* 68, 3560–3565. doi:10.1128/AEM.68.7.3560-3565.2002.

Geraci Joseph E., and Martin William J. (1954). Antibiotic therapy of bacterial endocarditis. *Circulation* 10, 173–194. doi:10.1161/01.CIR.10.2.173.

Giefing, C., Meinke, A. L., Hanner, M., Henics, T., Minh, D. B., Gelbmann, D., et al. (2008). Discovery of a novel class of highly conserved vaccine antigens using genomic scale antigenic fingerprinting of pneumococcus with human antibodies. *J. Exp. Med.* 205, 117–131. doi:10.1084/jem.20071168.

Gilmore, M. S., Lebreton, F., and van Schaik, W. (2013). Genomic transition of enterococci from gut commensals to leading causes of multidrug-resistant hospital infection in the antibiotic era. *Curr. Opin. Microbiol.* 16, 10–16. doi:10.1016/j.mib.2013.01.006.

Gilmore, M. S., Segarra, R. A., Booth, M. C., Bogie, C. P., Hall, L. R., and Clewell, D. B. (1994). Genetic structure of the *Enterococcus faecalis* plasmid pAD1-encoded cytolytic toxin system and its relationship to lantibiotic determinants. *J. Bacteriol.* 176, 7335–7344. doi:10.1128/jb.176.23.7335-7344.1994.

Ginda, K., Bezulska, M., Ziółkiewicz, M., Dziadek, J., Zakrzewska-Czerwińska, J., and Jakimowicz, D. (2013). ParA of *Mycobacterium smegmatis* co-ordinates chromosome segregation with the cell cycle and interacts with the polar growth determinant DivIVA. *Mol. Microbiol.* 87, 998–1012. doi:10.1111/mmi.12146.

Gransden, W. R., King, A., Marossy, D., and Rosenthal, E. (1998). Quinupristin/dalfopristin in neonatal *Enterococcus faecium* meningitis. *Arch. Dis. Child. - Fetal Neonatal Ed.* 78, 235–236. doi:10.1136/fn.78.3.F234d.

Greco-Stewart, V., Ramirez-Arcos, S., Liao, M., and Dillon, J. R. (2007). N terminus determinants of MinC from *Neisseria gonorrhoeae* mediate interaction with FtsZ but do not affect interaction with MinD or homodimerization. *Arch. Microbiol.* 187, 451–458. doi:10.1007/s00203-007-0210-4.

Gueiros-Filho, F. J., and Losick, R. (2002). A widely conserved bacterial cell division protein that promotes assembly of the tubulin-like protein FtsZ. *Genes Dev.* 16, 2544–2556. doi:10.1101/gad.1014102.

Guzmàn, C. A., Pruzzo, C., LiPira, G., and Calegari, L. (1989). Role of adherence in pathogenesis of *Enterococcus faecalis* urinary tract infection and endocarditis. *Infect. Immun.* 57, 1834–1838.

Haeusser, D. P., Garza, A. C., Buscher, A. Z., and Levin, P. A. (2007). The division inhibitor EzrA contains a seven-residue patch required for maintaining the dynamic nature of the medial FtsZ Ring. *J. Bacteriol.* 189, 9001–9010. doi:10.1128/JB.01172-07.

Haeusser, D. P., and Margolin, W. (2016). Splitsville: structural and functional insights into the dynamic bacterial Z ring. *Nat. Rev. Microbiol.* 14, 305–319. doi:10.1038/nrmicro.2016.26.

Halbedel, S., Hahn, B., Daniel, R. A., and Flieger, A. (2012). DivIVA affects secretion of virulence-related autolysins in *Listeria monocytogenes*. *Mol. Microbiol.* 83, 821–839. doi:10.1111/j.1365-2958.2012.07969.x.

Halbedel, S., Kawai, M., Breitling, R., and Hamoen, L. W. (2014). SecA is required for membrane targeting of the cell division protein DivIVA *in vivo*. *Front. Microbiol.* 5, 58. doi:10.3389/fmicb.2014.00058.

Halbedel, S., and Lewis, R. J. (2019). Structural basis for interaction of DivIVA/GpsB proteins with their ligands. *Mol. Microbiol.* 111, 1404-14150. doi:10.1111/mmi.14244.

Hammerum, A. M. (2012). Enterococci of animal origin and their significance for public health. *Clin. Microbiol. Infect. Off. Publ. Eur. Soc. Clin. Microbiol. Infect. Dis.* 18, 619–625. doi:10.1111/j.1469-0691.2012.03829.x.

Hamoen, L. W., Meile, J.-C., Jong, W. D., Noirot, P., and Errington, J. (2006). SepF, a novel FtsZ-interacting protein required for a late step in cell division. *Mol. Microbiol.* 59, 989–999. doi:10.1111/j.1365-2958.2005.04987.x.

Harry, E. J., and Lewis, P. J. (2003). Early targeting of Min proteins to the cell poles in germinated spores of *Bacillus subtilis*: evidence for division apparatus-independent recruitment of Min proteins to the division site. *Mol. Microbiol.* 47, 37–48. doi:10.1046/j.1365-2958.2003.03253.x.

Harry, E. J., Pogliano, K., and Losick, R. (1995). Use of immunofluorescence to visualize cell-specific gene expression during sporulation in *Bacillus subtilis*. *J. Bacteriol.* 177, 3386–3393. doi:10.1128/jb.177.12.3386-3393.1995.

Harry, E., Monahan, L., and Thompson, L. (2006). Bacterial Cell division: the mechanism and its precision. *International Review of Cytology*. 253, 27-94. doi:10.1016/S0074-7696(06)53002-5.

Harwood, C. R. (2007). *Bacillus subtilis* as a model for bacterial systems biology. *Encyclopedia of Life Sciences*. doi:10.1002/9780470015902.a0002027.

Hedlin, C. E. (2009). The essentiality of DivIVA$_{Ef}$ oligomerization for proper cell division in enterococcus faecalis and interaction with a novel cell division protein. Available at: https://harvest.usask.ca/handle/10388/etd-04152009-115838.

Heidrich, N., Chinali, A., Gerth, U., and Brantl, S. (2006). The small untranslated RNA SR1 from the *Bacillus subtilis* genome is involved in the regulation of arginine catabolism. *Mol. Microbiol.* 62, 520–536. doi:10.1111/j.1365-2958.2006.05384.x.

Heidrich, N., Moll, I., and Brantl, S. (2007). In vitro analysis of the interaction between the small RNA SR1 and its primary target ahrC mRNA. *Nucleic Acids Res.* 35, 4331–4346. doi:10.1093/nar/gkm439.

Heller, D. M., Tavag, M., and Hochschild, A. (2017). CbtA toxin of *Escherichia coli* inhibits cell division and cell elongation via direct and independent interactions with FtsZ and MreB. *PLoS Genet.* 13, 1007007. doi:10.1371/journal.pgen.1007007.

Henriques, A. O., Glaser, P., Piggot, P. J., and Jr, C. P. M. (1998). Control of cell shape and elongation by the rodA gene in *Bacillus subtilis*. *Mol. Microbiol.* 28, 235–247. doi:10.1046/j.1365-2958.1998.00766.x.

Hidron, A. I., Edwards, J. R., Patel, J., Horan, T. C., Sievert, D. M., Pollock, D. A., et al. (2008a). Antimicrobial-resistant pathogens associated with healthcare-associated infections: annual summary of data reported to the national healthcare safety network at the centers for disease control and prevention, 2006–2007. *Infect. Control Hosp. Epidemiol.* 29, 996–1011. doi:10.1086/591861.

Hidron, A. I., Schuetz, A. N., Nolte, F. S., Gould, C. V., and Osborn, M. K. (2008b). Daptomycin resistance in *Enterococcus faecalis* prosthetic valve endocarditis. *J. Antimicrob. Chemother.* 61, 1394–1396. doi:10.1093/jac/dkn105.

Hu, C.-D., Chinenov, Y., and Kerppola, T. K. (2002). Visualization of interactions among bZIP and Rel family proteins in living cells using bimolecular fluorescence complementation. *Mol. Cell* 9, 789–798. doi:10.1016/S1097-2765(02)00496-3.

Hussain, H., and Chong, N. F.-M. (2016). Combined overlap extension PCR method for improved site directed mutagenesis. *BioMed Res. Int.* 9, 15637. doi:10.1155/2016/8041532.

Huycke, M. M., and Gilmore, M. S. (1997). In vivo survival of *Enterococcus faecalis* is enhanced by extracellular superoxide production. *Adv. Exp. Med. Biol.* 418, 781–784. doi:10.1007/978-1-4899-1825-3_184.

Huycke, M. M., Joyce, W., and Wack, M. F. (1996). Augmented production of extracellular superoxide by blood isolates of *Enterococcus faecalis*. *J. Infect. Dis.* 173, 743–745. doi:10.1093/infdis/173.3.743.

Huycke, M. M., Sahm, D. F., and Gilmore, M. S. (1998). Multiple-drug resistant enterococci: the nature of the problem and an agenda for the future. *Emerg. Infect. Dis.* 4, 239–249. doi: 10.3201/eid0402.98021.

Ishikawa, S., Kawai, Y., Hiramatsu, K., Kuwano, M., and Ogasawara, N. (2006). A new FtsZ-interacting protein, YlmF, complements the activity of FtsA during progression of cell division in *Bacillus subtilis*. *Mol. Microbiol.* 60, 1364–1380. doi:10.1111/j.1365-2958.2006.05184.x.

Jacob, A. E., and Hobbs, S. J. (1974). Conjugal transfer of plasmid-borne multiple antibiotic resistance in *Streptococcus faecalis* var. zymogenes. *J. Bacteriol.* 117, 360–372.

James, N. G., and Jameson, D. M. (2014). Steady-state fluorescence polarization/anisotropy for the study of protein interactions. *Fluorescence Spectroscopy and Microscopy: Methods and Protocols.* 1076, 29–42. doi:10.1007/978-1-62703-649-8_2.

Jeffery, C. J. (1999). Moonlighting proteins. *Trends Biochem. Sci.* 24, 8–11. doi:10.1016/S0968-0004(98)01335-8.

Jeffery, C. J. (2016). Protein species and moonlighting proteins: Very small changes in a protein's covalent structure can change its biochemical function. *J. Proteomics* 134, 19–24. doi:10.1016/j.jprot.2015.10.003.

Jensen, S. O., Thompson, L. S., and Harry, E. J. (2005). Cell division in *Bacillus subtilis*: FtsZ and FtsA association is Z-ring independent, and FtsA is required for efficient midcell Z-ring assembly. *J. Bacteriol.* 187, 6536–6544. doi:10.1128/JB.187.18.6536-6544.2005.

Jett, B. D., Huycke, M. M., and Gilmore, M. S. (1994). Virulence of enterococci. *Clin. Microbiol. Rev.* 7, 462–478.

Kabeya, Y., Nakanishi, H., Suzuki, K., Ichikawa, T., Kondou, Y., Matsui, M., et al. (2010). The YlmG protein has a conserved function related to the distribution of nucleoids in chloroplasts and cyanobacteria. *BMC Plant Biol.* 10, 57. doi:10.1186/1471-2229-10-57.

Kaiser, P., Meierhofer, D., Wang, X., and Huang, L. (2008). Tandem affinity purification combined with mass spectrometry to identify components of protein complexes. *Methods Mol. Biol.* 439, 309-26. doi:10.1007/978-1-59745-188-8_21.

Kang, C.-M., Nyayapathy, S., Lee, J.-Y., Suh, J.-W., and Husson, R. N. (2008). Wag31, a homologue of the cell division protein DivIVA, regulates growth, morphology and polar cell wall synthesis in mycobacteria. *Microbiology*, 154, 725–735. doi:10.1099/mic.0.2007/014076-0.

Karimova, G., Dautin, N., and Ladant, D. (2005). Interaction network among *Escherichia coli* membrane proteins involved in cell division as revealed by bacterial two-hybrid analysis. *J. Bacteriol.* 187, 2233–2243. doi:10.1128/JB.187.7.2233-2243.2005.

Karimova, G., Pidoux, J., Ullmann, A., and Ladant, D. (1998). A bacterial two-hybrid system based on a reconstituted signal transduction pathway. *Proc. Natl. Acad. Sci.* 95, 5752–5756. doi:10.1073/pnas.95.10.5752.

Karlsson, R., and Fält, A. (1997). Experimental design for kinetic analysis of protein-protein interactions with surface plasmon resonance biosensors. *J. Immunol. Methods.* 200, 121–133. doi:10.1016/S0022-1759(96)00195-0.

Karoui, M. E., and Errington, J. (2001). Isolation and characterization of topological specificity mutants of minD in *Bacillus subtilis. Mol. Microbiol.* 42, 1211–1221. doi:10.1046/j.1365-2958.2001.02710.x.

Kaval, K. G., and Halbedel, S. (2012). Architecturally the same, but playing a different game. *Virulence.* 3, 406–407. doi:10.4161/viru.20747.

Kaval, K. G., Hauf, S., Rismondo, J., Hahn, B., and Halbedel, S. (2017). Genetic dissection of DivIVA functions in *Listeria monocytogenes. J. Bacteriol.* 199, 00421-17. doi:10.1128/JB.00421-17.

Kaval, K. G., Rismondo, J., and Halbedel, S. (2014). A function of DivIVA in *Listeria monocytogenes* division site selection. *Mol. Microbiol.* 94, 637–654. doi:10.1111/mmi.12784.

Kayaoglu, G., and Ørstavik, D. (2004). Virulence factors of *Enterococcus faecalis*: relationship to endodontic disease. *Crit. Rev. Oral Biol. Med.* 15, 308–320. doi: 10.1177/154411130401500506.

Kobayashi, K., Ehrlich, S. D., Albertini, A., Amati, G., Andersen, K. K., Arnaud, M., et al. (2003). Essential *Bacillus subtilis* genes. *Proc. Natl. Acad. Sci.* 100, 4678–4683. doi:10.1073/pnas.0730515100.

Kouidhi, B., Zmantar, T., Mahdouani, K., Hentati, H., and Bakhrouf, A. (2011). Antibiotic resistance and adhesion properties of oral Enterococci associated to dental caries. *BMC Microbiol.* 11, 1–7. doi:10.1186/1471-2180-11-155.

Kreft, B., Marre, R., Schramm, U., and Wirth, R. (1992). Aggregation substance of *Enterococcus faecalis* mediates adhesion to cultured renal tubular cells. *Infect. Immun.* 60, 25–30.

Kristich, C. J., Rice, L. B., and Arias, C. A. (2014). Enterococcal infection—treatment and antibiotic resistance. *Enterococci: From Commensals to Leading Causes of Drug Resistant Infection*. 62.

Król, E., Kessel, S. P. van, Bezouwen, L. S. van, Kumar, N., Boekema, E. J., and Scheffers, D.J. (2012). *Bacillus subtilis* SepF Binds to the C-terminus of FtsZ. *PLOS ONE.* 7, 43293. doi:10.1371/journal.pone.0043293.

Kurushima, J., Nakane, D., Nishizaka, T., and Tomita, H. (2015). Bacteriocin protein BacL1 of *Enterococcus faecalis* targets cell division loci and specifically recognizes l-Ala2-cross-bridged peptidoglycan. *J. Bacteriol.* 197, 286–295. doi:10.1128/JB.02203-14.

Land, A. D., Luo, Q., and Levin, P. A. (2014). Functional domain analysis of the cell division inhibitor EzrA. *PLoS ONE.* 9, 102616. doi:10.1371/journal.pone.0102616.

Land, A. D., Tsui, H.-C. T., Kocaoglu, O., Vella, S. A., Shaw, S. L., Keen, S. K., et al. (2013). Requirement of essential Pbp2x and GpsB for septal ring closure in *Streptococcus pneumoniae* D39. *Mol. Microbiol.* 90, 939-55. doi:10.1111/mmi.12408.

Land, A. D., and Winkler, M. E. (2011). The requirement for pneumococcal MreC and MreD is relieved by inactivation of the gene encoding PBP1a. *J. Bacteriol.* 193, 4166–4179. doi:10.1128/JB.05245-11.

Lara, B., Rico, A. I., Petruzzelli, S., Santona, A., Dumas, J., Biton, J., et al. (2005). Cell division in cocci: localization and properties of the *Streptococcus pneumoniae* FtsA protein. *Mol. Microbiol.* 55, 699–711. doi:10.1111/j.1365-2958.2004.04432.x.

Larsen, J., Schønheyder, H. C., Singh, K. V., Lester, C. H., Olsen, S. S., Porsbo, L. J., et al. (2011). Porcine and human community reservoirs of *Enterococcus faecalis*, Denmark. *Emerg. Infect. Dis.* 17, 2395–2397. doi:10.3201/eid1712.101584.

Le Gouëllec, A., Roux, L., Fadda, D., Massidda, O., Vernet, T., and Zapun, A. (2008). Roles of pneumococcal DivIB in cell division. *J. Bacteriol.* 190, 4501–4511. doi:10.1128/JB.00376-08.

Leaver, M., and Errington, J. (2005). Roles for MreC and MreD proteins in helical growth of the cylindrical cell wall in *Bacillus subtilis*. *Mol. Microbiol.* 57, 1196–1209. doi:10.1111/j.1365-2958.2005.04736.x.

Lebreton, F., Willems, R. J. L., and Gilmore, M. S. (2014). Enterococcus Diversity, Origins in Nature, and Gut Colonization. *Enterococci: From Commensals to Leading Causes of Drug Resistant Infection.*

Leclercq, R., Derlot, E., Duval, J., and Courvalin, P. (1988). Plasmid-mediated resistance to Vancomycin and Teicoplanin in *Enterococcus faecium*. *N. Engl. J. Med.* 319, 157–161. doi:10.1056/NEJM198807213190307.

LeDeaux, J. R., Solomon, J. M., and Grossman, A. D. (1997). Analysis of non-polar deletion mutations in the genes of the spo0K (opp) operon of *Bacillus subtilis*. *FEMS Microbiol. Lett.* 153, 63–69. doi:10.1111/j.1574-6968.1997.tb10464.x.

Lenarcic, R., Halbedel, S., Visser, L., Shaw, M., Wu, L. J., Errington, J., et al. (2009). Localization of DivIVA by targeting to negatively curved membranes. *EMBO J.* 28, 2272–2282. doi:10.1038/emboj.2009.129.

Lenz, L. L., and Portnoy, D. A. (2002). Identification of a second *Listeria* secA gene associated with protein secretion and the rough phenotype. *Mol. Microbiol.* 45, 1043–1056. doi:10.1046/j.1365-2958.2002.03072.x.

Levin, P. A., Kurtser, I. G., and Grossman, A. D. (1999). Identification and characterization of a negative regulator of FtsZ ring formation in *Bacillus subtilis*. *Proc. Natl. Acad. Sci.* 96, 9642–9647. doi:10.1073/pnas.96.17.9642.

Levin, P. A., Margolis, P. S., Setlow, P., Losick, R., and Sun, D. (1992). Identification of *Bacillus subtilis* genes for septum placement and shape determination. *J. Bacteriol.* 174, 6717–6728.

Licht, A., and Brantl, S. (2009). The transcriptional repressor CcpN from *Bacillus subtilis* uses different repression mechanisms at different promoters. *J. Biol. Chem.* 284, 30032–30038. doi:10.1074/jbc.M109.033076.

Licht, A., Preis, S., and Brantl, S. (2005). Implication of CcpN in the regulation of a novel untranslated RNA (SR1) in *Bacillus subtilis*. *Mol. Microbiol.* 58, 189–206. doi:10.1111/j.1365-2958.2005.04810.x.

Lleo, M. M., Canepari, P., and Satta, G. (1990). Bacterial cell shape regulation: testing of additional predictions unique to the two-competing-sites model for peptidoglycan

assembly and isolation of conditional rod-shaped mutants from some wild-type cocci. *J. Bacteriol.* 172, 3758–3771. doi:10.1128/jb.172.7.3758-3771.1990.

Lluch-Senar, M., Querol, E., and Piñol, J. (2010). Cell division in a minimal bacterium in the absence of ftsZ. *Mol. Microbiol.* 78, 278–289. doi:10.1111/j.1365-2958.2010.07306.x.

Low, H. H., Moncrieffe, M. C., and Löwe, J. (2004). The crystal structure of ZapA and its modulation of FtsZ polymerisation. *J. Mol. Biol.* 341, 839–852. doi:10.1016/j.jmb.2004.05.031.

Lutkenhaus, J., and Du, S. (2017). *E. coli* Cell Cycle Machinery. *Prokaryotic Cytoskeletons.* 27–65. doi:10.1007/978-3-319-53047-5_2.

Lutkenhaus, J., Pichoff, S., and Du, S. (2012). Bacterial cytokinesis: from Z ring to divisome. *Cytoskelet.* 69, 778–790. doi:10.1002/cm.21054.

Ma, X., Ehrhardt, D. W., and Margolin, W. (1996). Colocalization of cell division proteins FtsZ and FtsA to cytoskeletal structures in living *Escherichia coli* cells by using green fluorescent protein. *Proc. Natl. Acad. Sci.* 93, 12998–13003. doi:10.1073/pnas.93.23.12998.

MacCallum, W. G., and Hastings, T. W. (1899). A case of acute endocarditis caused by *Micrococcus zymogenes* (Nov. Spec.), with a description of the microorganism. *J. Exp. Med.* 4, 521–534. doi:10.1084/jem.4.5-6.521.

Machata, S., Hain, T., Rohde, M., and Chakraborty, T. (2005). Simultaneous deficiency of both MurA and p60 proteins generates a rough phenotype in *Listeria monocytogenes. J. Bacteriol.* 187, 8385–8394. doi:10.1128/JB.187.24.8385-8394.2005.

Mackay, J. P., Sunde, M., Lowry, J. A., Crossley, M., and Matthews, J. M. (2007). Protein interactions: is seeing believing? *Trends Biochem. Sci.* 32, 530–531. doi:10.1016/j.tibs.2007.09.006.

Maggi, S., Massidda, O., Luzi, G., Fadda, D., Paolozzi, L., and Ghelardini, P. (2008). Division protein interaction web: identification of a phylogenetically conserved common

interactome between *Streptococcus pneumoniae* and *Escherichia coli*. *Microbiol.* 154, 3042–3052. doi:10.1099/mic.0.2008/018697-0.

Maki, D. G., and Agger, W. A. (1988). Enterococcal bacteremia: clinical features, the risk of endocarditis, and management. *Medicine.* 67, 248-69.

Manson, J. M., Hancock, L. E., and Gilmore, M. S. (2010). Mechanism of chromosomal transfer of *Enterococcus faecalis* pathogenicity island, capsule, antimicrobial resistance, and other traits. *Proc. Natl. Acad. Sci.* 107, 12269–12274. doi:10.1073/pnas.1000139107.

Margolin, W. (2000). Themes and variations in prokaryotic cell division. *FEMS Microbiol. Rev.* 24, 531–548. doi:10.1111/j.1574-6976.2000.tb00554.x.

Marston, A. L., and Errington, J. (1999). Selection of the midcell division site in *Bacillus subtilis* through MinD-dependent polar localization and activation of MinC. *Mol. Microbiol.* 33, 84–96. doi:10.1046/j.1365-2958.1999.01450.x.

Marston, A. L., Thomaides, H. B., Edwards, D. H., Sharpe, M. E., and Errington, J. (1998). Polar localization of the MinD protein of *Bacillus subtilis* and its role in selection of the mid-cell division site. *Genes Dev.* 12, 3419–3430. doi:10.1101/gad.12.21.3419.

Massidda, O., Anderluzzi, D., Friedli, L., and Feger, G. (1998). Unconventional organization of the division and cell wall gene cluster of *Streptococcus pneumoniae. Microbiol.* 144, 3069–3078. doi:10.1099/00221287-144-11-3069.

Massidda, O., Nováková, L., and Vollmer, W. (2013). From models to pathogens: how much have we learned about *Streptococcus pneumoniae* cell division? *Environ. Microbiol.* 15, 3133–3157. doi:10.1111/1462-2920.12189.

Masson, S., Kern, T., Gouëllec, A. L., Giustini, C., Simorre, J.-P., Callow, P., et al. (2009). Central domain of DivIB caps the C-terminal regions of the FtsL/DivIC coiled-coil rod. *J. Biol. Chem.* 284, 27687–27700. doi:10.1074/jbc.M109.019471.

Mekonen, E. T., Noskin, G. A., Hacek, D. M., and Peterson, L. R. (1995). Successful treatment of persistent bacteremia due to Vancomycin-resistant, Ampicillin-resistant *Enterococcus faecium*. *Microb. Drug Resist.* 1, 249–253. doi:10.1089/mdr.1995.1.249.

Meniche, X., Otten, R., Siegrist, M. S., Baer, C. E., Murphy, K. C., Bertozzi, C. R., et al. (2014). Subpolar addition of new cell wall is directed by DivIVA in mycobacteria. *Proc. Natl. Acad. Sci.* 111, 3243–3251. doi:10.1073/pnas.1402158111.

Mierzejewska, J., and Jagura-Burdzy, G. (2012). Prokaryotic ParA–ParB–parS system links bacterial chromosome segregation with the cell cycle. *Plasmid* 67, 1–14. doi:10.1016/j.plasmid.2011.08.003.

Miller, J. H., and Lee, K. Y. (1984). Experiments in molecular genetics. *The Quart. Rev. Biol.* 2, 151.

Miller, M. D., Schwarzenbacher, R., von Delft, F., Abdubek, P., Ambing, E., Biorac, T., et al. (2004). Crystal structure of a tandem cystathionine-beta-synthase (CBS) domain protein (TM0935) from *Thermotoga maritima* at 1.87 A resolution. *Proteins* 57, 213–217. doi:10.1002/prot.20024.

Mingorance, J., Tamames, J., and Vicente, M. (2004). Genomic channeling in bacterial cell division. *J. Mol. Recognit.* 17, 481–487. doi:10.1002/jmr.718.

Miyagishima, S., Wolk, C. P., and Osteryoung, K. W. (2005). Identification of cyanobacterial cell division genes by comparative and mutational analyses. *Mol. Microbiol.* 56, 126–143. doi:10.1111/j.1365-2958.2005.04548.x.

Moellering, R. C., and Weinberg, A. N. (1971). Studies on antibiotic synergism against enterococci. *J. Clin. Invest.* 50, 2580–2584.

Mohamed, J. A., and Huang, D. B. (2007). Biofilm formation by enterococci. *J. Med. Microbiol.* 56, 1581–1588. doi:10.1099/jmm.0.47331-0.

Morlot, C., Noirclerc-Savoye, M., Zapun, A., Dideberg, O., and Vernet, T. (2004a). The d,d-carboxypeptidase PBP3 organizes the division process of *Streptococcus pneumoniae*. *Mol. Microbiol.* 51, 1641–1648. doi:10.1046/j.1365-2958.2003.03953.x.

Morlot, C., Zapun, A., Dideberg, O., and Vernet, T. (2003). Growth and division of *Streptococcus pneumoniae*: localization of the high molecular weight penicillin-binding proteins during the cell cycle. *Mol. Microbiol.* 50, 845–855. doi:10.1046/j.1365-2958.2003.03767.x.

Muchová, K., Kutejová, E., Pribisová, L., Wilkinson, A. J., and Barák, I. (2002). *Bacillus subtilis* division protein DivIVA - screen for stable oligomer state conditions. *Acta Crystallogr. D Biol. Crystallogr.* 58, 1542–1543. doi: 10.1107/s0907444902014336.

Mukherjee, P., Sureka, K., Datta, P., Hossain, T., Barik, S., Das, K. P., et al. (2009). Novel role of Wag31 in protection of mycobacteria under oxidative stress. *Mol. Microbiol.* 73, 103–119. doi:10.1111/j.1365-2958.2009.06750.x.

Mundt, J. O. (1961). Occurrence of Enterococci: Bud, Blossom, and Soil Studies. *Appl. Microbiol.* 9, 541–544.

Mundt, J. O. (1963). Occurrence of Enterococci in Animals in a Wild Environment. *Appl. Microbiol.* 11, 136–140.

Mundt, J. O., Coggin, J. H., and Johnson, L. F. (1962). Growth of *Streptococcus faecalis* var. *liquefaciens* on Plants. *Appl. Microbiol.* 10, 552–555.

Mura, A., Fadda, D., Perez, A. J., Danforth, M. L., Musu, D., Rico, A. I., et al. (2017). Roles of the essential protein FtsA in cell growth and division in *Streptococcus pneumoniae*. *J. Bacteriol.* 199, e00608-16. doi:10.1128/JB.00608-16.

Murray, B. E. (1990). The life and times of the Enterococcus. *Clin. Microbiol. Rev.* 3, 46–65. doi: 10.1128/cmr.3.1.46.

Murray, B. E. (2000). Vancomycin-resistant enterococcal infections. *N. Engl. J. Med.* 342, 710–721. doi:10.1056/NEJM200003093421007.

Nguyen, L., Scherr, N., Gatfield, J., Walburger, A., Pieters, J., and Thompson, C. J. (2007). Antigen 84, an effector of pleiomorphism in *Mycobacterium smegmatis*. *J. Bacteriol.* 189, 7896–7910. doi:10.1128/JB.00726-07.

Ni, H., Fan, W., Li, C., Wu, Q., Hou, H., Hu, D., et al. (2018). *Streptococcus suis* DivIVA protein is a substrate of Ser/Thr kinase STK and involved in cell division regulation. *Front. Cell. Infect. Microbiol.* 8, 85. doi:10.3389/fcimb.2018.00085.

Noirclerc-Savoye, M., Le Gouëllec, A., Morlot, C., Dideberg, O., Vernet, T., and Zapun, A. (2005). *In vitro* reconstitution of a trimeric complex of DivIB, DivIC and FtsL, and their transient co-localization at the division site in *Streptococcus pneumoniae. Mol. Microbiol.* 55, 413–424. doi:10.1111/j.1365-2958.2004.04408.x.

Norris, A. H., Reilly, J. P., Edelstein, P. H., Brennan, P. J., and Schuster, M. G. (1995). Chloramphenicol for the treatment of Vancomycin-resistant enterococcal infections. *Clin. Infect. Dis.* 20, 1137–1144. doi:10.1093/clinids/20.5.1137.

Nováková, L., Bezoušková, S., Pompach, P., Špidlová, P., Sasková, L., Weiser, J., et al. (2010). Identification of multiple substrates of the StkP Ser/Thr protein kinase in *Streptococcus pneumoniae. J. Bacteriol.* 192, 3629–3638. doi:10.1128/JB.01564-09.

Ogura, M., and Tanaka, T. (2009). The *Bacillus subtilis* late competence operon *comE* is transcriptionally regulated by *yutB* and under post-transcription initiation control by *comN* (*yrzD*). *J. Bacteriol.* 191, 949–958. doi:10.1128/JB.01429-08.

Oliva, M. A., Halbedel, S., Freund, S. M., Dutow, P., Leonard, T. A., Veprintsev, D. B., et al. (2010). Features critical for membrane binding revealed by DivIVA crystal structure. *EMBO J.* 29, 1988–2001. doi:10.1038/emboj.2010.99.

Ortiz, C., Natale, P., Cueto, L., and Vicente, M. (2016). The keepers of the ring: regulators of FtsZ assembly. *FEMS Microbiol. Rev.* 40, 57–67. doi:10.1093/femsre/fuv040.

Otto, M. (2006). Bacterial evasion of antimicrobial peptides by biofilm formation. *Antimicrob Pep and Human Dis.* 251–258. doi:10.1007/3-540-29916-5_10.

Paganelli, F. L., Willems, R. J., and Leavis, H. L. (2012). Optimizing future treatment of enterococcal infections: attacking the biofilm? *Trends Microbiol.* 20, 40–49. doi:10.1016/j.tim.2011.11.001.

Palmer, K. L., Kos, V. N., and Gilmore, M. S. (2010). Horizontal gene transfer and the genomics of enterococcal antibiotic resistance. *Curr. Opin. Microbiol.* 13, 632–639. doi:10.1016/j.mib.2010.08.004.

Patrick, J. E., and Kearns, D. B. (2008). MinJ (YvjD) is a topological determinant of cell division in *Bacillus subtilis*. *Mol. Microbiol.* 70, 1166–1179. doi:10.1111/j.1365-2958.2008.06469.x.

Paulsen, I. T., Banerjei, L., Myers, G. S. A., Nelson, K. E., Seshadri, R., Read, T. D., et al. (2003). Role of mobile DNA in the evolution of vancomycin-resistant *Enterococcus faecalis. Science.* 299, 2071–2074. doi:10.1126/science.1080613.

Pavlendová, N., Muchová, K., and Barák, I. (2007). Chromosome segregation in *Bacillus subtilis*. *Folia Microbiol.* 52, 563–572. doi:10.1007/BF02932184.

Pazos, M., Natale, P., Margolin, W., and Vicente, M. (2013). Interactions among the early *Escherichia coli* divisome proteins revealed by bimolecular fluorescence complementation. *Environ. Microbiol.* 15, 3282–3291. doi:10.1111/1462-2920.12225.

Perry, S. E., and Edwards, D. H. (2004). Identification of a polar targeting determinant for *Bacillus subtilis* DivIVA. *Mol. Microbiol.* 54, 1237–1249. doi:10.1111/j.1365-2958.2004.04363.x.

Perry, S. E., and Edwards, D. H. (2006). The *Bacillus subtilis* DivIVA protein has a sporulation-specific proximity to Spo0J. *J. Bacteriol.* 188, 6039–6043. doi:10.1128/JB.01750-05.

Peters, P. C., Migocki, M. D., Thoni, C., and Harry, E. J. (2007). A new assembly pathway for the cytokinetic Z ring from a dynamic helical structure in vegetatively growing cells of *Bacillus subtilis*. *Mol. Microbiol.* 64, 487–499. doi:10.1111/j.1365-2958.2007.05673.x.

Pilhofer, M., Rappl, K., Eckl, C., Bauer, A. P., Ludwig, W., Schleifer, K.H., et al. (2008). Characterization and evolution of cell division and cell wall synthesis genes in the bacterial

phyla Verrucomicrobia, Lentisphaerae, Chlamydiae, and Planctomycetes and phylogenetic comparison with rRNA genes. *J. Bacteriol.* 190, 3192–3202. doi:10.1128/JB.01797-07.

Pinho, M. G., and Errington, J. (2004). A *divIVA* null mutant of *Staphylococcus aureus* undergoes normal cell division. *FEMS Microbiol. Lett.* 240, 145–149. doi:10.1016/j.femsle.2004.09.038.

Poyart, C., and Trieu-Cuot, P. (1997). A broad-host-range mobilizable shuttle vector for the construction of transcriptional fusions to beta-galactosidase in gram-positive bacteria. *FEMS Microbiol. Lett.* 156, 193–198. doi: 10.1111/j.1574-6968.1997.tb12726.x.

Pucci, M. J., Thanassi, J. A., Discotto, L. F., Kessler, R. E., and Dougherty, T. J. (1997). Identification and characterization of cell wall-cell division gene clusters in pathogenic gram-positive cocci. *J. Bacteriol.* 179, 5632–5635. doi:10.1128/jb.179.17.5632-5635.1997.

Ragumani, S., Sauder, J. M., Burley, S. K., and Swaminathan, S. (2010). Structural studies on cytosolic domain of Magnesium transporter MgtE from *Enterococcus faecalis*. *Proteins* 78, 487–491. doi:10.1002/prot.22585.

Ramamurthi, K. S., and Losick, R. (2009). Negative membrane curvature as a cue for subcellular localization of a bacterial protein. *Proc. Natl. Acad. Sci.* 106, 13541–13545. doi:10.1073/pnas.0906851106.

Ramirez-Arcos, S. (2005). *Enterococcus faecalis* divIVA: an essential gene involved in cell division, cell growth and chromosome segregation. *Microbiology* 151, 1381–1393. doi:10.1099/mic.0.27718-0.

Ramirez-Arcos, S., Szeto, J., Beveridge, T., Victor, C., Francis, F., and Dillon, J. (2001). Deletion of the cell-division inhibitor MinC results in lysis of *Neisseria gonorrhoeae. Microbiol. Read. Engl.* 147, 225–237. doi:10.1099/00221287-147-1-225.

Ramos, A., Honrubia, M. P., Valbuena, N., Vaquera, J., Mateos, L. M., and Gil, J. A. (2003). Involvement of DivIVA in the morphology of the rod-shaped actinomycete *Brevibacterium lactofermentum*. *Microbiol. Read. Engl.* 149, 3531–3542. doi:10.1099/mic.0.26653-0.

Rams, T. E., Degener, J. E., and van Winkelhoff, A. J. (2013). Prevalence of β-lactamase-producing bacteria in human periodontitis. *J. Periodontal Res.* 48, 493–499. doi:10.1111/jre.12031.

Rao, V. S., Srinivas, K., Sujini, G. N., and Kumar, G. N. S. (2014). Protein-protein interaction detection: methods and analysis. *Int. J. Proteomics*. 147648. doi:10.1155/2014/147648.

Real, G., and Henriques, A. O. (2006). Localization of the *Bacillus subtilis* murB gene within the *dcw* cluster is important for growth and sporulation. *J. Bacteriol.* 188, 1721–1732. doi:10.1128/JB.188.5.1721-1732.2006.

Rico, A. I., Krupka, M., and Vicente, M. (2013). In the beginning, *Escherichia coli* assembled the proto-ring: an initial phase of division. *J. Biol. Chem.* 288, 20830–20836. doi:10.1074/jbc.R113.479519.

Rigden, M. D., Baier, C., Ramirez-Arcos, S., Liao, M., Wang, M., and Dillon, J.-A. R. (2008). Identification of the coiled-coil domains of *Enterococcus faecalis* DivIVA that mediate oligomerization and their importance for biological function. *J. Biochem.* 144, 63–76. doi:10.1093/jb/mvn044.

Rismondo, J., Cleverley, R. M., Lane, H. V., Großhennig, S., Steglich, A., Möller, L., et al. (2016). Structure of the bacterial cell division determinant GpsB and its interaction with penicillin-binding proteins. *Mol. Microbiol.* 99, 978–998. doi:10.1111/mmi.13279.

Rothfield, L. I., and Justice, S. S. (1997). Bacterial cell division: the cycle of the ring. *Cell.* 88, 581–584. doi:10.1016/s0092-8674(00)81899-1.

Rowlett, V. W., and Margolin, W. (2013). The bacterial Min system. *Curr. Biol.* 23, 553–556. doi:10.1016/j.cub.2013.05.024.

Rowlett, V. W., and Margolin, W. (2015). The bacterial divisome: ready for its close-up. *Philos. Trans. R. Soc. B Biol. Sci.* 370. doi:10.1098/rstb.2015.0028.

Russell, J. J., Theriot, J. A., Sood, P., Marshall, W. F., Landweber, L. F., Fritz-Laylin, L., et al. (2017). Non-model model organisms. *BMC Biol.* 15, 56. doi:10.1186/s12915-017-0391-5.

Sahm, D. F., Kissinger, J., Gilmore, M. S., Murray, P. R., Mulder, R., Solliday, J., et al. (1989). *In vitro* susceptibility studies of vancomycin-resistant *Enterococcus faecalis. Antimicrob. Agents Chemother.* 33, 1588–1591. doi: 10.1128/aac.33.9.1588.

Sandoe, J. A. T., Witherden, I. R., Cove, J. H., Heritage, J., and Wilcox, M. H. (2003). Correlation between enterococcal biofilm formation in vitro and medical-device-related infection potential *in vivo. J. Med. Microbiol.* 52, 547–550. doi:10.1099/jmm.0.05201-0.

Schleifer, K. H., and Kilpper-Bälz, R. (1984). Transfer of *Streptococcus faecalis* and *Streptococcus faecium* to the Genus Enterococcus nom. rev. as *Enterococcus faecalis* comb. nov. and *Enterococcus faecium* comb. nov. *Int. J. Syst. Evol. Microbiol.* 34, 31–34. doi:10.1099/00207713-34-1-31.

Schumacher, M. A. (2017). Bacterial Nucleoid Occlusion: Multiple Mechanisms for Preventing Chromosome Bisection During Cell Division. *Prokary. Cytoskele.* 267–298. doi:10.1007/978-3-319-53047-5_9.

Segarra, R. A., Booth, M. C., Morales, D. A., Huycke, M. M., and Gilmore, M. S. (1991). Molecular characterization of the *Enterococcus faecalis* cytolysin activator. *Infect. Immun.* 59, 1239–1246.

Servant, P., Le Coq, D., and Aymerich, S. (2005). CcpN (YqzB), a novel regulator for CcpA-independent catabolite repression of *Bacillus subtilis* gluconeogenic genes. *Mol. Microbiol.* 55, 1435–1451. doi:10.1111/j.1365-2958.2005.04473.x.

Sharma, K., Sultana, T., Liao, M., Dahms T. E. S., and Dillon, J. R. (2020). EF1025, a hypothetical protein from *Enterococcus faecalis*, interacts with DivIVA and affects cell length and cell shape. *Front. Microb.*, doi: 10.3389/fmicb.2020.00083

Shepard, B. D., and Gilmore, M. S. (1995). Electroporation and Efficient Transformation of *Enterococcus faecalis* Grown in High Concentrations of Glycine. *Electroporation Protocols for Microorganisms.* 217–226. doi:10.1385/0-89603-310-4:217.

Sieger, B., Schubert, K., Donovan, C., and Bramkamp, M. (2013). The lipid II flippase RodA determines morphology and growth in *Corynebacterium glutamicum*. *Mol. Microbiol.* 90, 966–982. doi:10.1111/mmi.12411.

Sievert, D. M., Ricks, P., Edwards, J. R., Schneider, A., Patel, J., Srinivasan, A., et al. (2013). Antimicrobial-resistant pathogens associated with healthcare-associated infections: summary of data reported to the National Healthcare Safety Network at the Centers for Disease Control and Prevention, 2009-2010. *Infect. Control Hosp. Epidemiol.* 34, 1–14. doi:10.1086/668770.

Sigrist, C. J. A., Cerutti, L., de Castro, E., Langendijk-Genevaux, P. S., Bulliard, V., Bairoch, A., et al. (2010). PROSITE, a protein domain database for functional characterization and annotation. *Nucleic Acids Res.* 38, D161-166. doi:10.1093/nar/gkp885.

Singh, J. K., Makde, R. D., Kumar, V., and Panda, D. (2007). A membrane protein, EzrA, regulates assembly dynamics of FtsZ by interacting with the C-terminal tail of FtsZ. *Biochem.* 46, 11013–11022. doi:10.1021/bi700710j.

Singh, K. V., Coque, T. M., Weinstock, G. M., and Murray, B. E. (1998). *In vivo* testing of an *Enterococcus faecalis* efaA mutant and use of efaA homologs for species identification. *FEMS Immunol. Med. Microbiol.* 21, 323–331. doi:10.1111/j.1574-695X.1998.tb01180.x.

Snyder, L. A. S., Saunders, N. J., and Shafer, W. M. (2001). A putatively phase variable gene (dca) required for natural competence in *Neisseria gonorrhoeae* but not *Neisseria meningitidis* is located within the Division Cell Wall (dcw) gene cluster. *J. Bacteriol.* 183, 1233–1241. doi:10.1128/JB.183.4.1233-1241.2001.

Song, J.-H., Ko, K. S., Lee, J.-Y., Baek, J. Y., Oh, W. S., Yoon, H. S., et al. Identification of essential genes in *Streptococcus pneumoniae* by allelic replacement mutagenesis. *Mol. Cells* 19, 365–374.

Soufo, H. J. D., Reimold, C., Linne, U., Knust, T., Gescher, J., and Graumann, P. L. (2010). Bacterial translation elongation factor EF-Tu interacts and colocalizes with actin-like MreB protein. *Proc. Natl. Acad. Sci.* 107, 3163–3168. doi:10.1073/pnas.0911979107.

Sourjik, V., and Berg, H. C. (2002). Binding of the *Escherichia coli* response regulator CheY to its target measured *in vivo* by fluorescence resonance energy transfer. *Proc. Natl. Acad. Sci.* 99, 12669–12674. doi:10.1073/pnas.192463199.

Stahlberg, H., Kutejová, E., Muchová, K., Gregorini, M., Lustig, A., Müller, S. A., et al. (2004). Oligomeric structure of the *Bacillus subtilis* cell division protein DivIVA determined by transmission electron microscopy. *Mol. Microbiol.* 52, 1281–1290. doi:10.1111/j.1365-2958.2004.04074.x.

Steele, S., Taft-Benz, S., and Kawula, T. (2014). A method for functional trans-Complementation of intracellular *Francisella tularensis*. *PLoS ONE* 9, 88194. doi:10.1371/journal.pone.0088194.

Steele, V. R., Bottomley, A. L., Garcia-Lara, J., Kasturiarachchi, J., and Foster, S. J. (2011). Multiple essential roles for EzrA in cell division of *Staphylococcus aureus*. *Mol. Microbiol.* 80, 542–555. doi:10.1111/j.1365-2958.2011.07591.x.

Stinemetz, E. K., Gao, P., Pinkston, K. L., Montealegre, M. C., Murray, B. E., and Harvey, B. R. (2017). Processing of the major autolysin of *E. faecalis*, AtlA, by the zinc-metalloprotease, GelE, impacts AtlA septal localization and cell separation. *PLOS ONE*. 12, 0186706. doi:10.1371/journal.pone.0186706.

Taguchi, A., Welsh, M. A., Marmont, L. S., Lee, W., Sjodt, M., Kruse, A. C., et al. (2019). FtsW is a peptidoglycan polymerase that is functional only in complex with its cognate penicillin-binding protein. *Nat. Microbiol.* 4, 587–594. doi:10.1038/s41564-018-0345-x.

Tamames, J., González-Moreno, M., Mingorance, J., Valencia, A., and Vicente, M. (2001). Bringing gene order into bacterial shape. *Trends Genet.* 17, 124–126. doi:10.1016/S0168-9525(00)02212-5.

Tännler, S., Fischer, E., Le Coq, D., Doan, T., Jamet, E., Sauer, U., et al. (2008). CcpN controls central carbon fluxes in *Bacillus subtilis*. *J. Bacteriol.* 190, 6178–6187. doi:10.1128/JB.00552-08.

Tavares, J. R., Souza, R. F. de, Meira, G. L. S., and Gueiros-Filho, F. J. (2008). Cytological characterization of YpsB, a novel component of the *Bacillus subtilis* divisome. *J. Bacteriol.* 190, 7096–7107. doi:10.1128/JB.00064-08.

Thanassi, J. A., Hartman-Neumann, S. L., Dougherty, T. J., Dougherty, B. A., and Pucci, M. J. (2002). Identification of 113 conserved essential genes using a high-throughput gene disruption system in *Streptococcus pneumoniae. Nucleic Acids Res.* 30, 3152–3162. doi: 10.1093/nar/gkf418.

Thomaides, H. B., Freeman, M., Karoui, M. E., and Errington, J. (2001). Division site selection protein DivIVA of *Bacillus subtilis* has a second distinct function in chromosome segregation during sporulation. *Genes Dev.* 15, 1662–1673. doi:10.1101/gad.197501.

Toledo-Arana, A., Valle, J., Solano, C., Arrizubieta, M. J., Cucarella, C., Lamata, M., et al. (2001). The enterococcal surface protein, Esp, is involved in *Enterococcus faecalis* biofilm formation. *Appl. Environ. Microbiol.* 67, 4538–4545. doi:10.1128/AEM.67.10.4538-4545.2001.

Torelli, R., Cacaci, M., Papi, M., Paroni Sterbini, F., Martini, C., Posteraro, B., et al. (2017). Different effects of matrix degrading enzymes towards biofilms formed by *E. faecalis* and *E. faecium* clinical isolates. *Colloids Surf. B Biointerfaces* 158, 349–355. doi:10.1016/j.colsurfb.2017.07.010.

Uehara, T., and Bernhardt, T. G. (2011). More than just lysins: peptidoglycan hydrolases tailor the cell wall. *Curr. Opin. Microbiol.* 14, 698–703. doi:10.1016/j.mib.2011.10.003.

Uttley, A. C., Collins, C. H., Naidoo, J., and George, R. C. (1988). Vancomycin-resistant enterococci. *The Lancet.* 331, 57–58. doi:10.1016/S0140-6736(88)91037-9.

Van Tyne, D., and Gilmore, M. S. (2014). Friend turned foe: evolution of enterococcal virulence and antibiotic resistance. *Annu. Rev. Microbiol.* 68, 337–356. doi:10.1146/annurev-micro-091213-113003.

Van Tyne, D., Martin, M. J., and Gilmore, M. S. (2013). Structure, function, and biology of the *Enterococcus faecalis* cytolysin. *Toxins.* 5, 895–911. doi:10.3390/toxins5050895.

Varley, A. W., and Stewart, G. C. (1992). The divIVB region of the *Bacillus subtilis* chromosome encodes homologs of *Escherichia coli* septum placement (minCD) and cell shape (mreBCD) determinants. *J. Bacteriol.* 174, 6729–6742.

Vicente, M., Álvarez, J., and Martínez-Arteaga, R. (2004). How similar cell division genes are located and behave in different bacteria. *Molecules in Time and Space: Bacterial Shape, Division and Phylogeny*. 239–248. doi:10.1007/0-306-48579-6_12.

Vicente, M., and Errington, J. (1996). Structure, function and controls in microbial division. *Mol. Microbiol.* 20, 1–7. doi:10.1111/j.1365-2958.1996.tb02482.x.

Vicente, M., and García-Ovalle, M. (2007). Making a point: the Role of DivIVA in Streptococcal polar anatomy. *J. Bacteriol.* 189, 1185–1188. doi:10.1128/JB.01710-06.

Vuyst, L. D., and Vandamme, E. J. (1994). Bacteriocins of Lactic Acid Bacteria: Microbiology, Genetics and Applications. Springer US. doi:10.1007/978-1-4615-2668-1.

Wang, X., and Lutkenhaus, J. (1993). The FtsZ protein of *Bacillus subtilis* is localized at the division site and has GTPase activity that is dependent upon FtsZ concentration. *Mol. Microbiol.* 9, 435–442. doi:10.1111/j.1365-2958.1993.tb01705.x.

Weber, L., Thoelken, C., Volk, M., Remes, B., Lechner, M., and Klug, G. (2016). The conserved dcw gene cluster of *R. sphaeroides* is preceded by an uncommonly extended 5' leader featuring the sRNA UpsM. *PLOS ONE.* 11, e0165694. doi:10.1371/journal.pone.0165694.

Weiser, J. N., Ferreira, D. M., and Paton, J. C. (2018). *Streptococcus pneumoniae*: transmission, colonization and invasion. *Nat. Rev. Microbiol.* 16, 355–367. doi:10.1038/s41579-018-0001-8.

White, C. L., Kitich, A., and Gober, J. W. (2010). Positioning cell wall synthetic complexes by the bacterial morphogenetic proteins MreB and MreD. *Mol. Microbiol.* 76, 616–633. doi:10.1111/j.1365-2958.2010.07108.x.

Whitman, R. L., Shively, D. A., Pawlik, H., Nevers, M. B., and Byappanahalli, M. N. (2003). Occurrence of *Escherichia coli* and enterococci in cladophora (chlorophyta) in nearshore water and beach sand of lake Michigan. *Appl. Environ. Microbiol.* 69, 4714–4719. doi:10.1128/AEM.69.8.4714-4719.2003.

Willems, R. J., Homan, W., Top, J., van Santen-Verheuvel, M., Tribe, D., Manzioros, X., et al. (2001). Variant esp gene as a marker of a distinct genetic lineage of vancomycin-resistant *Enterococcus faecium* spreading in hospitals. *Lancet Lond. Engl.* 357, 853–855. doi:10.1016/S0140-6736(00)04205-7.

Wu, L. J., and Errington, J. (2003). RacA and the Soj-Spo0J system combine to effect polar chromosome segregation in sporulating *Bacillus subtilis*: Chromosome segregation in *B. subtilis*. *Mol. Microbiol.* 49, 1463–1475. doi:10.1046/j.1365-2958.2003.03643.x.

Yang, S.-C., Lin, C.-H., Sung, C. T., and Fang, J.-Y. (2014). Antibacterial activities of bacteriocins: application in foods and pharmaceuticals. *Front. Microbiol.* 5, 241. doi:10.3389/fmicb.2014.00241.

Yogurtcu, O. N., and Johnson, M. E. (2018). Cytosolic proteins can exploit membrane localization to trigger functional assembly. *PLOS Comput. Biol.* 14, 1006031. doi:10.1371/journal.pcbi.1006031.

Zapun, A., Vernet, T., and Pinho, M. G. (2008). The different shapes of cocci. *FEMS Microbiol. Rev.* 32, 345–360. doi:10.1111/j.1574-6976.2007.00098.x.

Zou, Y., Li, Y., and Dillon, J.-A. R. (2017). The distinctive cell division interactome of *Neisseria gonorrhoeae*. *BMC Microbiol.* 17. doi:10.1186/s12866-017-1140-1.

Appendix

A. Ascertaining the interaction between EF1025 and DivIVA$_{Ef}$ using steady-state anisotropy and Surface Plasmon Resonance (SPR) assay.

The interaction between EF1025 and DivIVA$_{Ef}$ was ascertained using B2H, GST-pull down and co-immunoprecipitation previously in Chapter 2. These assays were qualitative and did not permit the quantification of these protein interactions in the micro- and nanomolar concentration range (James and Jameson, 2014; Douzi, 2017). To understand the binding affinities and association/dissociation kinetics of the protein complexes formed when EF1025 interacted with DivIVA$_{Ef}$, steady-state anisotropy and SPR was used. In steady-state anisotropy,

Material and methods

His-EF1025 or GST-DivIVA$_{Ef}$ fusions were overexpressed in *E. coli* BL21 cells and purified to homogeneity as described in Chapter 2. His-DivIVA$_{Ef}$ (Rigden et al., 2008) was overexpressed in *E. coli* C41 cells and purified to homogeneity as previously described (Rigden et al., 2008). GST-tag was removed from GST-DivIVA$_{Ef}$ by digestion with Thrombin (Thermofisher, CA) and was used for steady state anisotropy fluorescence measurement experiment which measures any change in the intensity of fluorescence of a fluorophore-labeled protein when it interacts with the unlabelled protein.

A steady-state rotational anisotropy experiment was performed to test the interaction between DivIVA$_{Ef}$ and EF1025. EF1025 was labelled with Flourscein EX dye as per manufacturer instructions (Thermofischer, CA) and titrated against unlabeled His-DivIVA$_{Ef}$ in a QuantaMaster QM-4 spectrofluorometer (Photon Technology International, USA) with a dual emission channel to collect data and calculate anisotropy. The sample was excited with vertically polarized light at 495 nm (6 nm band pass). Vertical and horizontal emissions were measured at 520 nm (6 nm band pass) to calculate the change in anisotropy. Flourscein labelled EF1025 was found to be highly unstable so DivIVA$_{Ef}$ without GST-tag was labelled with Flourscein EX dye and titrated against unlabeled His-EF1025 to observe a change in anisotropy.

For SPR spectrometry, purified His-EF1025 and GST-DivIVA$_{Ef}$ were used to test for potential protein-protein interactions using a Bio-Rad XPR36 (Bio-Rad Laboratories, CA) instrument with ProteOnTM HTE and GLC sensor Chips (Bio-Rad Laboratories, CA). For HTE

chip: chip surface was regenerated (0.5% SDS, 50 mM NaOH, 100 mM HCl and 300 mM EDTA), activated (500 μM of $NiSO_4$) and immobilized with His-EF1025 as ligand molecule at a concentration of 100 nM. This chip was then flooded with a one-fold dilution of analyte protein (GST-$DivIVA_{Ef}$) in PBST buffer (PBS buffer with Tween-20 i.e. 137 mM NaCl, 2.7 mM KCl, 10 mM Na_2HPO_4, 1.8 mM KH_2PO_4, 0.1% BSA, 0.05% Tween-20, pH 7.9), followed by an injection of PBST buffer. A reference channel flowed with only PBST buffer, and a chip surface immobilized with His-EF1025 flowed with GST in PBST served as negative controls. For the GLC sensor chip: immobilization step was performed using an anti-GST antibody (Genscrpit, USA) which was then coupled to $DivIVA_{Ef}$ and was flooded with analyte protein (i.e. His-EF1025) for binding experiments. Each experiment was performed in triplicates and titrated with 10-12 dilutions of the unlabelled protein.

All SPR data were analyzed with ProteOn Manager™ (Bio-Rad Laboratories) to test the binding affinity of these two proteins and calculate any change in the response Units (RU) due to the interaction between ligand and analyte molecule. The raw signal detected by the machine for was first subtracted from the signal from interspot that did not have immobilized proteins (EF1025 or $DivIVA_{Ef}$) and then from the reference channel. Then, the signal was subtracted with the RU signal with running buffer and ligand immobilized on the chip.

Results and discussion

A change in anisotropy was observed when unlabeled EF1025 was titrated against unlabeled $DivIVA_{Ef}$ but a saturation stage could not be achieved. During the experiment, the initial change in anisotropy was slow but data points were scattered (data not shown). A small change in anisotropy was observed when the anisotropy for an unbound fraction (no GST-$DivIVA_{Ef}$) was subtracted from bound fraction (with GST-$DivIVA_{Ef}$) (Fig. A.1). A similar observation was made when labelled $DivIVA_{Ef}$ was titrated with EF1025, therefore, a change in anisotropy was calculated for the bound and unbound fractions of EF1025. An interaction between $DivIVA_{Ef}$, a decamer (Ramirez et al., 2008) and EF1025, a decamer (this study) might collectively be forming a massive complex. Such a small change in total anisotropy could have been due to the breakdown of one decamer into monomeric units which might be associating with each other. Weak binding between $DivIVA_{Ef}$ and EF1025 could have caused the monomeric units to reassemble therefore a lack of an equilibrium stage. Such a breakdown and re-assemblage will maintain a total change in

anisotropy of the complex as constant. Although a change in anisotropy was detected, labelled EF1025 was observed to be unstable during titration.

In SPR, the sensorgram for EF1025 binding to $DivIVA_{Ef}$ indicated nonspecific binding of EF1025 to the interspot/empty regions when HTE or the GLC sensor chip was used (Fig. A.2). To minimize nonspecific binding of EF1025 to the chip surface, various concentrations of bovine serum albumin (BSA), Arginine, and Glutathione S-transferase (GST) were used in the running buffer. A small decrease in non-specific interactions was observed, however, after comparing with reference channels, the interaction was inconclusive due to the presence of non-specific interactions. This indicated that SPR was not a suitable technique to study this interaction.

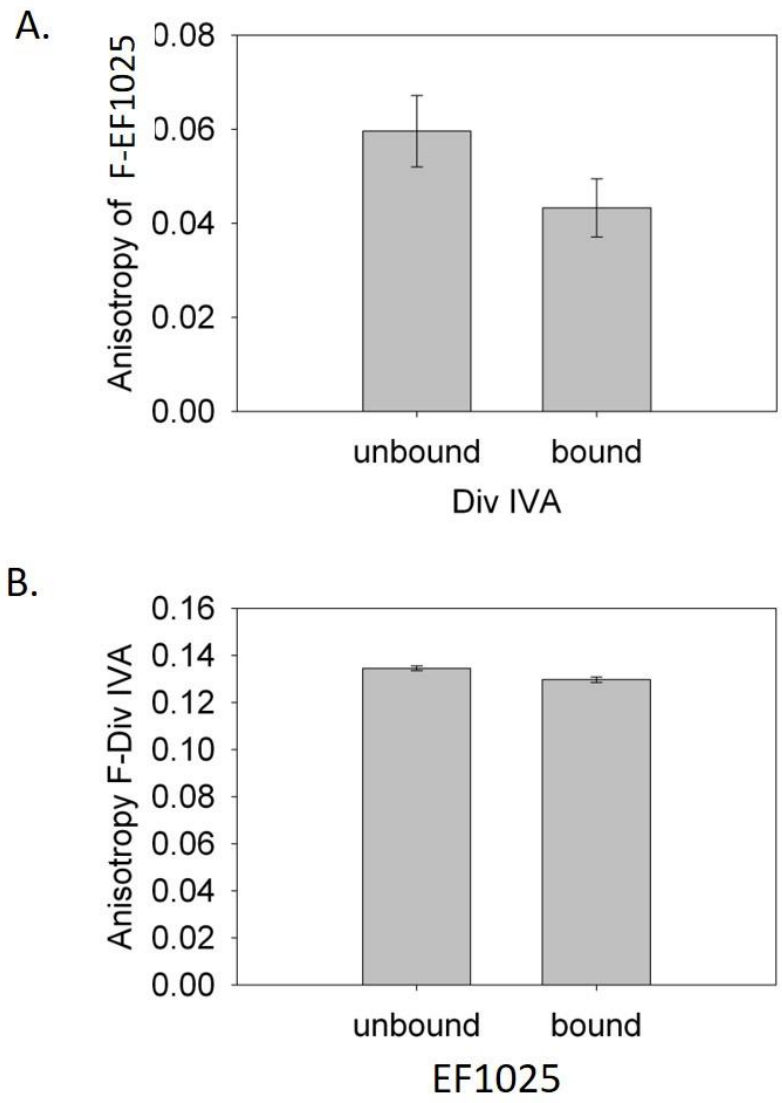

Figure A.1. Binding affinities of EF1025 and DivIVA$_{Ef}$. (A) DivIVA$_{Ef}$ was used as a substrate where EF1025 was fluorescently labelled. A change in anisotropy occurred when titrated with increasing concentrations of EF1025. The unbound fraction indicates anisotropy recorded for fluorescently labelled EF1025 without the substrate (i.e. DivIVA$_{Ef}$). B. EF1025 was used as a substrate where DivIVA$_{Ef}$ was fluorescently labelled. A comparatively lower change in anisotropy was observed when titrated with the substrate. Values are an average from three independent experiments.

A.

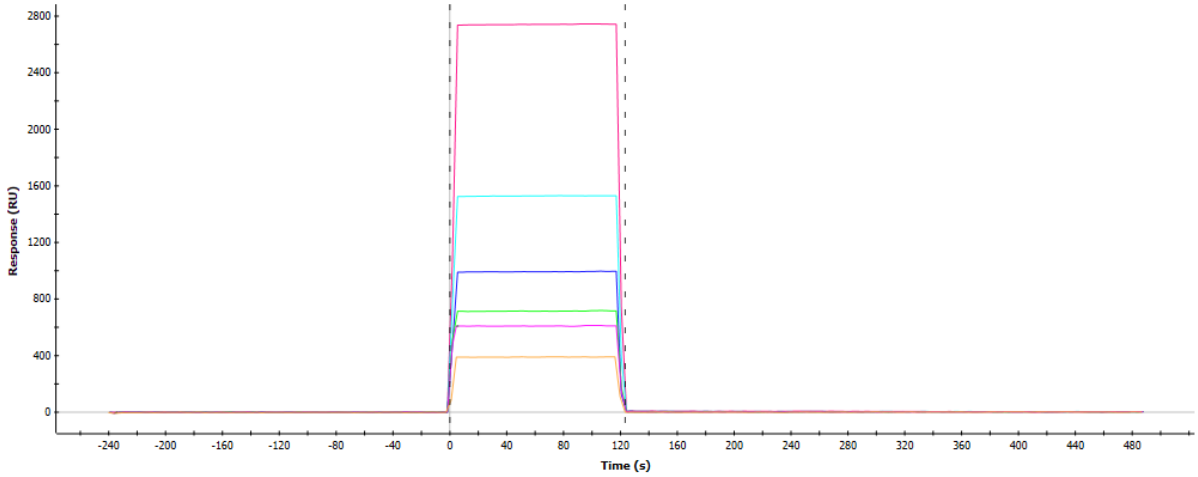

B.

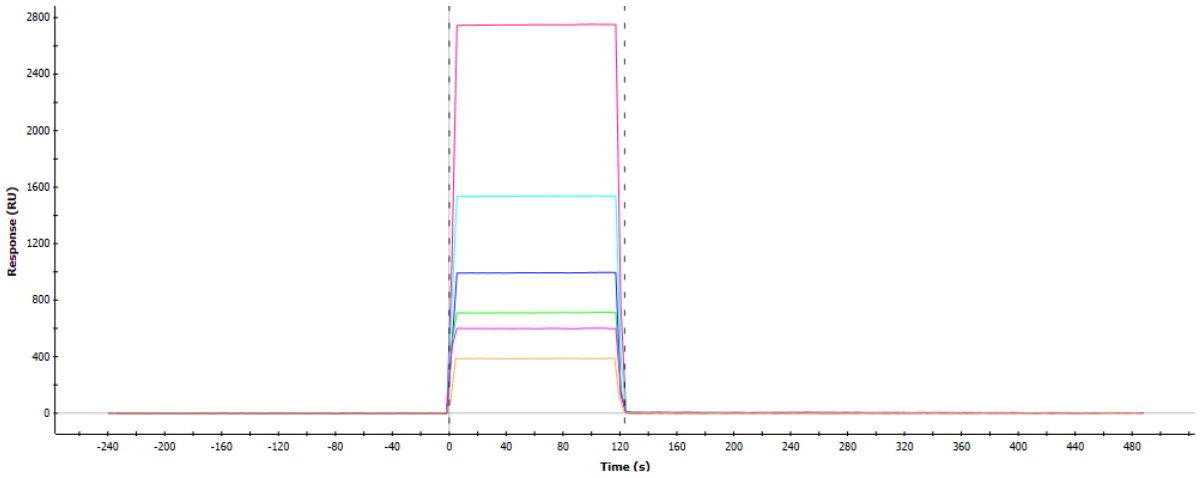

Figure A.2. SPR measurement for studying the interaction of EF1025 with $DivIVA_{Ef}$ using a GLC chip. 10uM GST tagged $DivIVA_{Ef}$ (ligand) was immobilized and flooded with 22uM of His-EF1025 (analyte). A. Response units recorded for "Reference" channel without immobilized GST tagged DivIVAEf. B. Response unit recorded for "Test" channel flooded with His-EF1025. The reference channel and test channel recorded similar RU for the interaction.

B. Generation of a plasmid construct where the control the expression of *EF1025* is under a Nisin inducible promoter using the vector pMSP3545 and transform it into *E. faecalis* JH2-2 cells to study the effect of EF1025 expression on *E. faecalis* morphology.

Previously showed that insertional inactivation or deletion of *EF1025* resulted in the loss of viability of *E. faecalis* unless the gene was complemented by *in trans EF1025* expression. To control the expression of *EF1025* in *E. faecalis* using the plasmid pMSP3545, which utilizes a nisin-controlled expression (NICE) system due to the presence of *nisR* and *nisK*, and a nisin inducible promoter (P_{nis}) (Bryan et al., 2000). The products of *nisR* and *nisK* constitute a regulator which allow transcription from P*nis* in the presence of nisin. pMSP3545 has an erythromycin marker and can replicate in *E. coli* as well as in *E. faecalis*.

Materials and methods

To clone *EF1025* under the control of P_{nis}, *EF1025* was PCR amplified using primer pair EF1025npF/R (Chapter 2- Table S3D) from *E. faecalis* genomic DNA and was digested with *Nco*I and *Xba*I restriction enzymes. pMSP3545 was digested using *Nco*I and *Xba*I restriction enzymes. Digested *EF1025* and pMSP3545 were ligated and electroporated into electrocompetent *E. faecalis* JH2-2 cells as previously described (Ramirez-Arcos, 2005), creating the strain *E. faecalis* NIE1. Transformants were selected on LB plates supplemented with erythromycin 150 µg/mL. Transformed colonies were isolated and tested for the presence of *EF1025* downstream of P_{nis} using primer pair EF1025npF/PnisA (Chapter 2- Table S3D and AATCTATGTTACTAAA) followed by DNA sequencing.

To express *EF1025* in *E. faecalis* NIE1, *E. faecalis* NIE1 was grown in five tubes for 8-10 hrs, each containing 10 ml of BHI broth with nisin in the concentration range of 0 ng/mL to 25 ng/mL. To identify *EF1025* expression levels, cells from each tube were centrifuged and lysed in 5 mL of PBS buffer containing 0.1mg/mL of lysozyme (Sigma, CA). An added step of sonication was performed to ensure cell lysis. Cell lysate containing a known amount of total cell protein was loaded on a 12% SDS-PAGE for separation followed by Western blotting using anti-EF1025 antibody as described previously (Ramirez-Arcos, 2005). Nisin inducible overexpression was also tested at concentration range 50 ng/mL and 100 ng/mL.

Results and discussion

Cloning was successful as confirmed by DNA sequencing. However, western blotting revealed no change in the expression levels of *EF1025* when induced with the highest concentration of nisin (i.e. 25 ng/mL; Fig. B.1). All samples (induced or non-induced) showed a band corresponding to *EF1025* of equal intensity when blotted with the anti-EF1025 antibody. Due to unknown reasons, P_{nis} was observed to have a leaky expression of *EF1025*. At higher concentrations of nisin (>50 ng/mL), precipitated cell aggregates at the bottom of the growth medium were observed.

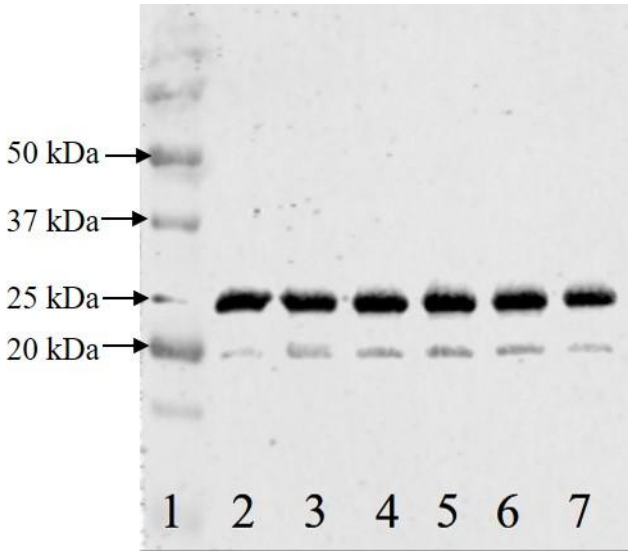

Figure B.1. Western blot probed with the anti-EF1025 antibody showing expression of *EF1025* in *E. faecalis* NIE1 when induced with nisin. Lane 1- Protein ladder; Lane 2- non-induced *E. faecalis* NIE1 showing a 25 kDa band; Lane 3-7: samples induced with nisin at concentrations 5 ng/mL, 10 ng/mL, 15 ng/mL, 20 ng/mL and 25 ng/mL. 20 kDa band is a non-specific band.

C. Ascertaining the interaction between CcpN and DivIVA from *B. subtilis* using Surface Plasmon Resonance (SPR) assay.

In Chapter 3, the interaction between CcpN and $DivIVA_{Bs}$ was ascertained using B2H and GST-pull down. I was interested in understanding the quantitative aspects of this interaction, therefore, SPR was used to quantify the binding affinities and association/dissociation kinetics of the protein complexes formed when CcpN interacted with $DivIVA_{Bs}$.

Materials and method:

GST-$DivIVA_{Bs}$ or 6×His-CcpN fusions were overexpressed in *E. coli* C41 (DE3) and purified to homogeneity as described previously in Chapter 3. A fraction of purified GST-tagged $DivIVA_{Bs}$ was also subjected to Thrombin cleavage to remove GST-tag for SPR experiment. Potential interaction between His-CcpN and $DivIVA_{Bs}$ was examined by SPR using the Reichert 2SPR instrument with Gold plain sensor chips having HTE and GLC sensor coating (Reichert Technologies). HTE chip surface was regenerated (0.5% SDS, 50 mM NaOH, 100 mM HCl and 300 mM EDTA), activated (500 µM of $NiSO_4$) and immobilized with 10 µM of $DivIVA_{Bs}$ as ligand molecule. This immobilized chip was then flooded with 22 µM of analyte protein (His-CcpN) at a flow rate of 30 µl/min in PBST buffer (PBS buffer with Tween-20 i.e. 137 mM NaCl, 2.7 mM KCl, 10 mM Na_2HPO_4, 1.8 mM KH_2PO_4, 0.1% BSA, 0.05% Tween-20, pH 7.9), followed by an injection of PBST buffer. A reference channel flowed with only PBST buffer, and a chip surface immobilized with $DivIVA_{Bs}$ flowed with GST in PBST served as negative controls. For GLC sensor chip, immobilization step was performed using anti-GST antibody which was then flooded with 50 µM GST-$DivIVA_{Ef}$ and was then flooded with 22 µM of analyte protein (i.e. His-CcpN) for binding experiments.

The sensorgram (i.e. a representation of the response unit versus time) was produced using SPR data that was analyzed with ProteOn Manager™ (Bio-Rad Laboratories) as previously discussed.

Results and discussion:

The sensorgram for CcpN binding to $DivIVA_{Bs}$ indicated a positive interaction when the HTE chip was used, although an equilibrium stage was absent (Fig. C.1). To improve the sensorgram, higher concentration of CcpN (25 µM and above) was used which resulted in the loss

of interaction. When a high flow rate (i.e. 30 µl/min) and a low concentration (i.e. 22 µM) of CcpN was used, this interaction was restored. A reduction in flow rate for the analyte protein 15 µl/min also resulted in the loss of this interaction. Interaction processes usually dominate more at higher flow rates, since mass transport is faster (Karlsson and Fält, 1997). The loss of interaction at higher concentrations of His-CcpN could be due to the aggregation of CcpN since CcpN was found to precipitate at higher concentrations (>2 mg/mL) during purification protocol. No interaction was observed when the GLC chip was used. Such third-party interaction showed very high non-specific binding to the chip surface as was noticed in Appendix A.1.

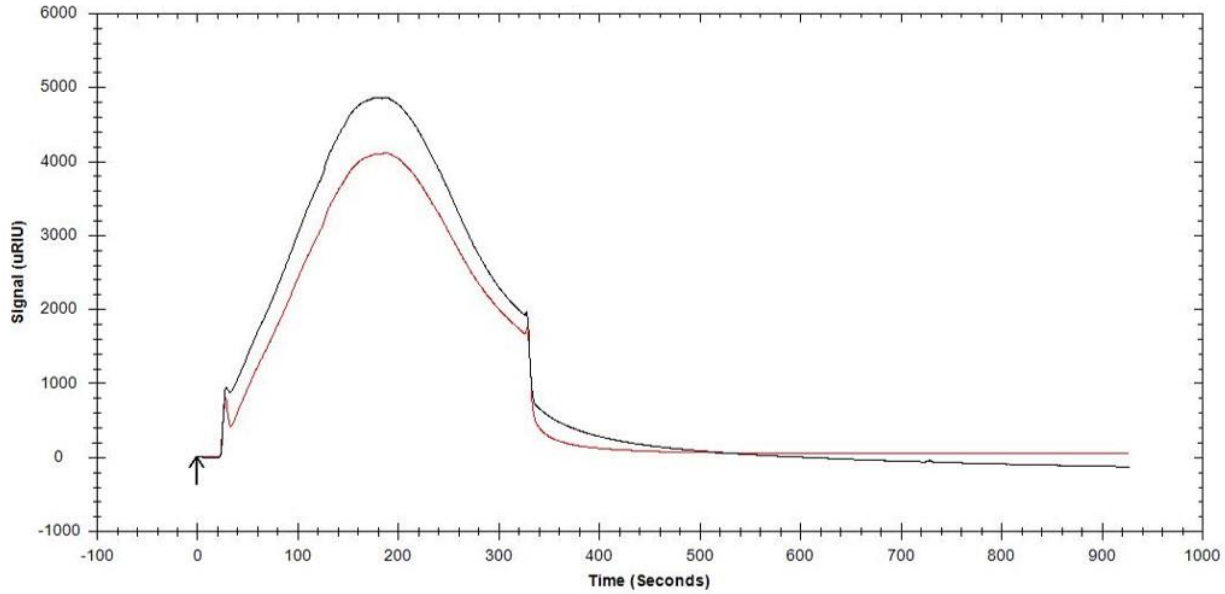

Figure C.1. SPR measurement for $DivIVA_{Bs}$ and CcpN interaction after subtracting reference channel RUs from Test channel. 10 µM $DivIVA_{Bs}$ (ligand) was immobilized and flooded with 22 µM of His-CcpN (analyte). Red line- "Reference" channel with no immobilized $DivIVA_{Bs}$; Black line- test channel with captured His-CcpN. Response unit recorded for "Test" channel after subtracting RUs from the reference channel. Test channel shows the change in RUs, hence a positive interaction.